Critical Reviews™ *in Biomedical Engineering*, 48(6):327–418 (2020)

Meta-Analysis of Efficacy of Chemotherapy Delivered by Mesoporous Silica Nanoparticles to Tumor-Bearing Mice

Anthony J. McGoron

Department of Biomedical Engineering, Florida International University, Miami, FL 33174; Tel.: (305) 348-1352; Fax: (305) 348-6954, E-mail: Mcgorona@fiu.edu

ABSTRACT: Nanomedicines have played an important role in the management of cancer patients with PEGylated liposomal doxorubicin (e.g., Doxil) and nab-paclitaxel (Abraxane) being two examples that have been commercially successful. However, the number of patients benefitting from these therapies is small compared with the potential impact. While off-site toxicities have been reduced, long term survival has not been realized. Thus, there continues to be a need for improved therapies and nanomedicine (delivery of drugs using nanoparticle carriers) that provide advantages over the delivery of free drug. Mesoporous silica nanoparticles (MSNs) are a unique class of nanomedicine that offers high loading capacity, the ability of targeting specificity, potential for stimulated drug release and are considered generally safe and non-toxic. This paper provides a comprehensive analysis of 166 published studies in which MSNs were evaluated *in vivo* and tumor response was reported. Eleven studies with liposomal doxorubicin and 3 studies with Abraxane are also included in the analysis. The MSN formulations exhibit a wide range of size, charge, drug loading and drug release. The tumor inhibition ratio (TIR) of some MSN formulations compared favorably to the FDA approved nanomedicines. However, TIR reached at least 99% in only 14 MSN formulations reported. On average, targeted MSNs and MSNs with combined therapy (multiple drugs, or drugs combined with thermal therapy) performed best. Survival was reported in 14 MSN studies. The reported increased life survival (ILS) tended to be longer for liposomal doxorubicin and Abraxane than for the MSN formulations. The paper also provides an overview of MSN synthesis strategies and compares the development timeline of MSNs to that of Doxil and Abraxane, discussing the barriers to commercialization. Finally, the paper provides recommendations to advance the development and commercialization of MSNs for cancer therapy.

KEY WORDS: nanomedicine, drug delivery, tumor volume, chemotherapy, liposome, albumin-bound paclitaxel

I. INTRODUCTION

A. Mesoporous Silica Nanoparticles

Since the first report of a unique characteristic of solid tumor microenvironment (i.e., increased capillary permeability and lack of lymphatics), later termed the enhanced permeability and retention (EPR) effect,[1–4] drug-polymer, drug-protein, and drug-nanoparticle complexes have been investigated as possible "silver bullets" for cancer therapy. Several reviews of FDA approved nanomedicines have been published recently.[5–8] The growth in nanomedicine funding has also been described.[9] Excellent reviews have been published outlining the advantages and disadvantages of the different nanoparticle materials and formulations for drug delivery applications; including liposomes,[10–13] albumin-bound drugs in nanoparticle form,[14,15] organic (polymer)[16,17] and inorganic materials (silica, gold, silver, iron oxide),[18–25] dendrimers,[26,27] and micelles,[28,29] as well as polymer-drug and antibody drug conjugates.[30–32] This paper will examine the current state of the development of mesoporous silica nanoparticles (MSNs) for drug delivery in cancer and compare and contrast the pre-clinical *in vivo* tumor growth inhibition of drug loaded MSNs to FDA approved Doxil (generic: Lipodox or liposomal doxorubicin) and Abraxane for delivery of doxorubicin (DOX) and paclitaxel respectively. The paper will also investigate the inconsistencies in experimental design and reporting of data, which may contribute to the lack of progress in moving new Nanomedicine based drug delivery formulations to commercialization. Finally, the paper will provide recommendations for standardizing pre-clinical Nanomedicine drug delivery experimental design and reporting of results.

The preparation of mesoporous silica-gel structures was introduced around 1980.[33] The first appearance of porous silica nanoparticles for cancer drug delivery applications was in 2000[34] (Table 1). In 2003 Lin introduced the acronym MSNs for mesoporous silica nanosphere.[35] A recent comprehensive review of the development of ordered mesoporous materials provides a nice history,[36] but leaves out the beginning of the story. In 1968 a method for forming small spherical non-porous SiO_2 particles of uniform and controllable size was reported and is now commonly referred to as the Stöber method (or Stöber reaction),[37] and has been cited over 10,500 times. The synthesis is a sol-gel process with a silicate precursor (typically tetraethylorthosilicate-TEOS, soluble in alcohol and organic solvents) which undergoes hydrolysis in H_2O in an alcoholic solution and then in the presence of an acid or base catalyst (HCl, HNO_3, ammonium, NaF, or NaOH) undergoes condensation. In 1992 a new family of molecular sieves was introduced[38,39] (which together has been cited almost 25,000 times) using a quaternary ammonium surfactant and tetramethylammonium silicate organosilicate. The ordered mesoporous silicas (M41S family, of which MCM41 or MCM-41 is an example) self-assemble into hexagonal arrayed pore of sizes from 15 Å to 100 Å and surface area of 700 m^2/g. The structure and pore dimensions highly depend on the surfactant template structure (such as chain length) (see Table 2 for a list of different MSN types). In 1999 the organosilane 1,2-bis(trimethoxysilyl)ethane (BTME, an organosilane monomer containing two trialkoxysilyl groups) with the surfactant octadecyltrimethylammonium chloride was used to create highly ordered organic-inorganic mesoporous materials with pore diameters of ~ 30 Å and surface areas of 750–1170 m^2/g.[40]

Excellent reviews have been published detailing the synthesis and structure relationships of mesoporous silica materials for general applications,[41] and biomedical applications (theranostics, imaging, drug monitoring and sensing),[25,42] including post-synthesis funciontalization.[43] Mesoporous (between micro and macro porous) materials are those with pore sizes from about 20 to 500 Å (2–50 nm). Material characteristics typically reported include overall size and shape, pore shape, pore arrangement, pore size, pore volume, Brunauer–Emmett–Teller (BET) surface area, wall thickness, lattice constant (the physical dimension of unit cell in a crystal lattice) and d spacing (distance between planes of atoms). Synthesis conditions controlling the crystal structure include temperature, solvent, the structure and chain length of the surfactant or structure directing agent template (which may be anionic, cationic or neutral, most typically a quaternary ammonium surfactant), the catalyst (which may be basic or acidic), the silica source (TEOS, TMOS, tetramethylammonium silicate), possibly with a bock copolymer (e.g., PEO-PPO-PEO), and the synthesis conditions (pH, temperature, time). IUPAC (International Union of

TABLE 1: Results from a Web of Science™ search (conducted December 23, 2020) for nanoparticle drug formulation development

Key words	Articles	Reviews	Proceedings	Book chapters	First year in database	First drug approved[a]
Liposome* AND *Cancer*	31,088	6306	4825	915	1974[†]	1995[b]
Albumin-Bound AND *Cancer*	1972	467	176	48	1985	2005[c]
Silica* AND *particle* AND *Cancer*	9799	1733	533	270	2002	N/A
Silica* AND *particle* AND *porous AND *Cancer*	7677	1205	190	152	2000	N/A

[a]For Cancer therapy; [b]Doxil®; [c]Abraxane®; N/A, not applicable. [†]Bangham[225] cites the first description of liposomes in 1964. *Search variant wildcard.

TABLE 2: MSN types

Material (phase)	Template/ surfactant	Catalyst	+Block co-polymer	Lattice structure	Pore size	Ref.
MCM-41	Cation	Base	N	Hexagonal	15 to > 100 Å	38,226,227
MCM-48	Cation	Base	N	Cubic	30–100 Å	226,228
MCM-50	Cation	Base	N	Lamellar	Not Reported	227,229
SBA-1	Cation	Acid	N	Cubic	24 Å	227
SBA-2	Cation	Acid/Base	N	Hexagonal	30 Å	227
SBA-3	Cation	Acid	N	Hexagonal	40 Å	227
SBA-6	Gemini	Base	N	Cubic	75 Å	230
SBA-8	Bolaform	Base	N	"ribbon like"	29 Å	231,232
SBA-11	Nonionic	Acid	Y	Cubic	25 Å	233
SBA-12	Nonionic	Acid	Y	Hexagonal	31 Å	233,234
SBA-15	Nonionic	Acid	Y	Hexagonal	50 Å	233,235
SBA-16	Nonionic	Acid	Y	"cage"	54 Å	233
FDU-1	Nonionic pluronic	Acid	Y	"caged" cubic	120 Å	236
FDU-2	Multicharge cationic	Basic	N	Cubic	30 Å	237
FDU-5	Nonionic	Acidic	Y	Cubic	45–95 Å	238
FDU-11	Bolaform	Basic	N	Tetragonal	27 Å	239
FDU-12	Nonionic pluronic	Acid	Y	Cubic	200 Å	240,241
FDU-13	Bolaform	Basic	N	Tetragonal	18 Å	239
MCF	nonionic	Acidic	Y	Not reported	"ultra large"	242
FSM-16	Cationic	Basic	N	Hexagonal	15–40 Å	243
MSU	Nonionic	Slightly basic	N	Hexagonal	20–60 Å	244

Common acid (e.g., HCl, HBr) or base (e.g., NaOH, tetramethylammonium hydroxide). Note the conditions listed are as described in the publication cited. In some cases, the material has been reported to be formed in other conditions. Pore size distributions are generally narrow. The range of pore size listed in the table is due to different templates/surfactants used, or more specifically, with templates/surfactants with different chain lengths.
The search is from 1965-present. Note that keywords are only searched in the Title, Abstract and Keywords (Author Keywords and Keywords Plus®) of an article's record and so some articles will be missed if the words appear elsewhere in the article.
MCM: Mobil Composition Matter (or Mobil Crystalline Matter); SBA: UC Santa Barbara Amorphous; FDU: Fudan University; MCF: Mesostructured Cellular Form; FSM: Folded Sheet Mesoporous; MSU: Michigan State University

Pure and Applied Chemistry) nomenclature of the structural and compositional characteristics of porous materials was published in 1994[44] and for ordered mesoporous structures in 2001.[45] The tables for the classification of crystal families and systems can be found here[46] and a tutorial on how to interpret the tables here.[47] Ohsuna et al.[48] developed a software package to simulate mesoporous crystal structure based on TEM images for structure type identification.

Most template methods (often referred to as "modified Stöber") that have been proposed for drug delivery applications employ the surfactant cetyltrimethylammonium bromide (CTAB) or chloride (CTAC) as the template, typically mixed in H_2O or H_2O:alcohol, to create a microemulsion for better control of the hydrolysis step before the condensation step is initiated by the base.[49–51] The surfactant is then removed by either burning it off (referred to as calcination) or by solvent extraction with an acid:alcohol solution,

most typically under reflux conditions. Controlling the two synthesis steps by adjusting the ratio of the reactants, time and rate of adding the reactants and the reaction temperature and time, allows for controlling size, shape and the number and size of the pores. MSN syntheses processes reported also include a reverse (or inverse) micro-emulsion (water in oil) method[52–54] and an oil in water emulsion method using vinyltriethoxysilane-VTES (or TVES) as the organosilica (which is slightly soluble in H_2O) with Aerosol-OT (AOT) and butanol as surfactant and co-surfactant, respectively.[55–58] Collectively, these methods are also referred to as ORMOSILs (organically modified silica). Another modification is to functionalize the surface of the pores with reactive amine, thiol or carboxyl groups for conjugating drugs, imaging agents, targeting moieties, polymers, etc. The first use of the term ORMOSIL seems to be in 1986,[59] though the application was for solid-state conductors. In fact, porous silica nano and microparticles, due to their ordered pair structure, high pore surface area, and good control of over physical properties, such as size and shape, have many applications, including as catalysts, in chromatography, CO_2 sequestration, filters, water filtration, optoelectronic devices, biomedical applications such as sensors and drug delivery, and many others. Therefore, the large-scale manufacturing of these materials is well developed and the physical and chemical characteristics are well understood.

Table 3 lists the primary chemicals used to synthesize MSNs. The most common surfactant used for MSN synthesis is CTAB. CTAC, the chloride salt form of CTAB, is used less often.[60,61] Differences between the characteristics of CTAB and CTAC were investigated and described by Atkin et al.[62] Triton X-100 is a non-ionic surfactant used in a water-in-oil emulsion modified Stöber technique, the oil phase is typically n-hexane and/or n-hexanol.[63–65] Sodium bis(ethyl-hexyl) sulfosuccinate (Aerosol-OT, AOT) is an anionic surfactant that has been used in oil-in-water emulsion modified Stöber methods, often with a co-surfactant such as 1-butanol.[56,58,66–68] A co-surfactant may be a second surfactant or an alcohol and is often added to ionic surfactants to help reduce surface tension and rigidity in the surfactant film around the emulsion droplet. Tween-80 (Polysorbate 80) is another non-ionic surfactant used to create micelles for a modified Stöber MSN synthesis technique, but it is not commonly used.[69,70] The microemulsion formed during MSN synthesis is highly dependent on the characteristics of the surfactant (and co-surfactants), such as chain length and charge, and the presence of electrolytes, which influences the properties of the silica-aqueous solution. The constituent conditions control the curvature of the water-surfactant (or water-oil-surfactant) interface and influences the colloid size and shape, which in turn controls the rate of condensation of the organosilica compound and ultimately the growth of the nanoparticle.

To date, there have been no clinical trials using MSNs for drug delivery (https://www.clinicaltrials.gov), possibly for safety concerns, but also perhaps because they have performed no better than the already FDA approved nanomedicines in pre-clinical studies. Though there is persistent concern about the potential adverse health effects of nanoparticle materials,[23] in general, ORMOSIL nanoparticles are considered biocompatible and nontoxic.[71–74] For both liposomes and albumin-bound drug carriers for cancer, the first article appeared about 20 years before the first FDA approved drug. The motivation for delivering drugs by a nanocarrier or polymer conjugate is primarily to (1) improve the solubility of poorly water-soluble drugs, (2) increase plasma residence time ("stealth") to improve pharmacokinetics (PK), (3) to reduce kidney excretion, (4) add a targeting and/or (5) imaging functionality without affecting the pharmacodynamics (PD) of the drug. Drugs that are generally effective but have undesirable toxicities can be re-purposed to improve PK-PD and thus potentially improve patient outcomes. Table 4 lists primary drugs that have been delivered by MSNs and evaluated in tumor-bearing mice in the studies reviewed in this paper. The choice of delivery vehicle is driven by the physical and chemical characteristics of the drug (molecular weight, charge, solubility, pKa, LogP etc.). The pKa is the negative base-10 logarithm of the acid dissociation constant (Ka) and relates drug solubility to the pH of the solvent/ststem. P (also referred to as $K_{o/w}$) is the octanol/water partition coefficient and a measure of lipophilicity, a higher logP being more compatible with a lipophilic solvents and carrier. These characteristics influence drug loading,

TABLE 3: List of chemicals commonly used in the synthesis of MSNs for drug delivery applications

Chemical name	Abbreviation	Purpose/Use	Structure/Formula
Cetyltrimethylammonium bromide	CTAB	Cationic surfactant	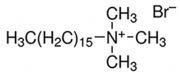
Cetyltrimethylammonium chloride	CTAC	Cationic surfactant	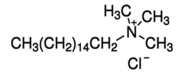
Triton X-100		Non-ionic surfactant used in a water-in-oil emulsion	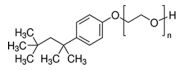
Tween-80 (Polysorbate 80)		Non-ionic surfactant that is used to create micelles	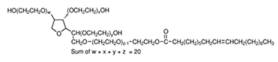
Dioctyl sulfosuccinate sodium salt	Aerosol-OT, AOT	Anionic surfactant used in oil-in-water emulsion	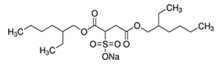
Igepal Co-520		Nonionic surfactant	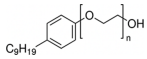
Pluronic 127		Co-surfactant	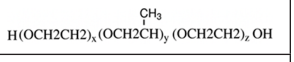
1-Butanol		Co-surfactant	
n-hexanol		Co-surfactant	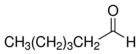
n-hexane		Co-surfactant	$CH_3(CH_2)_4CH_3$
Aminopropyl)triethoxysilane	APTES	For amine functionalization	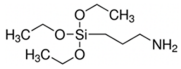
(3-mercaptopropyl) trimethoxysilane	MPTMS	For thiol functionalization	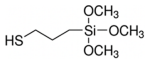
5-(Triethoxysilyl)pentanoic acid		For carboxyl functionalization	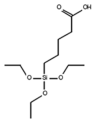
3-(trihydroxysilyl) propyl methylphosphonate		Silica source	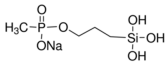
3-(Trimethoxysilyl)propyl methacrylate	TMP; MPS	Silica source	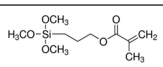
1,2-bis(triethoxysilyl)-ethane	BTEE	Silica source	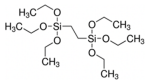
Triethylamine	TEA	Base catalyst	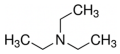
Ammonium solution		Base catalyst	NH_3
Triethanolamine	TEOA	Base catalyst	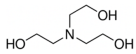
Sodium hydroxide		Base catalyst	NaOH
Ammonium hydroxide		Base catalyst	NH_4NO_3
Tetraethyl orthosilicate	TEOS	Silica source	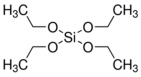

TABLE 3: (*continued*)

Chemical name	Abbreviation	Purpose/Use	Structure/Formula
Triethoxyvinylsilane	TEVS or VTES	Silica source	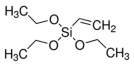
3-isocyanato propyl trimethoxy silane		Silica source	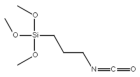
Trimethylsilyl chloride	Cl-TMS	Silica source	
Trihydroxy-silylpropylmethyl-phosphonate		Silica source	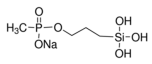
(3-triethoxysilylpropylsuccinic Anhydride)	TPS	Silica source	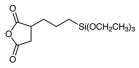
N-(2-aminoethyl)-3-aminopropyltrimethoxysilane	AEAPS	Silica source	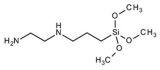
bis(trimethoxysilyl)ethane	BTSE; BTME	Silica source	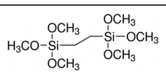
Octadecyltrimethoxysilane	C_{18}TMS	Silica source	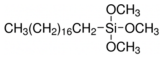
Polyethylamine	PEI	Cationic polymer	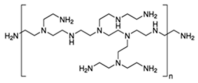
Polydopamine	PDA	Polymer from oxidation of dopamine	unknown
Ammonium nitrate		Removes surfactant from msns	NH_4NO_3
Sodium carbonate		To etch SiO_2 for hollow msns	Na_2CO_3
Dimethyl sulfoxide	DMSO	Solvent and oil phase for emulsion	
Cyclohexane		oil phase for emulsion	C_6H_{12}
Decahydronaphthalene	decalin	oil phase for emulsion	$C_{10}H_{18}$
Triethylammmonium sucrose octasulfate	TEA_8SOS	remote loading trapping agent	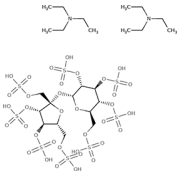

release and compatibility with the solvents and other chemicals used in the synthesis of the nanocarrier.

B. Commercialization

Anthacyclines are the most widely prescribed anti-cancer agents due to their broad spectrum efficacy towards cancer, but high, dose-limiting cardioctoxicity and immune suppression was largely the driving force to develop drug carrier systems. Doxorubicin (DOX) is the most widely used anthracycline. The 20 year path to FDA approval of Doxil (PEGylated liposomal DOX approved in 1995), which was the first approved nanoparticle-based drug larger than a polymer-drug or antibody-drug conjugate, has been very well described.[75] By 1995 (the year of

TABLE 4: List of the most common drugs (and their characteristics) employed in the studies analyzed in this paper

Drug	Abbreviation	Mechanism of action	Structure	MW	pKa	LogP	H_2O solubility
All-trans retinoic acid	ATRA	N/A	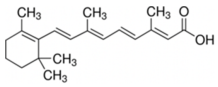	300.4	N/A	6.9	Nearly insoluble
Arsenic trioxide	ATO	Induces apoptosis	As_2O_3	197.8	N/A	N/A	Slightly
Berberine	Ber	Alkylation agent	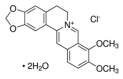	336.4	N/A	3.6	Slightly
Camptothecin	CPT	Topoisomerase inhibitor	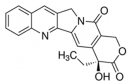	348.4	N/A	1	Low
Chlorin	Ce6	PDT photosensitizer		312.4	N/A	3.7	DMSO, not H_2O
Cisplatin (platinum agent)	cisPt/CDDP	Alkylation agent	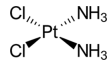	300	N/A	N/A	Soluble
Curcumin	Cur	Adjuvant	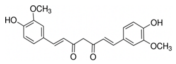	368.4	8.5	3.29	Isoluble
Docetaxel	Doc	Microtubular inhibitor	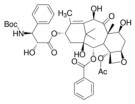	807.9	N/A	1.6	Insoluble
Doxorubicin	DOX	Topoisomerase inhibitor	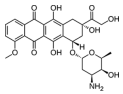	543.5	7.3-9.5	1.3	HCl salt form
Epirubicin	EPI	Topoisomerase inhibitor	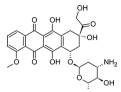	543.5	~ 9.2-12.7	1.3	HCl salt form
Erlotinib HCl		EGFR inhibitor	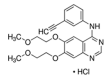	393.4	1	2.7	Soluble
5-fluorouracil	5-FU	Antimetabolite		130.1	8	N/A	Acids and DMSO
Gemcitabine-HCl	GEM	DNA synthesis inhibitor		263.2	3.6	–1.5	Soluble

TABLE 4: (*continued*)

Drug	Abbreviation	Mechanism of action	Structure	MW	pKa	LogP	H_2O solubility
Irinotecan	Ir	Topoisomerase inhibitor		586.7	N/A	3	Soluble
Mefuparib hydrochloride	MPH	Poly(ADP-ribose) polymerase inhibitor		334.8	N/A		Soluble
Paclitaxel	PTX	Microtubular inhibitor		853.9	10.4	2.5	Insoluble
Protoporphyrin IX	PpIX	PDT photosensitizer		562.7	N/A	4.6	Poorly
Quercetin	QC	N/A		303.2	1.5	N/A	Poorly
Resveratrol	RSV	Multiple mechanisms		228.4	9-10.6	3.1	Low
Ruthenium polypyridyl	RuPOP	Induces apoptosis		N/A	N/A	N/A	Soluble
Temoporfin		PDT photosensitizer		680.8	N/A	8.8	DMSO, not H_2O
Sorafanib		RAF kinase inhibitor		464.8	N/A	4.1	DMSO

TABLE 4: (*continued*)

Topotecan		Topoisomerase 1 inhibitor		421.4	1.7–9.8	0.5	Soluble
Vincristine	VCR	Binds to microtubules		825	5–7.4	2.8	Slightly in alcohol

pKa is the negative base-10 logarithm of the acid dissociation constant (Ka). P is the octanol/water partition coefficient and a measure of lipophilicity. (source: pubchem.ncbi.nlm.nih.gov and material data safety sheets, MSDS). Some data are not available (N/A).

approval) there were 205 patents awarded in liposomal based drug delivery for cancer. Shinozawa[76] reported on the efficacy of both neutral and charged (non PEGylated) liposomal DOX in 1981, 14 years before the approval of Doxil. While cardiolipin is not a component of FDA approved liposomal formulations, it was a component in most of the early formulations due to strong binding of anthracyclines to cardiolipin, which was considered early on to be a possible cause of the high toxicity of anthracyclines to the heart.[77–80] In contrast, Abraxane (ABI-007, albumin-bound paclitaxel, nab-paclitaxel) was developed and approved in 2005 and is based on the discovery of the binding of paclitaxel to serum proteins. By 2005 only 7 patents were awarded in nano-albumin-bound drugs for cancer. Interestingly, a Web of Science search returned two pre-clinical studies demonstrating *in vivo* tumor control,[81,82] published after Abraxane was approved. This is compared with many more such studies of liposomal doxorubicin.

Antunes[83] conducted a patent search and found 2,306 nanoparticle focused patents in the pharmaceutical sector by 2013. Table 5 lists the number of awarded patents from the Derwent Innovations Index™. While these numbers likely overestimate the number of directly related patents, since the search terms may appear as background information and many of the patents may not be specifically for drug formulations or drug carriers, they do attest to the strong interest in commercializing nano-based pharmaceuticals towards cancer. Figure 1 shows that 2018 and 2019 were particularly strong years. These results may provide an indication of potential future commercialization of new nanomedicines. However, the majority of the patents are from universities or institutes, not companies, and identifying commercial partners to license this type of technology is a big challenge.

As stated previously, Doxil was FDA approved in 1995 and the first patent issued for liposomal drug delivery for cancer was in 1976 (20 years prior) while the first publication appeared in 1974, a little more than 20 years prior. For Abraxane, FDA approved in 2005, the first patent appeared 10 years prior, and the first publication 20 years prior. For MSN drug delivery applications for cancer, the first patent and first publication both appeared in 2006. The earliest clinical trial of a liposomal formulation for cancer listed in the ClinicalTrials database was in 1997 (two year after the approval of Doxil) and for albumin-bound paclitaxel, 2001 (4 years before the approval of Abraxane). However, Gabizon et al., published the results of a Phase I study of liposomal DOX in 1989.[84] Segal et al., published a human clinical study of liposomal bleomycin in 1976.[85] The first published human clinical trial of nab-paclitaxel was in 2001.[86] Of Doxil in particular, Barenholz et al.[87] stated that "the first provisional patents were filed in 1987/1988 based on work started 7 ½ years earlier." Given comparable timelines, perhaps companies are working on commercializing MSN formulation for cancer therapy (first reported in the literature in 2006 and the first patent issued the same year). A patent issued in 2003 (Nanoparticle Assembled Hollow Spheres) described nanoparticles containing silica as a component for drug delivery, but it did not mention mesoporous. Nevertheless, there are no current clinical trials on record (ClinicalTrials.gov) testing MSN formulations for drug delivery. There are however 3 current studies (phase 1 and 2) evaluating cRGDY-PEG-Cy5.5-C dots (NCT02106598), 89Zr-DFO-cRGDY-PEG-Cy5-C' dots (NCT03465618) and 64Cu-NOTA-PSMAi-PEG-Cy5.5-C' dots (NCT04167969) for fluorescence nodal mapping and positron (PET) imaging of brain tumors and prostate cancer. C dots (Cornell dots) are ultra-small dye-encapsulated core-shell silica particles synthesized by the Stöber method with alcohol as the solvent and C′ (C prime) dots are similar except grown in water.[88,89] The success of these trials may provide supporting evidence to investigate MSNs for delivering chemotherapy drugs.

If we compare the timeline from the first reported use of pegylated liposomal DOX or albumin-bound paclitaxel in tumor-bearing rodents (~ 1980 and 2002 respectively) to their first test in humans (1989 and 2001 respectively), to their eventual FDA approval (1995 and 2005 respectively), we might get a sense of how long to expect before one is to see MSNs commercialized. However, the lack of complete response of Doxil; and Abraxane in humans may have dampened the enthusiasm for

TABLE 5: Results of a search of awarded patents in the nanomedicine drug delivery space (as of December 23, 2020)

Key words	Total	World	China	US	EU	Japan	Canada	India	First year
(pharma* OR drug*) AND (nano* OR liposom*)	24,508	8327	10,992	9302	5216	4704	2252	1978	1966
(pharma* OR drug*) AND nano*	20,275	6571	9662	7097	3730	3156	1606	1698	1966
(pharma* OR drug*) AND (nano* OR liposom*) AND cancer	7630	2963	3762	3005	1794	1375	884	641	1976
(pharma* OR drug*) AND nano* AND cancer”	6057	2202	3231	2188	1200	795	598	511	1996
(pharma* OR drug*) AND liposom*	5341	2139	1941	2288	1637	1705	749	363	1976
(pharma* OR drug*) AND liposom* AND cancer	2040	957	785	999	706	653	339	178	1976
(pharma* OR drug*) AND nano* AND albumin AND cancer	232	74	147	42	41	28	23	19	1995
(pharma* OR drug*) AND nano* AND (*silica*) AND *cancer*	299	69	196	72	30	17	12	12	2001
(pharma* OR drug*) AND nano* AND *silica* AND *porous* AND *cancer*	170	28	126	34	15	9	6	5	2006

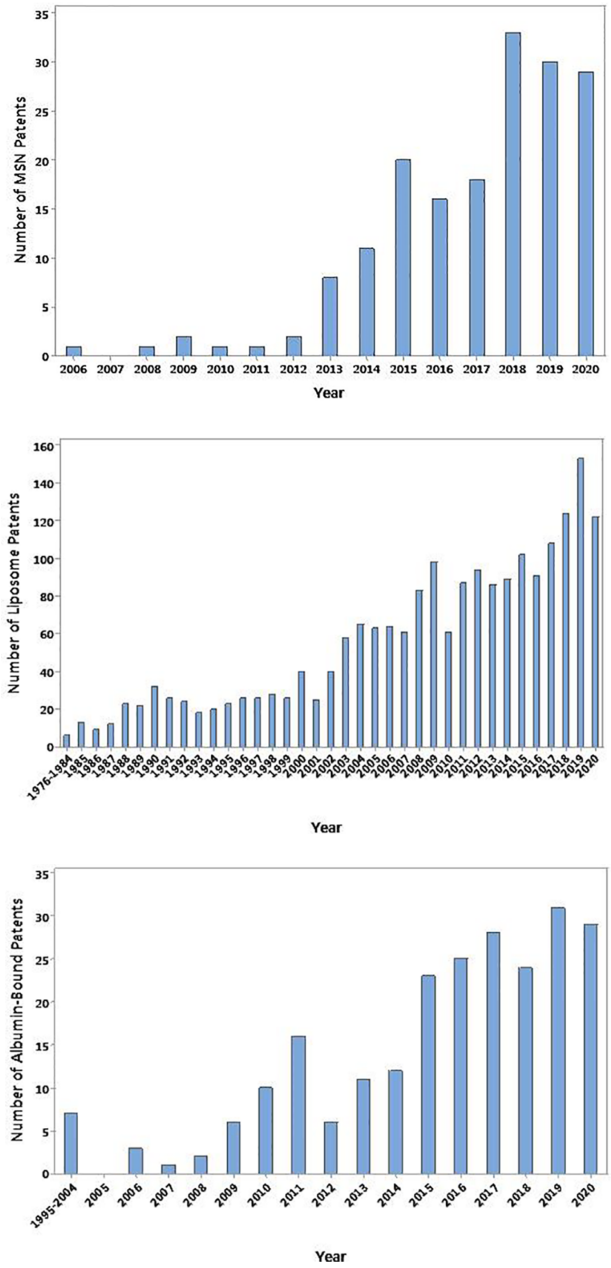

FIG. 1: Results of patent search (as of December 1, 2020) using (top): Key-words: (pharma* OR drug*) AND nano* AND (*porous silica) AND cancer. (middle): Key-words: (pharma* OR drug*) AND liposom* AND cancer. (bottom): Key-words: (pharma* OR drug*) AND (nano* AND albumin) AND cancer.

the cost and time to fully develop MSNs for drug delivery. It should also be questioned, what, if any, advantage MSNs might have over already approved nanoparticle formulations, for example, greater efficacy (either reduced toxicity or improved survival or both) in certain populations or cancer types. Even in animal models, complete response (eradication of tumor) was not generally observed for Doxil or Abraxane. But increased survival and reduced systemic toxicity was observed.

C. Barriers to Commercialization

Several papers have been published that describe the barriers to commercialization of nanomedicines for drug delivery.[90–92] It is well recognized that EPR is not universal in solid tumors and it has been argued as to how much of a contribution EPR has had on the success of nanomedicines to date.[93–96] The liposomal and albumin-bound drug formulations are arguably less complicated than formulations with mesoporous silica nanoparticles, and possibly involve less risk. However, the choice of the most effective liposome composition and developing the strategy for maximizing drug loading was not trivial and similar optimization studies would need to be done for MSNs. The pre-clinical animal studies with liposomal and albumin-bound drug formulations were largely positive and promising that they might not only reduce side effects but even lead to a cure, or at least substantial improvements in survival in humans. Eradication of the tumor was observed in some studies (or more specifically, the tumor was no longer palpable). However, while the translation to humans was successful, the degree of efficacy observed in tumor-bearing rodents did not translate to humans with the same level of response. The potential reasons for this (i.e., differences between rodent models and human disease, and poor patient selection) has been extensively reported on.[97–99] So, with all the money and time spent, papers published, patents awarded, why have nanoparticle-based drug delivery systems not led to cures in cancer? While there has been considerable progress there is little argument that the so-called "silver bullet" remains out of reach. While these therapies have proven to add benefit to patient's lives (in terms of quality of life, reduced side-effects and possibly some progression free survival), they have generally not led to an increase in disease free life and certainly

not a cure for the majority of patients receiving the treatments.[11,100–103]

In the past decade, several reviews, opinion pieces, editorials, etc. have appeared in reputable journals questioning the value of continuing to expend money, resources and time in this pursuit.[104–113] After all, resources are finite. Several articles have offered the argument that the reason for a lack of translating the exciting promise of pre-clinical success into the clinic is due to either (1) lack of appropriate animal models that accurately reflect the disease in humans, (2) the lack of appropriate selection of the patient populations that might benefit most from the therapy and/or (3) the difficulty in bringing a cancer therapeutic to market because of expense or technology to make manufacturing scale-up practical. The challenge of using animal models to predict clinical outcomes is well known and much discussed.[114–118] The cost of bringing a new drug to market is estimated to be around ~$2.8B for anti-neoplastic drug, which includes the cost of failed drugs, and is increasing at a rate well above general inflation.[119,120] New drugs for oncology applications have the lowest success rate through phase III trials[121] but the overall success rate for approval after submission to FDA is comparable to drugs for other therapeutic areas (81.7%).[120] The median duration spent in clinical trials for oncology drugs was 13.1 years.[121] The general attractiveness of nanoparticle-based and polymer-based drug delivery has been in the potential to re-package existing drugs for improved delivery (PK-PD). The reformulation of existing drug molecules onto or into a new delivery format has many advantages, especially if the general safety can be demonstrated and if the carrier does not interfere with the drug activity at the target site. However, the considerable challenge is the efficient delivery to and off-loading of drug at the target site. This point is addressed below.

Abou-El-Enein et al.[122] suggest a 12-step process for improving the translation of biomedical science to clinical success. Anchordoquy et al.[123] summarized a workshop titled "Mechanisms and Barriers in Nanomedicine" to facilitate improvements in translating Nanomedicine research to the clinic. Sanna et al.[124] provided a review of targeted nanomedicine which presented a multifactorial optimization of the synthesis parameters and characteristics for the development of BIND-014, a targeted polymeric micelle which completed phase 1 and 2 clinical trials (another phase 2 trial was terminated).[7] It was ultimately not pursued but the basic "BIND" polymer nanoparticle technology is still being investigated clinically with AZD2811 nanoparticles (ClinicalTrials NCT03217838).[125,126] These examples may provide useful guides to improve the potential for overcoming barriers to nanomedicine commercialization.

D. Inconsistency in Experimental Design and Data Reporting

The way that the nanomedicines (nanoparticles or nanoformulations) are categorized in the literature is confusing and makes comparing the results among different groups challenging. A general classification might be as follows; liposomes (typically PEGylated), polymer-drug conjugate (typically PEGylated), nanoparticles from natural or synthetic polymers (often PEGylated), antibody-drug conjugates, aptamer-drug conjugate, lipid nanoparticles, micelles, inorganic nanoparticles (typically iron oxide, gold, silica, or combinations), proteins, protein-conjugates, nanocrystals, and virosomes. There is considerable overlap in how the formulations are described in the literature. Many review papers are unable to directly compare various nanomedicine formulations because of the lack of consistency in experimental design, reporting of data or incomplete or confusing details in the materials and methods description. There needs to be consistency in the way the nanomedicines are categorized, characterized (physio-chemical properties), and tested in pre-clinical *in vivo* studies. For example, the pH (and contents) of the solvent used for measuring zeta potential are often not provided, providing both DLS (hydrodynamic) and SEM/TEM diameter is important because they report different characteristics, polydispersity index (PDI), or size (or molecular weight) distribution is often not reported, loading efficiency and capacity should both be reported, drug release and degradation to near 100% under conditions comparable to plasma, tumor interstitial space, and endosomes or lysozomes, depending on

their intracellular fate or intended use is often not reported. Percent surface coating of targeting moiety are usually not reported. When reporting the size of the particles, some provide a range, while others provide PDI and still others the standard deviation. Many papers do not report how freeze-drying (lyophilization) affects the formulation stability and size after resuspension.

Two recent analyses by the same group[127,128] reported that about 1% of an injected nanoparticle formulation is actually taken up by a tumor and that less than 0.0014% actually makes it into cancer cells. A more recent analysis found higher delivery efficiency of 2.23%.[129] While these studies are thorough, many studies reported in the literature are not included in their analyses due to inconsistency in experimental design, or data reporting, or insufficient number of pharmacokinetics data points to calculate area under the curve (AUC). A closer examination of[127] finds that most of the papers included in the analysis were for imaging (i.e., not therapy). Few of the papers reported the amount of drug (or imaging tracer) loaded into the nanoparticle carrier, so it is not possible to estimate how much drug (or tracer) was actually delivered to the tumor. In fact, a review of Nanomedicine drug delivery papers shows that in many, either the data are not provided, or the data provided are incomplete. For example, some papers report drug loading efficiency (i.e., the percentage of the drug added during the synthesis process divided by the drug loaded into the carrier) but do not report the actual amount of drug in the particle, i.e., the drug loading capacity (mass of drug per mass of carrier in wt%). It is often not possible to interpret the drug loading capacity from the loading efficiency based on the experimental details provided. Often, the term "loading efficiency" is used without explicitly defining what it means, or "efficiency" is used when it apparently (or even explicitly) means "capacity." In other words, the precise meaning of loading efficiency is not always clear when it is used. While loading efficiency is important from a materials conservation perspective (especially for expensive drugs), it is the loading capacity (drug content) that is most important in predicting the amount of active drug that actually reaches the target (tumor).

Size and surface charge are other particle characteristics that are reported very inconsistently across articles. When size is reported it is not always clear if the size is hydrodynamic (i.e., measured by dynamic light scattering or a similar method) or by electron microscopy (SEM or TEM). If SEM or TEM size is reported, it is not always clear how many particles were measured, or if it is simply an estimate from a single image view. Often a plot of hydrodynamic size distribution may be provided (generally on a log scale), but not the actual mean value. Sometimes the size of the base mesoporous silica nanoparticle is reported, but not for the final loaded and coated product, or it may not be clear. The surface charge (zeta potential) is often not reported, or not reported for the final product, and typically measured in H_2O or PBS and not in the presence of plasma proteins. Often synthesis condition details are vague and not explicitly stated (volumes, concentrations, reaction temperature, details of the process and conditions for removing surfactants, etc.).

For a therapeutic drug carrier, the drug must be released from the carrier close enough to its site of action to be effective. Another major inconsistency is the reporting of drug release from the nanoparticle carrier. Either the experimental conditions are not clear, the experiment is not carried out long enough to estimate the time for more than 90% of the drug to be released, or even the data might not be presented at all. When the dialysis membrane method is used, including a free-drug group is necessary to accurately model the release kinetics. For positively charged drugs electrostatically bound to MSN release is enhanced at low pH. Therefore, many experimental designs for MSNs include a low pH condition to simulate the conditions in a tumor. The pH in the experimental conditions reviewed in this paper range from as low as 1 to 6.8 pH units. While acidosis has been reported and explained,[130–134] due to tumor microenvironment heterogeneity, it is not settled that tumor micro-environment pH levels are consistently low enough to induce drug release in all tumors or even in all regions of a tumor.[135,136] Other release triggering mechanisms have been designed into the formulations and have been reported, most often glutathione (GSH) or reactive oxygen species (ROS).[137–140] DOX release from Doxil under

physiological conditions is reported to be slow, ~ 0.5% at 2 h at pH 7.4 and < 3% at pH 5.5 at 2 h[141] or ~ 30% at 12 d at pH 7.4.[142] Russell[142] measured an ~ 2× greater rate constant at pH 5. Based on these two studies, DOX release from Doxil appears to be comparable to that from MSNs.

Here, we present the case of MSNs presenting evidence from pre-clinical studies that showed promise in tumor-bearing mice (and in a few cases, rats). Since there are no reported clinical trials using MSNs to deliver therapeutics in cancer (https://www.clinicaltrials.gov) it may be assumed that, for whatever reason, none of these formulations is close to becoming a commercial clinical product. Our contention is that, in addition to the limitations listed above, there is also a big problem with the lack of consistent reporting of results from pre-clinical *in vivo* studies, the complexity of the formulations reported that make them impractical for scale-up and manufacturing, and possibly a difficulty in reproducing data reported in the literature, as discussed in,[143,144] with recommendations for the reporting of Nanomedicine data presented at the end of the paper.

II. METHODOLOGY

In the analysis for this paper a Web of Science™ search was conducted for articles that report studies investigating MSNs carrying chemotherapy drugs that have been tested in tumor bearing rodents and in which tumor response was reported. Studies in which drug was injected directly into the tumor were not included. Studies that described encapsulating DNA, RNA or proteins but without chemotherapy were also not included. The analysis concentrates chiefly on carrier size, charge, surface coating, drug loading, drug release and tumor response. However, as will become clear, it is difficult to arrive at firm conclusions due to the fact that the experimental design and data reporting are so inconsistent among research groups.

The literature search was conducted using search terms to find as many relevant papers as possible. However, it is possible that some relevant papers were not captured. The original research articles were evaluated to determine if drug loading and release from the carrier were reported and if tumor response was measured. Studies that reported the delivery of proteins or DNA/RNA, but not chemotherapy, were excluded. Of the studies included, some incorporated cellular or vascular targeting (other than passive EPR targeting). Some report the size of the carrier from SEM/TEM measurements and/or DLS, either as a graphic only or explicitly as a number. Some report zeta potential, typically in PBS or water dispersant. For data that were reported in graphical form, but the values were not explicitly stated, the program GetData Graph Digitizer (version 2.26.20.20; http://getdata-graph-digitizer.com/) was used to extract data from the plots.

Tumor inhibition ratio (TIR) is defined as $(1-W_T/W_C)$ where W_T is the weight (or volume) of the tumor at the end of the study in the treatment group and W_C is the tumor weight (or volume) in the placebo group. If tumor *ex vivo* weight at the end of the study was provided, then TIR was calculated from the weight, otherwise it was calculated from the *in vivo* volume measurements. Increased life survival (ILS) is defined as 100 × (treated mean survival)/(control mean survival) – 100. Mean survival time is determined from a Kaplan-Meier plot as (number of days of the first death + number of days of the last death)/2. If all animals were not dead by the end of the study, the data are reported as % surviving at the last time point. Group means of nanoparticle characteristics and TIR were compared by ANOVA and Pearson Correlation using Minitab 19 with $p < 0.05$ used for hypothesis testing. Comparing TIR among groups, the ANOVA was followed by a *post hoc* Dunnett comparison with either Free-DOX or MSN-DOX [without targeting, thermal therapy (TT), photodynamic therapy (PDT), or radiation therapy (RT)] as the control group.

III. RESULTS

In total, data from 166 MSNs, 13 liposomal doxorubicin and 3 Abraxane studies are included in this paper. Some papers tested in multiple tumor models. Several chemotherapy drugs were used (Table 4), including various shRNA, DNA, enzyme inhibitors, herbal or dietary supplements, as well as combinations (though not listed in the table). Table 6 provides

TABLE 6: Distribution of the types of formulations included in this paper

Formulation	No. of studies	With PEG	With targeting	With triggered release (pH)	With triggered release (heat; GSH; ROS, etc.)	Solid core other than MSNs	Hollow core
DOX w/o combination therapy	50	16	27	12	9	9	4
DOX + TT	22	8	12	6	7	10	6
DOX + PDT	7	3	3	1	1	1	2
DOX + RT	1	1	1	0	0	1	0
DOX + other chemo drugs	23	20	11	3	4	6	1
Other chemo-drugs	55	28	29	7	4	13	5
PDT only	3	1	1	0	0	0	1
TT only	2	0	0	0	0	2	0
PDT + TT	3	2	3	2	2	2	0
Total	166	79	87	31	27	44	19

Note that the two columns of "triggered" release formulations may be greater than the number of studies because some formulation possessed both pH responsive and molecular responsive release characteristics.

a distribution of the types of formulations. Some of the MSN studies reported multiple formulations. Some formulations induced PDT or TT. The thermal therapy was induced by external stimulation with near infrared (NIR) light of gold (Au), copper sulfide (CuS) or indocyanine green (ICG) or alternating magnetic field (AMF) or radiofrequency (RF) stimulation of Fe_3O_4. One study combined MSN loaded DOX with RT. One study combined chemotherapy, PDT and TT and three studies combined TT and PDT without chemotherapy drug. Numerous studies did not report loading capacity. In several papers, neither the loading capacity nor loading efficiency was reported. An attempt was made to contact those authors and some responded with the data.

The synthesis methods employed in the papers reviewed for this analysis include the Stöber method, modified Stöber method, micro-emulsion (oil-in-water), and reverse micro-emulsion (water-in-oil). For emulsion methods several surfactants were used, different silica precursors and different base initiators (Table 3). Some MSNs were not functionalized, and some were functionalized with amines, carboxyl or suflhydryl groups. Most of the formulations in this review included a step to remove excess surfactant; by solvent extraction (using various solvents with (71) or without (20) reflux condition or with sonication (4)), calcination (19), centrifuge washing with various solvents (23), ion-exchange (2), dialysis (2). Others did not report doing this step. Some formulations included a core-shell design in which the core was of a material other than silica (e.g., iron oxide, gold) and some were hollow. Many formulations included a hydrophilic coating (e.g., PEG). Many formulations depend on pH triggering such that the strong electrostatic interactions of negative charge of the silica-oxide surface and positively charged drug is weakened under low pH conditions allowing the drug to be released, or a thiol linker is incorporated so that the drug will be released in the high GSH environment of the tumor, or the MSN cores are capped with a molecule that will release the drug in the presence of either low pH, elevated temperature, GSH, or ROS. Table 7 provides the nanoparticle characteristics of each study, Tables 8–11 present the *in vivo* efficacy data for the MSN studies and Table 12 the efficacy studies for liposomal and Abraxane studies. In several

TABLE 7: MSN formulation characterization

Author	DOX LC	Size TEM	Size DLS	ZP (mV)	Target	TT/PDT	Template	Drug(s)	PEG	Core	Coated/ capped
Studies with DOX w/o combination therapy											
Chen 2020[199]	31.4	~~31.4~~	~~375~~	–28	N	N	CTAB	DOX	N	$dSiO_2$ (120 nm)	PLL(cit)
Chen 2020[245]	16.3	~~16.3~~	~~60~~	~~104~~	~~–51~~	~~A-CAIX Ab~~	CTAC	DOX	N	MSN	N
Chen 2016[195]	8.41	~~8.41~~	~~200~~	~~302~~	~~–45~~	~~HA/CD44~~	CTAB	DOX	N	MSN	β-cyclodextrin
Cheng 2017[246]	7.8	~~7.8~~	193	~~193~~	~~–4.8~~	~~FA~~	CTAB	DOX	Y	MSN	olydopamine
Cheng 2017[247]	10.1	~~10.1~~	221	~~221~~	~~2.6~~	N	CTAB	DOX	Y	MSN	PDA
Dai 2015[248]	4.9	~~4.9~~	117	~~117~~	~~–16.3~~	~~FA~~	CTAB	DOX	N	MSN	Salphdc
Fang 2019[249]	25	160			HA/CD44	N	CTAB	DOX	N	FeO4	N
Gao 2012[201]	15		131	0.4	FA	N	Stober	DOX	N	SiO_2	SiO_2
Han 2016[194]	17		48	–22.6	TAT	N	CTAB	DOX	N	MSN	Galactose
Hou 2017[250]	35.4		210	24.0	FA	N	CTAB	DOX	Y	Hollow	PDA
Hou 2016[251]	57.5	255	289		N	N	Commercial	DOX	N	MSN	N
Huang 2017[252]	14.6		116	–24.3	Lactobionic acid	N	CTAB	DOX	N	SiO_2 core	N
Jiang 2018[70]	1		190		N	N	Tween-80	DOX	N	MSN	N
Kang 2019[253]			99	–18.9	HA/CD44	N	CTAB	DOX	N	MSN	N
Khatoon 2016[254]	15.6		150	–12.6	N	N	CTAB	DOX	N	MSN	N
Li 2018[196]	12.2	114	600		Peptide + magnet	N	CTAB	DOX	N	Fe3O4	N
Li 2018[147]	21.1		134	–35.4		N	CTAC	DOX	N	MSN	N
Li 2017[215]	3	35	68		TSH	N	Commercial	DOX	Y	MSN	N
Li 2014[255]		200		21	N	N	CTAB	DOX	N	MSN	Polymer
Lin 2018[63]	11.2		130		Biotin	N	CTAB	DOX	Y	MSN	N
Liu 2020[256]	21	96		–15	N	N	CTAB	DOX	Y	MSN	PEG-b-PLLDA
Liu 2019[257]	26		110	–14.9	HA/CD44	N	CTAB	DOX	N	MSN	N
Liu 2019[258]	4.2		154	–19.8	N	N	CTAC	DOX	N	MSN	N
Liu 2017[259]	29.1	150			N	N	CTAB	DOX	N	MSN	sericin
Liu 2016[260]	10	120		7.4	N	N	CTAB	DOX	Y	Hollow	beta-cyclodextrin
Meng 2011[200]	3		50	46.7	N	N	Pluronic F127-CTAB	DOX	N	MSN	phosphonate

TABLE 7: (*continued*)

Author	DOX LC	Size TEM	Size DLS	ZP (mV)	Target	TT/PDT	Template	Drug(s)	PEG	Core	Coated/ capped
Studies with DOX w/o combination therapy											
Palanikumar 2018[261]	32		150	–3	N	N	CTAB	DOX	Y	MSN	PDS
Qiao 2019[262]	28.6	100				N	Hexadecyltrime-thylammonium bromide	DOX	N	MSN	tryptophan mediated Fe_3O_4 cap
Ramaya 2017[263]	9.3		125	25.6	FA	N	Stober	DOX	N	Gold	N
Shao 2016[264]	20	300		6.59	mag	N	CTAB	DOX	Y	Fe_3O_4	MSN
Shen 2019[265]	28		50	–0.1	N	N	CTAC	DOX	Y	MSN	MPTMS
Si 2020[266]	66	150	190	–10	MUC-1	N	CTAB	DOX	N	MSN	N
Tian 2016[267]	26.5	100	108		Tf	N	CTAB	DOX	N	MSN	N
Turan 2019[202]	20	80		–32.5	CREKA	RF	CTAB	DOX	Y	Iron Oxide	N
Turan 2019[203]	19.5	74			RGD/ CREKA	RF	CTAB	DOX	Y	Iron Oxide	N
Wan 2020[268]	10.2	120	245	–29.8	N	N	CTAB	DOX	N	Fe_3O_4	MSN
Wang 2019[269]	40	70	90	–34.7	ICAM-1	N	CTAB	DOX	Y	MSN	N
Wei 2017[270]	16.3		170	–15.9	peptide	N	CTAB	DOX	N	MSN	N
Xu 2013[271]	6.5	109	110	0.9	N	N	CTAB	DOX	N	MSN	gelatin
Yang 2017[272]	4.8	50		–20.6	N	N	Hyper-branched polyglycerol	DOX	N	MSN	N
Yang 2016[273]	25.6		201	–32.1	N	N	CTAB	DOX	N	MSN	N
Yang 2016[204]	15.9		155		FA	N	CTAB	DOX	N	Hollow	DBA capping agent
Yang 2016[273]	25.6	140	201	–32.1	HA/CD44	N	CTAB	DOX	N	MSN	hyaluronic acid /Sodium alginate
You 2017[274]	42	100		–8.8	FA	N	CTAC	DOX	Y	MSN	PEI-PEG
Zhang 2017[275]	33.4	60	80	10	N	N	CTAB	DOX	Y	MSN	N
Zhang 2014[276]	5	48.3	61	–15.2	FA	N	CTAC	DOX	Y	MSN	N
Zhao 2018[277]	3.9		160		N	N	CTAB	DOX	N	MSN	N
Zhao 2016[278]	2.8		128		N	N	Triton-X-100	DOX	N	MSN	N
Zhou 2018[279]	20		158		Tf	N	CTAB	DOX	N	Hollow	N

TABLE 7: (*continued*)

Zhu 2017[280]	20.56		253	–11.9	VEGF	N	CTAB	DOX	N	MSN	LDH
DOX + TT											
Cao 2020[281]	20.6		187	–38.8	FA	PTT	CTAB	DOX	N	Hollow	PDA
Chai 2018[282]	47		294	5.4	N	PTT	C18TMS	DOX; MoSe2	Y	Hollow	PDA
Chen 2019[283]	15.4		169	–17.3	HA/CD44	PTT	CTAB	DOX	N	MSN	PDA
Cheng 2018[284]	15.9		223	–17.9	N	PTT	CTAB	DOX	N	MSN	CuS
Fang 2018[285]	41	120	206	–16.7	HA/CD44	PTT	C18TMS	DOX	N	Hollow	QDs
Feng 2020[286]	43		287	28.2	N	TT	CTAB	DOX	N	Hollow	ZnO caps
Gao 2018[198]	46		750		FA	AMF	CTAB	DOX	Y	Fe_3O_4	N
Jin 2018[287]	42	100		–8.8	FA	N	CTAB	DOX	Y	Gold	N
Lei 2019[288]			200	–2	N	PTT	CTAB	DOX	N	MSN	PDA
Lei 2016[289]	1.4;6.68	60	82	4.8	RGD	PTT	CTAC	DOX;ICG	Y	MSN	β-cyclodextrin
Li 2020[290]	42.9		118	21.3	N	PTT	CTAC	DOX	N	Hollow	N
Li 2020[206]	22.5	76X35		–8.5	TAT-RhB	PTT	CTAB	DOX	Y	GNR	N
Li 2019[207]	5.3	50	138	–16.3	RGD	PTT	CTAB	DOX	N	Ag_2S3 DQ	N
Li 2018[205]	60.9			–4	Her-2	PTT	Stober	DOX	N	PVP-Bi2-S3 NP	N
Lu 2018[291]	49.9	100	120	–13.2	RGD	PTT	CTAC	DOX	Y	Bi_2S_3	N
Ren 2020[193]	77.4	150		30	FA	PTT	CTAB	DOX	N	MSN	BPQDs
Wang 2019[292]	19.9		139	–13	N	PTT	CTAB	DOX	Y	Gold	N
Wang 2018[197]	68.7	95X145	600	21.4	N	PTT	CTAB	DOX	N	GNR	N
Wei 2018[208]	20.2	110	120	~ 0	N	PTT	NR	DOX	N	MSN	CuS
Yang 2020[293]	50		250	37.3	FA	PTT	CTAB	DOX	Y	Hollow	N
Zhang 2020[209]	10		168	NR	N	PDT	CTAB	DOX	N	CuS	MnO_2 cap
Zhong 2020[294]	21.8		201	–7.0	N	PTT	CTAB	DOX	N	GNR	N
DOX + PDT											
Fang 2019[295]	9.6		274	–20	N	N	Stober	DOX; Ce6	N	Hollow	N
Li 2018[296]	45.7 DOX; 11.6 PpIX		120	15	RGD	PDT	CTAC	DOX; PpIX	Y	Hollow	MSN
Liu 2017[297]			235	–18	Magnetic+ FA	PDT	CTAB	DOX	Y	Fe_3O_4	Lipid bilayer
Rao 2018[298]	16.2		116	–34	N	N	CTAB	DOX; Ce6	Y	MSN	N

TABLE 7: (*continued*)

Author	DOX LC	Size TEM	Size DLS	ZP (mV)	Target	TT/PDT	Template	Drug(s)	PEG	Core	Coated/ capped
DOX + PDT											
Su 2017[299]	39.8		108	–14.0	N	N	CTAB	DOX; Ce6	N	MSN	RBCV
Wang 2019b[300]			140	–9.2	Magnet	N	CTAB	DOX; Ce6	Y	MSN	Fe_3O_4
Xu 2020[301]	10.5; 36.8	150	200	–43	N	PDT	CTAB	DOX; Ce6	N	MSN	N
DOX + Radiotherapy (RT)											
Wang 2017[302]	61.7	225X110			FA	N	CTAB	DOX	Y	GNR	N
DOX + Non-DOX drug											
Chen 2016[303]		130	184	64.5	N	N	CTAB	DOX; shRNA	N	MSN	shABCG2
Ding 2020[304]	4.1; 7.6	130	263	–8.3	peptide	N	CTAC	DOX; α-TOS	N	MSN	carboxymethyl chitin
Fang 2018[65]	32.6		102	–28.6	HA/CD44	N	Triton-X-100	DOX; Quercetin	N	MSN	N
He 2020[305]	8.3	120	166		N	N	CTAB	DOX; Curcumin	N	MSN	N
He 2016[306]		80		–38	N	N	Stober	DOX; erlotinib	N	MSN	SPC/ HHG2C18/ Chol
Hu 2017[307]	5.1		159	14	N	N	CTAC	DOX; alpha-TOS	Y	MSN	N
Kankala 2020[308]		100			N	N	CTAB	DOX:Platinum	N	MSN	Chitosan
Kong 2017[309]	11.6		243	–12	N	N	CTAC	DOX; IL2; ATRA	Y	Hollow	N
Li 2018[210]	2.9		190	–21.3	FA	PTT	CTAB	DOX; DNA	N	Ag_2S QD	N
Li 2017[211]	21		327	52	N	N	CTAB	DOX; shRNA	N	SiO_2	N
Li 2017[211]			204	–10.8	EpCAM aptamer	N	CTAB	DOX; DM1	Y	MSN	hydrochloride dopamine
Liu 2018[310]	8.2 DOX	100	183	23.3	WL8 peptide	N	CTAB	DOX; miRNA-145	Y	MSN	PEI
Nie 2020[212]	25.8; 20.2		189	–23.8	N	N	CTAB	DOX; MPH	Y	MSN	CCM
Ramasamy 2018[311]	8.1		100	–35.0	N	PTT	CTAB	DOX; Se	N	GNR (40X9 nm)	MSN
Su 2014[312]	2.75		108	–11.2	EGF	N	none	DOX; CA-4	Y	liposome	SiO_2
Wang 2018[64]	6	66	100	19.2	FA	PTT	Triton-X-100	DOX; Se	Y	MSN	N
Xie 2020[313]	2.15; 10.89	37	200	35.3	N9	N	CTAC	DOX; NuBCP9	N	MSN	G5
Xing 2020[213]	11.6		130	–18.2	N	PTT	CTAB	DOX; PTX	N	Gold	N
Xue 2017[314]			262	12.0	N	N	CTAC	DOX; miR-375	Y	MSN	lipid

TABLE 7: (*continued*)

Yin 2018[315]	12.1 DOX	93.9	107	–33.6	iRGD	N	CTAB	DOX; let-7a mRNA	Y	$ZnFe_2O_4$	PEI
Zhang 2019[316]	58.1; 54.2	300X100		–15.4	HA/CD44	N	CTAB	DOX; berberine	N	MSN	N
Zhang 2014[317]	6	165			Aptamer	N	CTAB	DOX; CytC	N	MSN	N
Zhao 2017[214]	23.2	110	124	–47.4	N	N	CTAB	DOX; siRNA	N	MSN	N
Non-DOX drug w/o PDT or TT											
Ansari 2018[318]	16.2	19			magnetic	N	Pluronic F127 + CTAB	Epirubicin	N	Fe_3O_4	N
Babaei 2020[319]	32		125	1	AS1411 DNA aptamer	N	CTAB	Campothecin; iSur shRNA	Y	MSN	N
Che 2015[320]	9.7		273	–5			CTAB	paclitaxel	N	Fe_3O_4 (10 nm)	gelatin
Chen 2020[321]	15.3		197	–23.7	N	N	CTAC	paclitaxel	Y	Hollow	PDA
Chen 2019[322]	8.7; 7.6		128	–26.4	N	N	CTAB	5-FU + ß-lap NQO1 inhibitor	Y	MSN	N
Choi 2016[323]	21		120	1	N	N	CTAB	axitinib; celas	Y	MSN	Lipid bilayer
Ding 2015[324]	35.7	100	180	10	N	N	CTAC	(-)-epigallocatechin-3-gallate	N	MSN	N
Du 2019[325]	7.63	40			HA/CD44	N	CTAC	PTX	N	MSN	Poly (L-lysine)
Fei 2017[326]	6.8	152	150	20	RGD	N	CTAB	ATO	Y	Hollow	lipid
Feng 2019[327]	56; 84	160	230	–36	N	N	CTAB	Evodiamine; Berberine	Y	MSN	NIPAM
Gao 2019[328]	3.2; 32.2	180			N	N	CTAB	paclitaxel; curcumin	Y	MSN	Lipid bilayer
Goto 2017[329]	7.9		105	–2.8	N	N	CTAB	GEM	Y	MSN	PICsomes polymeric vessel
Hanafi-Bojd 2015[330]	8.4		383	–7	N	N	CTAB	Epirubicin	Y	MSN	N
Hanafi-Bojd 2016[331]			248	–20.2	N	N	Pluronic F127 + CTAB	EPI	Y	MSN	N
Hu 2019[332]	9.4		155	–23	N	N	CTAB	resveratrol	N	MSN	N
Huo 2017[333]	16.6; 15.9		255	–27.6	N	N	CTAB	Gox; Fe_3O_4	Y	MSN	N
Ke 2018[334]	32	180	220	–36.0	transferrin Tf	N	CTAB	sorafenib	N	Hollow	N
Kundo 2020[335]	12.6		414	–36.6	FA	N	CTAB	umbelliferone/ coumarin	N	MSN	poly acrylic acid
Li 2020[336]	5.5; 1.8		299	–51.6	FA	N	CTAB	pactlitaxel; TanIIA	Y	MSN	Lipid bilayer

TABLE 7: (*continued*)

Author	DOX LC	Size TEM	Size DLS	ZP (mV)	Target	TT/PDT	Template	Drug(s)	PEG	Core	Coated/ capped
Non-DOX drug w/o PDT or TT											
Li 2020[217]	7.5		90	–12.2	asialoglycoprotein receptor	N	CTAB	irinotecan (CPT-11)	N	MSN	lipid
Li 2019[337]	27.2; 32.7	365	428	–15.9; 33.1	N	N	CTAB	Losartan;GEM	N	Fe_3O_4	N
Liu 2020[338]	5.3; 5.1		227		chondroitin sulfate	N	CTAB	paclitaxel; quercetin	N	MSN	chondroitin sulfate
Liu 2020[338]	4.23; 2.46			neutral	FA	N	CTAB	norcantharidin (DM-NCTD); ABT-737	N	MSN	Lipid Bilayer
Liu 2019[149]	40	78	130	–11	N	N	CTAC	irinotecan	Y	MSN	N
Liu 2018[339]	10; 2.2	130	156	–2.4	N	N	CTAB	GEM; Pt	N	MSN	Chitosan
Lu 2010[340]	1		130		FA	N	CTAB	CPT	N	MSN	N
Meng 2015[341]	25; 2.5	75	101	–27.2	N	N	CTAC	GEM; PTX	Y	MSN	Liposome
Mu 2017[342]	21.5	160		–13.8	N	N	CTAB	sorafenib	Y	MSN	PLH-PEG
Murugan[343]	15.5; 20.1	50	48	18.4	RGD/TAT	N	CTAC	Topotecan (TPT)/ metformin (MT)	N	MSN	N
Pan 2017[344]	7.5	136	199	–8.7	RGD	N	CTAB	5-FU	N	MSN	N
Paredes 2020[345]		116	323	6.4	FA	N	CTAB	(MSN-AP-Sn)	N	MSN	N
Qu 2018[346]			110		FA	N	CTAB	Topotecan (TPT)	N	MSN	N
Ren 2018[347]		100			N	N	CTAB	Campothecin	N	MSN	MnOx-SPION
Tang 2013[348]	14.8	46	73		N	N	Stober	Camptothecin	Y	MSN	N
Tao 2019[349]	8.2		142	–13.9	N	N	CTAB	ATO	Y	MSN	Polyacrylic acid
Wang 2017[350]	NR	90	150	NR	LA	N	CTAB	PTX	Y	MSN	N
Wu 2020[351]	20.3				N	N	CTAB	CaO2	N	Hollow	polyacrylic acid
Xu 2017[352]	24	100			FA	N	CTAB	PTX	Y	MSN	N
Zhang[353]	8.6; 3.2	45	260	5.0	N	N	Igepal CO-520	cisplatin; acriflavine	Y	cisplatin	N
Zhao 2017[354]	20.5	80	211	7.7	lactobionic acid	N	CTAC	sorafenib	N	MSN	N
	21.3	80	197	6.3	lactobionic acid	N	CTAC	ursolic acid	N	MSN	N

TABLE 7: (*continued*)

Non-DOX chemo + TT and/or PDT and/or RT											
Huang 2020[355]	NR		115	–10.5		N	NR	quercetin	N	MSN	cancer cell membrane
Hu 2019[356]	16.7	141X66		–20.4	AE105-peptide	TT	CTAB	Cisplatin	N	GNR	PEI
Li 2019[357]	0.15 MB; 0.25 Pt	45		39.0	FA	PDT	CTAB	MB; Pt	N	MSN	Protein shell
Li 2019[218]	19.1	225X110		4.7	FA	PTT	CTAB	Berberine	Y	GNR	N
Liu 2012[216]			185	–9.5	Tf	PTT	Stober	Docetaxel	Y	SiO_2	SiO_2
Luo 2016[358]	1.9	54X24		–13.4	LA	TT+PDT	CTAB	Cisplatin; AIPsS4	Y	GNR	SiO_2 + β-cyclodextrin
Shao 2020[219]	15 CQ		235		N	PTT	CTAB	Chloroquine; Glucose oxidase	N	PDA polydopamine	N
Sun 2019[220]	10	70		24.0	N	PTT	CTAB	Zoledronate	N	GNR	N
Thapa 2017[222]	10 IR820		160	–30.0	cyclosporine	PDT	CTAB	bortezomib	Y	MSN	Lipid bilayer
Wang 2020[359]	6.23	135		–32.6	CCM	PTT	CTAB	irinotecan	N	ZGGO	CCM
Wang 2019[360]	8.1		260		FA	PTT	CTAB	tirapazamine TPZ	Y	MSN	N
Wu 2019[221]	46.1; 13.8		115	–8.7	N	PTT	CTAC	ICG; paclitaxel	Y	Hollow	N
Xing 2018[361]	19.9	100X250			Mag	MTT	CTAB	curcumin	Y	Fe_3O_4	MSN
Zhang 2019[362]	3.5; 1.5		220	–18.5	EGFR	PTT	CTAC	erlotinib; ICG	N	MSN	ZnO QD cap
Zhao 2017[354]	24.6	206X112		–21.4	Tf	PDT	CTAB	GEM	Y	MSNR	Gold
Studies with PDT only											
Brezániová 2018[363]	20	44	174		N	PDT	CTAC	temoporfin	N	MSNN	
Du 2020[364]	19.7	275	320		N	PDT	C18TMS	Ce6; MnOx	Y	Hollow	N
Ma 2018 Ru@ MSNs-20[148]	23.7	20	24	37.1	FA-PEI	N	CTAB	RuPOP	N	MSN	N
Ma 2018 Ru@ MSNs-40[148]	21.1	40	44	18.8	FA-PEI	N	CTAB	RuPOP	N	MSN	N
Ma 2018 Ru@ MSNs-80[148]	17.6	80	106	21.2	FA-PEI	N	CTAB	RuPOP	N	MSN	N

TABLE 7: (*continued*)

Author	DOX LC	Size TEM	Size DLS	ZP (mV)	Target	TT/PDT	Template	Drug(s)	PEG	Core	Coated/ capped
TT only (no chemo)											
Yang 2019[365]	57.2		210	–28.6	N	PDT	CTAB	TPPS4 (NIR PTT sensitizer)	N	MSNR	Gold
Zhang 2020[366]					N	PDT	CTAB	N/A	N	GNR	N
TT and PDT (no chemo)											
Liu 2018[367]	6	79X37		–9.4	N	PDT + PTT	CTAB	ICG	Y	GNR (58X16 nm)	CS(DMA)-PEG
Wang 2019[368]	10.8	250X100	300	–20.0	Cancer Cell Membrane	TT + PDT	CTAB	Ce6	N	Fe_3O_4	MCF-7 cell-derived CM
Zhang 2020[369]	11 Ce6		204	–26.5	FA	PTT + PDT	CTAB	Ce6; CuS	Y	MSN	PDA

TABLE 8: Tumor inhibition ratio for MSN formulations with DOX without TT, PDT, or RT

Study	Group	Target	Ex stim	Tumor	Mouse	Drug	Dose (mg/kg)	Start TV (mm^3)	%TIR
Chen 2020[199]	DOX	N/A	N/A	4T1 mouse epithelial breast	Balb/c	DOX	7 × 5	70	29
	DOX@HMSN-SS-PLL	—	—	—	—	—	—	—	47
	DOX@ HMSN-SS-PLL(sa)	—	—	—	—	—	—	—	67
	DOX@ HMSN-SS-PLL(cit)	—	—	—	—	—	—	—	86
Chen 2020[245]	DOX@MSNs	A-CAIX Ab	N/A	4T1 mouse epithelial breast	Balb/c	DOX	4 × 6	360	39
	DOX@MSNs-CAIX	—	—	—	—	—	—	234	62
Chen 2016[195]	DOX@MSN-ss-COOH	HA/CD44	N/A	4T1 mouse epithelial breast	—	DOX	7 × 3	30	29
	DOX	—	—	—	—	—	—	—	37
	DOX@MSN-ss-GHA	—	—	—	—	—	—	—	58
Cheng 2017[246]	MSNs@PDA−PEG−FA	FA	N/A	HeLA human cervical	nude	DOX	4 × 5	80	14
	DOX	—	—	—	—	—	—	—	56
	MSNs-DOX@ PDA−PEG	—	—	—	—	—	—	—	73
	MSNs-DOX@ PDA−PEG−FA	—	—	—	—	—	—	—	84
Cheng 2017[247]	drug-free MSNs@ PDA-TPGS	N/A	N/A	A549- human alveolar carcinoma	—	DOX	5 × 5	80	21
	DOX	—	—	—	—	—	—	—	60
	MSNs-DOX@ PDA-PEG	—	—	—	—	—	—	—	76
	MSNs-DOX@ PDA-TPGS	—	—	—	—	—	—	—	90
Dai 2015[248]	HPSN	FA	N/A	HepG2 human liver	nude	DOX	20 × 3	50	5
	DOX	—	—	—	—	—	—	—	38

TABLE 8: (*continued*)

Study	Group	Target	Ex stim	Tumor	Mouse	Drug	Dose (mg/kg)	Start TV (mm^3)	%TIR
	DOX@HPSN	—	—	—	—	—	—	—	46
	DOX@ HPSN−Salphdc−FA	—	—	—	—	—	—	—	68
Fang 2019[249]	DOX	HA/CD44	N/A	4T1 mouse epithelial breast	Balb/c	DOX	7 × 1	50	83
	HA-MSN	—	—	—	—	—	—	—	6
	DOX-HA-MS	—	—	—	—	—	—	—	61
	DOX-NH2-MSN	—	—	—	—	—	—	—	72
	DOX-HA-MSN	—	—	—	—	—	—	—	80
Gao 2012[201]	FA-SN	FA	N/A	HeLA human cervical	nude	DOX	4 × 10	100	4
	DOX	—	—	—	—	—	—	—	82
	DOX-SN	—	—	—	—	—	—	—	63
	DOX-FA-SN	—	—	—	—	—	—	—	96
Han 2016[194]	bare CSNP	TAT	N/A	H22 murine hepatic	Kumming	DOX	4 × 2	110	5
	DOX	—	—	—	—	—	—	—	46
	CSNP w/non-cleavable PEG	—	—	—	—	—	—	—	68
	CSNP w/non-charge-reversible shell	—	—	—	—	—	—	—	68
	CSNP w/o PEG	—	—	—	—	—	—	—	76
	CSNP w/o GAL	—	—	—	—	—	—	—	80
	CSNP w/o TAT	—	—	—	—	—	—	—	80
	CSNP (low dose)	—	—	—	—	—	—	—	86
	CSNP w TAT	—	—	—	—	—	—	—	92
Hou 2017[250]	silica@PDA-PEG	FA	N/A	4T1 mouse epithelial breast	Balb/c	DOX	7 × 5	NR	9
	silica@PDA/DOX-PEG	—	—	—	—	—	—	—	24
	silica@PDA/ DOX-PEG-FA	—	—	—	—	—	—	—	62

TABLE 8: (*continued*)

Hou 2016[251]	DOX	N/A	N/A	PC3 Human prostate	nude	DOX	6	350	71
	HMON	—	—	—	—	—	—	—	79
Huang 2017[252]	HMSNs-DOX	lactobionic acid	N/A	HepG2 human liver	nude	DOX	20 × 3	50	15
	DOX	—	—	—	—	—	—	—	49
	HMSN@DOX	—	—	—	—	—	—	—	60
	HMSN-S-S-CPA-CytC-LA@DOX	—	—	—	—	—	—	—	83
Jiang 2018[70]	placebo	N/A	N/A	EMT6 murine mammary	Balc/c	DOX	5 × 10	300	—
	DOX	—	—	—	—	—	—	—	10
	SiNPs/DOX	—	—	—	—	—	—	—	54
Kang 2019[253]	DOX	HA/CD44	N/A	4T1 mouse epithelial breast	NR	DOX	5	86	18
	DOX@MAN/HAP	—	—	—	—	—	—	—	38
	HA-DOX@MSN/HAP	—	—	—	—	—	—	—	63
	oHA-DOX@MSN/HAP	—	—	—	—	—	—	—	92
Khatoon 2016[254]	DOX	N/A	N/A	SCC7 murine squamous cell	NR	DOX	4 × 5	160	27
	DOX-MSN	—	—	—	—	—	—	—	61
	DOX-Z-MSN	—	—	—	—	—	—	—	76
Li 2018[196]	Peptide- Fe_3O_4@MSN/DOX	peptide + mag	N/A	HT-1080 human fibrosarcoma	nude	DOX	7 × 1.6	100	76
	Peptide-Fe_3O_4@MSN/DOX + Magnet	—	—	—	—	—	—	—	84
Li 2018[147]	DOX	N/A	N/A	H22 murine hepatic	Kunming	DOX	3 × 4	100	70
	MSN5	—	—	—	—	—	—	—	24
	DOX/MSN2	—	—	—	—	—	—	—	85
	DOX/MSN5	—	—	—	—	—	—	—	97

TABLE 8: (*continued*)

Study	Group	Target	Ex stim	Tumor	Mouse	Drug	Dose (mg/kg)	Start TV (mm^3)	%TIR
Li 2017[215]	DOX	TSH	N/A	FTC-133 human follicular thyroid carcinoma	NOD SCID	DOX	3 × 5	212	47
	SiO_2@DOX	—	—	—	—	—	—	—	67
	TSH-SiO_2@DOX	—	—	—	—	—	—	—	82
Li 2014[255]	DOX	N/A	N/A	HeLA human cervical	nude	DOX	6 × 4	7	40
	DOX-loaded LbL-MS	—	—	—	—	—	—	—	63
Lin 2018[63]	DOX	Biotin	N/A	HTC-116 human colorectal	nude	DOX	7 × 5	100	11
	DOX/SLN-PEG	—	—	—	—	—	—	—	32
	DOX/SLN-PEG-Biotin	—	—	—	—	—	—	—	68
Liu 2020[256]	RCMSN	N/A	N/A	MCF/ADR	nude	DOX	4 × 5	100	–4
	DOX	—	—	—	—	—	—	—	–7
	DOX@UCMSN	—	—	—	—	—	—	—	61
	DOX@RCMSN	—	—	—	—	—	—	—	70
Liu 2019[257]	DOX	HA/CD44	N/A	A549- human alveolar carcinoma	nude	DOX	8 × 5	100	19
	DMMA-MSN/DOX	—	—	—	—	—	—	—	47
	HA-MSN/DOX	—	—	—	—	—	—	—	60
	HA-JMSN/ DOX-DMMA	—	—	—	—	—	—	—	79
Liu 2019[258]	MSN@$CaCO_3$@CM	N/A	N/A	LNCaP-AI	nude	DOX	3 × 5	100	0
	DOX/MSN@$CaCO_3$@ CM	—	—	—	—	—	—	—	71
	DOX	—	—	—	—	—	—	—	38
Liu 2017[259]	SMSN	N/A	N/A	MCF-7/MDR human breast	nude	DOX	4 × 5	100	–3
	DOX	—	—	—	—	—	—	—	28

TABLE 8: (*continued*)

	DOX@SMNS	—	—	—	—	—	—	—	71
Liu 2016[260]	HMSN	N/A	N	HepG2 human liver	nude	DOX	9 × 3	100	14
	HMSNs-b-CD/ Ada-PEG	—	—	—	—	—	—	—	7
	DOX	—	—	—	—	—	—	—	51
	HMSNs@DOX	—	—	—	—	—	—	—	62
	HMSNs-b-CD/Ada-PEG@DOX	—	—	—	—	—	—	—	87
Meng 2011[200]	NP3	N/A	N/A	KB-31 human cervical	nude	DOX	3 × 4	15	–11
	DOX	—	—	—	—	—	—	—	70
	DOX-NP3	—	—	—	—	—	—	—	85
Palanikumar 2018[261]	PMSN	N/A	N/A	SCC7 murine squamous cell	nude	DOX	6 × 2	200	8
	DOX	—	—	—	—	—	—	—	12
	DOX-BCP	—	—	—	—	—	—	—	4
	DOX-PMSN	—	—	—	—	—	—	—	73
Qiao 2019[262]	HRN	N/A	N/A	HepG2 human liver	nude	DOX	1 × 5	40	–4
	DOX	—	—	—	—	—	—	—	58
	DOX-HRN	—	—	—	—	—	—	—	84
Ramaya 2017[263]	Au@SiO_2-CS-FA	FA	N/A	EAC murine Ehrlich ascites carcinoma	Balb/c	DOX	14 × 1	140	3
	Au@SiO_2-DOX-CS	—	—	—	—	—	—	150	26
	Au@SiO_2-DOX-CS-FA	—	—	—	—	—	—	140	71
	DOX	—	—	—	—	—	—	140	44
	Lipodox	—	—	—	—	—	—	140	53
Shao 2016[264]	M-MSN-PEG	mag	N	H22 murine hepatic	ICR	DOX	5 × 1	68	5
	DOX	—	—	—	—	—	—	—	94

TABLE 8: (*continued*)

Study	Group	Target	Ex stim	Tumor	Mouse	Drug	Dose (mg/kg)	Start TV (mm^3)	%TIR
	M-MSN-DOX-M-	—	—	—	—	—	—	—	23
	M-MSN-DOX-M +	—	—	—	—	—	—	—	51
Shen 2019[265]	DOX	N/A	N/A	SMMC-7721 human liver	nude	DOX	7 × 5	100	36
	DOX-POMSN	—	—	—	—	—	—	—	71
Si 2020[266]	MSN	MUC-1	N/A	MCF-7 human breast	nude	DOX	7 × 5	80	3
	DOX	—	—	—	—	—	—	—	35
	NAN	—	—	—	—	—	—	—	28
	SMRAN	—	—	—	—	—	—	—	49
Tian 2016[267]	DOX	Tf	N	A549- human alveolar carcinoma	Balb/c	DOX	4 × 5 i.p.	100	44
	DOX-HSMN-SH	—	—	—	—	—	—	—	32
	DOX-HSMN-s-s-Tf	—	—	—	—	—	—	—	71
Turan 2019[202]	TMZ	CREKA	RF	GL261 murine glioma cranial	nude	DOX	3 × 5	15	–30
	TMZ (+RF)	—	—	—	—	—	—	—	0
	DOX (+RF)	—	—	—	—	—	—	—	34
	Fe@MSN -DOX(+RF)	—	—	—	—	—	—	—	–30
	Targeted Fe@MSN-DOX (–RF)	—	—	—	—	—	—	—	58
	Targeted Fe@MSN-DOX (+RF)	—	—	—	—	—	—	—	95
Turan 2019[203]	DOX RF	RGD/ CREKA	RF	GL261 murine glioma cranial	nude	DOX	3 × 2	5	0
	RGD-NP no RF + DOX	—	—	—	—	—	3 × 2	—	–71
	CREKA-NP no RF + DOX	—	—	—	—	—	3 × 5	—	59
	CREKA-NP RF + DOX	—	—	—	—	—	3 × 5	—	90
	RGD-NP RF + DOX	—	—	—	—	—	3 × 2	—	81

TABLE 8: (*continued*)

	RGD-NP + CREKA-NP RF + D	—	—	—	—	—	3 × 7	—	99
Wan 2020[268]	DOX	N/A	N/A	4T1 mouse epithelial breast	Balb/c	DOX	1 × 5	100	37
	DOX@MMSN-SS-PEI	—	—	—	—	—	—	—	56
	DOX@ MMSN-SS-PEI-cit	—	—	—	—	—	—	—	87
Wang 2019[269]	DOX	ICAM-1	N	MDA-MB-231	nude	DOX	3 × 10	NR	16
	DOX@PMO-Cy5.5	—	—	—	—	—	—	—	27
	DOX@ PMO-Cy5.5-ICAM	—	—	—	—	—	—	—	60
Wei 2017[270]	DOX	peptide	N/A	HT-1357 human Bladder	nude	DOX	4 × 10	80	48
	DOX-MSN@PDA	—	—	—	—	—	—	—	66
	DOX-MS@PDA-PEP	—	—	—	—	—	—	—	88
Xu 2013[271]	MSN@Gel	N/A	N/A	HT-29 human colorectal	Balc/c nude	DOX	4 × 10	60	–5
	DOX	—	—	—	—	—	—	—	50
	DOX-MSN	—	—	—	—	—	—	—	67
	DOX-MSN@Gel	—	—	—	—	—	—	—	84
Yang 2017[272]	DOX	N/A	N/A	MCF-7 human breast	nude	DOX	5 × 1	25	38
	PGSN-DOX	—	—	—	—	—	—	—	43
Yang 2016[273]	DOX	N/A	N/A	MCF-7/MDR human breast	nude	DOX	5 × 5	57	33
	DOX/HHS-MSN	—	—	—	—	—	—	—	77
	DOX/HH-MSN	—	—	—	—	—	—	—	65
	DOX/SHS-MSN	—	—	—	—	—	—	—	53
Yang 2016[204]	HMS	FA	N	HeLA human cervical	nude	DOX	1 × 8	65	6
	DOX	—	—	—	—	—	—	—	46
	HMS@FTD	—	—	—	—	—	—	—	95

TABLE 8: (*continued*)

Study	Group	Target	Ex stim	Tumor	Mouse	Drug	Dose (mg/kg)	Start TV (mm^3)	%TIR
Yang 2016[273]	DOX	HA/CD44	N/A	MCF-7/ADR	nude	DOX	5 × 5	50	33
	DOX/SHS-MSN	—	—	—	—	—	—	—	53
	DOX/HH-MSN	—	—	—	—	—	—	—	66
	DOX/HHS-MSN	—	—	—	—	—	—	—	78
You 2017[274]	DOX	FA	N/A	CNE2 nasopharyngeal	NR	DOX	12 × 4	200	39
	MSNR-DOX (2)	—	—	—	—	—	—	—	45
	MSNR-DOX (4)	—	—	—	—	—	—	—	71
Zhang 2017[275]	DOX	N/A	N/N	MCF-7	nude	DOX	3 × 7.5	200	26
	DOX@ MONs-Cy5.5-PEG	—	—	—	—	—	—	—	49
	DOX@ MONs-Cy5.5-PHLIP	—	—	—	—	—	—	—	81
Zhang 2014[276]	DOX	FA	N/A	MDA-MB-231 human breast	nude	DOX	3 × 1.5	7.5	12
	DOX@PEG-MSNPs48-CD-PEG	—	—	—	—	—	—	—	30
	DOX@PEG-MSNPs48-CD-PEG-FA	—	—	—	—	—	—	—	80
	PEG-MSNPs72	—	—	—	—	—	—	—	—
	PEG-MSNPs100	—	—	—	—	—	—	—	—
Zhoa 2018[277]	MSN + TPGS	N/A	N/A	MCF-7/MDR human breast	SCID	DOX	5	100	1
	DOX	—	—	—	—	—	—	—	15
	DOX@MSN	—	—	—	—	—	—	—	30
	DOX@MSN-TPGS	—	—	—	—	—	—	—	65
Zhoa 2016[278]	DOX	N/A	N/A	HepG2 human liver	nude	DOX	7 × 5 s.c.	100	40
	DOX-substrate/SSLN	—	—	—	—	—	—	—	73

TABLE 8: (*continued*)

Zhou 2018[279]	HMSN	Tf	N/A	MDA-MB-231 human breast	nude	DOX	7 × 1	110	3
	DOX	—	—	—	—	—	—	—	51
	HMSN@DOX	—	—	—	—	—	—	—	73
	HMSN-S-S-Tf@DOX	—	—	—	—	—	—	—	86
Zhu 2017[280]	SiO_2@LDH	VEGF (Avastin)	N/A	SH-SY5Y	nude	DOX	7 × 5	150	16
	DOX	—	—	—	—	—	—	—	72
	SiO_2@LDH-DOX	—	—	—	—	—	—	—	34
	SiO_2@LDH-Bev	—	—	—	—	—	—	—	11
	SiO_2@LDH-Bev-DOX	—	—	—	—	—	—	—	59

TABLE 9: Tumor inhibition ratio for MSN formulations with DOX with TT, PDT, or RT

Study	Group	Target	Ex stim	Tumor	Mouse	Drug	Dose (mg/kg)	Start TV (mm^3)	%TIR
DOX + thermal therapy									
Cao 2020[281]	DOX	FA	NIR	H22 murine hepatic	Kunming	DOX	1 × 5	400	15
	DOX-HPC	—	—	—	—	—	—	—	26
	DOX-HPCF	—	—	—	—	—	—	—	49
	HPC + NIR	—	—	—	—	—	—	—	39
	HPCF + NIR	—	—	—	—	—	—	—	64
Chai 2018[282]	DOX	N/A	NIR	MDA-MB-231	nude	DOX	3 × 7.5	100	12
	PM@HMSNs + laser	—	—	—	—	—	—	—	36
	PM@HMSNs-DOX	—	—	—	—	—	—	—	42
	PM@HMSNs-DOX + laser	—	—	—	—	—	—	—	74
Chen 2019[283]	DOX	HA/CD44	NIR	HeLA human cervical	nude	DOX	1 × 3	100	25
	MSNs-PDA	—	—	—	—	—	—	—	50
	MSNs-PDA-HA	—	—	—	—	—	—	—	58
	MSNs-PDA-HA + NIR	—	—	—	—	—	—	—	92
Cheng 2018[284]	DOX	N/A	NIR	S10 muring sarcoma	nude	DOX	9 × 5	100	25
	YSPMO(DOX)@CuS	—	—	—	—	—	—	—	58
	YSPMO(DOX)@CuS + NIR	—	—	—	—	—	—	—	83
Fang 2018[285]	DOX	HA/CD44	NIR	HeLA human cervical	nude	DOX	3 × 5	100	23
	HA-HMCN@GQDs + laser	—	—	—	—	—	—	—	47
	HA-HMCN(DOX)@GQD	—	—	—	—	—	—	—	52
	HMCN(DOX)@GQDs + laser	—	—	—	—	—	—	—	73
	HA-HMCN(DOX)@ GQDs + laser	—	—	—	—	—	—	—	86

TABLE 9: (*continued*)

Feng 2020[286]	Saline + NIR	N/A	NIR	4T1 mouse epithelial breast	Balb/c	DOX	1 × 10	175	–7
	DOX	—	—	—	—	—	—	—	18
	HMC-SS-Zno + NIR	—	—	—	—	—	—	—	51
	Dox/HMC-SS-ZnO	—	—	—	—	—	—	—	45
	Dox/HMC-SS-ZnO + NIR	—	—	—	—	—	—	—	94
Gao 2018[198]	DOX	FA	AMF	MCF-7 human breast	Balb/c	DOX	12 × 1.5	NR	27
	IOMSN@uIO(DOX)	—	—	—	—	—	—	—	54
	IOMSN@uIO(DOX)-FA	—	—	—	—	—	—	—	82
	IOMSN@uIO(DOX)-FA + AMF	—	—	—	—	—	—	—	88
Jin 2018[287]	MSN-Fe-AuNP	N/A	NIR	WHU-HN6-human squamous	nude	DOX	1 × 10	100	22
	DOX	—	—	—	—	—	—	—	35
	MSN-Fe-AuNP-DOX	—	—	—	—	—	—	—	60
	MSN-Fe-AuNP + NIR	—	—	—	—	—	—	—	83
	MSN-Fe-AuNP-DOX + NIR	—	—	—	—	—	—	—	93
Lei 2019[288]	MSN-SS-PDA/DOX	N/A	NIR	4T1 mouse epithelial breast	Balb/c	DOX	5 × 10	125	23
	MSN-SS-PDA + NIR	—	—	—	—	—	—	—	23
	DOX	—	—	—	—	—	—	—	77
	MSN-SS-PDA/DOX + NIR	—	—	—	—	—	—	—	91
Lei 2016[289]	I/D@MSN + NIR	RGD	NIR	4T1 mouse epithelial breast	Balb/c	DOX;ICG	1 × (1.15; 5)	100	93
	ICG/DOX + NIR	—	—	—	—	—	—	—	70
	PBS + NIR	—	—	—	—	—	—	—	14
	I/D@MSN	—	—	—	—	—	—	—	35
	ICG/DOX	—	—	—	—	—	—	—	22

TABLE 9: (*continued*)

Study	Group	Target	Ex stim	Tumor	Mouse	Drug	Dose (mg/kg)	Start TV (mm^3)	%TIR
Li 2020[290]	DOX	N/A	NIR	Saos-2	nude	DOX; Cu	1 × (7.5; 4.8)	100	32
	CuS@BSA-HMONs + laser	—	—	—	—	—	—	—	46
	CuS@BSA-HMONs-DOX	—	—	—	—	—	—	—	65
	CuS@BSA-HMONs-DOX + laser	—	—	—	—	—	—	—	94
Li 2020[206]	NIR	TAT-RhB	NIR	CT26	Balb/c		1 × 2	75	–8
	DOX	—	—	—	—	—	—	—	49
	AuNR@SiO_2/DOX + NIR	—	—	—	—	—	—	—	60
	AuNP@SiO_2-TAT/DOX	—	—	—	—	—	—	—	58
	AuNR@SiO_2-TAT-NIR	—	—	—	—	—	—	—	81
	AuNR@SiO_2-TAT/DOX + NIR	—	—	—	—	—	—	—	99
Li 2019[207]	PBS + NIRX1	RGD	NIR	HeLA human cervical	nude	DOX	1 × 5.3	200	11
	DOX	—	—	—	—	—	—	—	44
	Ag_2S@M/D-P-RGD	—	—	—	—	—	—	—	26
	Ag_2S@M-P-RGD + NIRX1	—	—	—	—	—	—	—	77
	Ag_2S@M/D-P-RGD + NIRX1	—	—	—	—	—	—	—	100
	AG_2S@M-P-RGD + NIRX3	—	—	—	—	—	—	—	86
	Ag_2S@M/D-P-RGD + NIRX3	—	—	—	—	—	—	—	99
Li 2018[205]	DOX + NIR	Her-2	NIR	SKBR-3 human breast	nude	DOX	1 × 1.2	50	26
	Tam-Bi_2S_3@mPS/DOX	—	—	—	—	—	—	—	57
	Bi_2S_3@mPS/DOX + NIR	—	—	—	—	—	—	—	71
	Tam-Bi_2S_3@mPS + NIR	—	—	—	—	—	—	—	82

TABLE 9: (*continued*)

	Tam-Bi_2S_3@mPS/DOX + NIR	—	—	—	—	—	—	—	100
Lu 2018[291]	DOX + NIR	RGD	NIR	UMR-106 rat osteosarcoma	nude	DOX	1 × 2.5	110	2
	RGD-Bi_2S_3@MSN/DOX	—	—	—	—	—	—	—	38
	Bi_2S_3@MSN/DOX + NIR	—	—	—	—	—	—	—	68
	RGD-Bi_2S_3@MSN + NIR	—	—	—	—	—	—	—	88
	RGD-Bi_2S_3@MSN/DOX + NIR	—	—	—	—	—	—	—	95
Ren 2020[193]	DOX	FA	NIR	H22 murine hepatic	Balb/c	DOX	1 × 7.7	150	51
	FMSN@BP	—	—	—	—	—	—	—	1
		—	—	—	—	—	—	—	—
	FMSN@BP-DOX	—	—	—	—	—	—	—	—
	FMSN@BP-DOX-FA	—	—	—	—	—	—	—	—
	FMSN@BP-FA + NIR	—	—	—	—	—	—	—	—
	FMSN@BP-DOX + NIR	—	—	—	—	—	—	—	—
	FMSN@BP-DOX-FA + NIR	—	—	—	—	—	—	—	—
Wang 2019[292]	DOX	N/A	NIR	4T1 mouse epithelial breast	Balb/c	DOX	1 × 5	70	13
	GNR@P-SiO_2/DOX	—	—	—	—	—	—	—	20
	GNR@P-SiO_2 + NIR	—	—	—	—	—	—	—	53
	GNR@P-SiO_2/DOX + NIR	—	—	—	—	—	—	—	73
Wang 2018[197]	GNR/Ppy/m-SiO_2 + Laser	N/A	NIR	CT26 mounse colon	Balb/c	DOX	1 × 5	100	97
	GNR/Ppy/m-SiO_2-DOX	—	—	—	—	—	—	—	19
	GNR/Ppy/m-SiO_2-DOX + Laser	—	—	—	—	—	—	—	99
Wei 2018[208]	CuSNDs	N/A		MDA-MB-231	nude	DOX; Cu	NR	NR	8
	DOX	—	—	—	—	—	—	—	23
	MDN	—	—	—	—	—	—	—	15
	CuSNDs + NIR	—	—	—	—	—	—	—	46

TABLE 9: (*continued*)

Study	Group	Target	Ex stim	Tumor	Mouse	Drug	Dose (mg/kg)	Start TV (mm^3)	%TIR
	MDN + NIR	—	—	—	—	—	—	—	100
Wei 2018[208]	CuSNDs	N/A	—	HepG2 human liver	nude	DOX; Cu	NR	NR	44
	DOX	—	—	—	—	—	—	—	38
	MDN	—	—	—	—	—	—	—	31
	CuSNDs + NIR	—	—	—	—	—	—	—	44
	MDN + NIR	—	—	—	—	—	—	—	97
Yang 2020[293]	Saline + NIR	FA	NIR	HeLA human cervical	nude	DOX	3 × 5	100	8
	FaPCH	—	—	—	—	—	—	—	3
	FaPCH + NIR	—	—	—	—	—	—	—	37
	DOX	—	—	—	—	—	—	—	42
	FaPCHD	—	—	—	—	—	—	—	65
	FaPCHD + NIR	—	—	—	—	—	—	—	95
Zhang 2020[209]	NIR	N/A	NIR	HeLa	nude	DOX	1 × 2	180	6
	$CuS@mSiO_2$	—	—	—	—	—	—	—	19
	DOX	—	—	—	—	—	—	—	40
	$CuS@mSiO_2@MnO_2$	—	—	—	—	—	—	—	30
	$CuS@mSiO_2@MnO_2$ + NIR	—	—	—	—	—	—	—	66
	$CuS@mSiO_2@MnO_2$/DOX	—	—	—	—	—	—	—	72
	$CuS@mSiO_2@MnO_2$/DOX + NIR	—	—	—	—	—	—	—	100
Zhong 2020[294]	PBS + NIR	N/A	NIR	H22	nude	DOX	1 × 5	200	10
	GNR@HPMO@PVMSN	—	—	—	—	—	—	—	13
	GNR@HPMO@PVMSN + NIR	—	—	—	—	—	—	—	35
	GNR@HPMO@ PVMSN–DOX	—	—	—	—	—	—	—	44

TABLE 9: (*continued*)

	GNR@HPMO@PVMSN–DOX + NIR	—	—	—	—	—	—	—	88
DOX + radiation therapy									
Wang 2017[302]	FA-GSJNs	FA	N/A	SMMC-7721	nude	DOX	7 × 1	80	25
	FA-GSJNs + RT	—	—	—	—	—	—	—	75
	DOX	—	—	—	—	—	—	—	83
	GSJNs-DOX	—	—	—	—	—	—	—	67
	FA-GSJNs-DOX	—	—	—	—	—	—	—	83
	GSJNs-DOX + RT	—	—	—	—	—	—	—	94
	FA-GDJMS-DOX + RT	—	—	—	—	—	—	—	98
DOX + photodynamic therapy									
Fang 2019[295]	DOX	N/A	NIR	HeLA human cervical	nude	DOX; Ce6	1 × (2.7; 3.3)	100	29
	BMHDC	—	—	—	—	—	1 × 2	—	43
	HMSNs-DOX-Ce6 + laser	—	—	—	—	—	—	—	71
	BMHDC + laser	—	—	—	—	—	—	—	86
Li 2018[296]	US	RGD	s 450 nm +	SMMC-7721	nude	DOX; PpIX	1 × 2	100	3
	DOX	—	—	—	—	—	—	—	21
	DOX@ HMONs-PpIX-PEG	—	—	—	—	—	—	—	44
	DOX@ HMONs-PpIX-PEG + US	—	—	—	—	—	—	—	72
	DOX@HMONs-PpIX-RGD + US	—	—	—	—	—	—	—	84
Liu 2017[297]	DOX	Mag + Methotrexate	NIR	HeLA human cervical	Balb/c	nude	7 × 4	120	58
	DOX/ZnPc-FMLM	—	—	—	—	—	—	—	90
Rao 2018[298]	DOX	N/A	NIR	SCC7 murine squamous cell	nude	DOX; Ce6	1 × 5	150	18
	R-MSN + NIR	—	—	—	—	—	—	—	27

TABLE 9: (*continued*)

Study	Group	Target	Ex stim	Tumor	Mouse	Drug	Dose (mg/kg)	Start TV (mm^3)	%TIR
	DOX-MSN	—	—	—	—	—	—	—	36
	DOX-R-MSN + NIR	—	—	—	—	—	—	—	55
Su 2017[299]	RMSN + laser	N/A	NIR	4T1 mouse epithelial breast	nude	DOX; Ce6	8 × (5; 2.5)	100	10
	DOX	—	—	—	—	—	—	—	32
	DOX/Ce6 + laser	—	—	—	—	—	—	—	44
	MSN-DOX/Ce6 + laser	—	—	—	—	—	—	—	56
	RMSN-Ce6 + laser	—	—	—	—	—	—	—	65
	RMSN-DOX	—	—	—	—	—	—	—	72
	RMSN-DOX/Ce6 + laser	—	—	—	—	—	—	—	94
Wang 2019[300]	DOX	Mag	NIR	MCF-7/MDR human breast	nude	DOX; Ce6	1 × 3	200	4
	nanocompposite	—	—	—	—	—	—	—	25
	nanocomposite +	—	—	—	—	—	—	—	38
Xu 2020[301]	DOX	N/A	US	MDA-MB-231	nude	DOX; Ce6	5 × (3; 10)	100	37
	DOX + Ce6 + US	—	—	—	—	—	—	—	56
	MSN-DOX-Ce6 + US	—	—	—	—	—	—	—	76

TABLE 10: TIR for MSN formulations combination of DOX with other chemotherapy

Study	Group	Targeting	Ext stim	Tumor	Mouse	Drug	Dose (mg/kg)	TV at start	%TIR
Chen 2016[303]	DOX	N/A	N/A	Hep3B CSCs	nude	DOX; shRNA	15 × 1 mg NP	NR	20
	MSN/DOX	—	—	—	—	—	—	—	34
	MSN-SS-PEI/ DOX	—	—	—	—	—	—	—	45
	MSN-SS-PEI/ DOX/shCrtl	—	—	—	—	—	—	—	61
	MSN-SS-PEI/DOX/ shABCG2	—	—	—	—	—	—	—	84
Ding 2020[304]	DOX	GRP78P	pH; H2O2	4T1	Balb/c	DOX; α-TOS	1 × 5 DOX	100	68
	DOX/α-TOS loaded HMSNs	—	—	—	—	—	—	—	31
	DOX/α-TOS loaded HMSN-NH2-CMCH-GRP78P	—	—	—	—	—	—	—	58
	DOX/α-TOS loaded HMSN-NH2-CMCH-GRP78P	—	—	—	—	—	—	—	51
	DOX/α-TOS loaded HMSN-TK-CMCH	—	—	—	—	—	—	—	44
	DOX/α-TOS loaded HMSN-TKCMCH-GRP78P	—	—	—	—	—	—	—	80
Fang 2018[65]	Q + D	HA/CD44	N/A	SGC-7901/ADR human gastric	nude	DOX; Quercetin	7 × (5; 5)	100	44
	HA-SiLN/D	—	—	—	—	—	—	—	45
	HA-SiLN/Q	—	—	—	—	—	—	—	31

TABLE 10: (*continued*)

Study	Group	Targeting	Ext stim	Tumor	Mouse	Drug	Dose (mg/kg)	TV at start	%TIR
	HA-SiLN/QD	—	—	—	—	—	—	—	74
He 2020[305]	DOX/SP-FS-USMNS cluster	N/A		HepG2	nude	DOX; Curcumin	5 × 1	90	49
	Cur-SOX/SP-FS-USMSN cluster	—	—	—	—	—	—	—	56
He 2016[306]	(E + D)	N/A	N/A	LLC (Lewis lung carcinoma)	C57BL/6	DOX; erlotinib	5 × (2; 0.77)	NR	29
	M-SPC-L(E + D)	—	—	—	—	—	—	—	34
	M-HHG2C18-L(D)	—	—	—	—	—	—	—	13
	M-HHG2C18-L(D) + E	—	—	—	—	—	—	—	11
	M-HHG2C18-L(E + D)	—	—	—	—	—	—	—	77
Hu 2017[307]	D@RSMSN	N/A	N/A	MCF-7 human breast	nude	DOX; α-TOS	3 × (5; 2.5)	100	23
	DOX	—	—	—	—	—	—	—	54
	T/D@RSMSN	—	—	—	—	—	—	—	85
Kankala 2020[308]	DOX			MCF-7/ADR human breast	nude	DOX; Platinum	7 × NR	100	37
	Zn-MSN	—	—	—	—	—	—	—	1
	Zn-MSN-DOX	—	—	—	—	—	—	—	59
	Zn-MSN@CS/Pt	—	—	—	—	—	—	—	0
	Zn-MSN-DOX@CS/Pt	—	—	—	—	—	—	—	69
Kong 2017[309]	DOX	N/A	N/A	B16F10 murine melanoma	C67/BL6	DOX; Il2; ATRA	3 × (5; 2; 15)	30	17
	D/I	—	—	—	—	—	—	—	37
	A/D	—	—	—	—	—	—	—	47
	A/D/I	—	—	—	—	—	—	—	52

TABLE 10: (*continued*)

	D-dHMLB	—	—	—	—	—	—	—	43
	D/I-dHMLB	—	—	—	—	—	—	—	59
	A/D-dHMLB	—	—	—	—	—	—	—	62
	A/D/I-dHMLB	—	—	—	—	—	—	—	85
Li 2018[210]	QD@M-DNA/FA	FA	NIR	HeLA human cervical	nude	DOX; db-DNA	5 × (1.5; 0.2)	200	44
	QD@M-DNA/FA + NIR	—	—	—	—	—	—	—	58
	QD@M/D-Avidin/FA + NIR	—	—	—	—	—	—	—	75
	QD@M/D-DNA/FA + NIR	—	—	—	—	—	—	—	96
Li 2017[211]	SL-IDMSN	N/A	N/A	H22 murine hepatic	Kunming	DOX; iSur-pDNA	9 × (4; 1)	130	21
	DOX	—	—	—	—	—	—	—	52
	SL-IDMSN/pDNA	—	—	—	—	—	—	—	63
	SL-IDMSN@DOX/pGL	—	—	—	—	—	—	—	78
	DMSN@DOX/pDNA	—	—	—	—	—	—	—	87
	SL-IDMSN@DOX/pDNA	—	—	—	—	—	—	—	97
Liu 2018[310]	TMSN	peptide (WIFP	N/A	SW480 human colorectal	nude	DOX; miRNA-145	5 × 3 mg/kg; 75 nmol/kg	NR	3
	m@TMSN	—	—	—	—	—	—	—	61
	D@TMSN	—	—	—	—	—	—	—	48
	Dm@MSN	—	—	—	—	—	—	—	43
	Dm@TMSN	—	—	—	—	—	—	—	86
Nie 2020[212]	CCM-DOX-MPH	N/A	N/A	MCF-7 human breast	nude	DOX; MPH	6 × (5; 4)	150	71

TABLE 10: (*continued*)

Study	Group	Targeting	Ext stim	Tumor	Mouse	Drug	Dose (mg/kg)	TV at start	%TIR
	CCM@LM-DOX-MPH	—	—	—	—	—	6 × (1; 0.78)	—	95
	L@LM-DOX-MPH	—	—	—	—	—	—	—	86
	LM-DOX-MPH	—	—	—	—	—	—	—	89
	Doxil	—	—	—	—	—	6 × 5	—	87
	CCM-DOX	—	—	—	—	—	—	—	34
	L@LM-DOX	—	—	—	—	—	—	—	47
	LM-DOX	—	—	—	—	—	—	—	63
	CCM@ LM-DOX	—	—	—	—	—	—	—	71
Ramasamy 2018[311]	DOX	N/A	NIR	MDA-MB-231	Balc/c nude	DOX; Se	4 × 5 DOX	90	26
	Nano Se	—	—	—	—	—	—	—	41
	Au@mSiO$_2$/ DOX (NIR-)	—	—	—	—	—	—	—	51
	Au@mSiO$_2$/ DOX (NIR +)	—	—	—	—	—	—	—	55
	Se@Au@ mSiO$_2$/DOX (NIR-)	—	—	—	—	—	—	—	67
	Se@Au@ mSiO$_2$/DOX (NIR+)	—	—	—	—	—	—	—	79
Su 2014[312]	RIV-L[C]	EGF (RIV)	N/A	A375 human melanoma	nude	DOX; CA-4	6 × (0.8; 25)	75	57
	RIV-L[D]	—	—	—	—	—	—	—	55
	RIV-L[D] + RIV-L[C]	—	—	—	—	—	—	—	75
	l[CD]	—	—	—	—	—	—	—	71
	RIV-L[CD]	—	—	—	—	—	—	—	90

TABLE 10: (*continued*)

Wang 2018[64]	Se@ SiO_2-FA-CuS	FA	NIR	HeLA human cervical	nude	DOX; Se	1;3.5	25	10
	DOX	—	—	—	—	—	—	—	28
	Se@SiO_2-FA-CuS/ DOX	—	—	—	—	—	—	—	48
	Se@SiO_2-FA-CuS + NIR	—	—	—	—	—	—	—	76
	Se@SiO_2-FA-CuS/DOX + NIR	—	—	—	—	—	—	—	100
Xie 2020[313]	N9	N9 peptide	N/A	HepG2-Bcl2-GFP	nude	DOX; N9	7 × (0.5; 1.75)	80	3
	DOX	—	—	—	—	—	—	—	16
		—	—	—	—	—	—	—	
	N9 + DOX	—	—	—	—	—	—	—	17
	M~G5	—	—	—	—	—	—	—	1
	N9@M~G5	—	—	—	—	—	—	—	84
	N9@ M~G5~DOX	—	—	—	—	—	—	—	88
Xing 2020[213]	DOX	N/A	NIR	LLC (Lewis lung carcinoma)	C57BL/6	DOX; PTX	5 × (4; 0.28)	80	35
	PTX	—	—	—	—	—	—	—	49
	Au-MSN JNP	—	—	—	—	—	—	—	0
	Au-MSN JNP + NIR	—	—	—	—	—	—	—	46
	Au-MSN-DOX JNP	—	—	—	—	—	—	—	37
	PTX-Au-MSN JNP	—	—	—	—	—	—	—	13
	PTX-Au-MSN-DOX JNP	—	—	—	—	—	—	—	60
	placebo	—	—	—	—	—	—	—	—

TABLE 10: (*continued*)

Study	Group	Targeting	Ext stim	Tumor	Mouse	Drug	Dose (mg/kg)	TV at start	%TIR
Xue 2017[314]	LH/miR-375	N/A	N/A	HepG2/ADR human liver	nude	DOX; miR-375	3 × 6 mg/kg; 3 × 4 nmol/kg	75	19
	DOX	—	—	—	—	—	—	—	20
	LHD	—	—	—	—	—	—	—	29
	LHD/miR-375	—	—	—	—	—	—	—	55
Yin 2018[315]	MSNP-DOX	iRGD	N/A	MDA-MB-231	nude	DOX; let-7a mRNA	12 × (0.6; 0.129)	100	17
	MSP/Let-7a	—	—	—	—	—	—	—	61
	MSNP-DOX/ Let-7a	—	—	—	—	—	—	—	88
Zhang 2019[316]	MSN	HA/CD44	N/A	H22 murine hepatic	ICR	DOX; berberine	3 × (1; 2)	250	3
	DOX	—	—	—	—	—	—	—	46
	DOX + BER	—	—	—	—	—	—	—	75
	MSN@DB	—	—	—	—	—	—	—	55
	HA-MSN@DB	—	—	—	—	—	—	—	81
Zhang 2014[317]	MSN	Aptamer	N/A	HepG2 human liver	nude	DOX; CytC	9 × 3 DOX	38	4
	MSN-CtyC-Apt	—	—	—	—	—	—	—	21
	DOX	—	—	—	—	—	—	—	49
	MSN@DOX	—	—	—	—	—	—	—	71
	MSN-CtyC-Apt@DOX	—	—	—	—	—	—	—	87
Zhao 2017[214]	DOX	N/A	N/A	MCF-7	SCID	DOX; siRNA	8 × 1.2 DOX	50	71
	MSN@DOX	—	—	—	—	—	—	—	83
	MSN-SS-siRNA@DOX	—	—	—	—	—	—	—	96

TABLE 11: TIR for MSN formulations combination of drugs other than DOX

Study	Group	Targeting	Ext stim	Tumor	Mouse	Drug	Dose (mg/kg)	Start TV (mm^3)	%TIR
Ansari 2018[318]	MMSN	Mag	N/A	C-26 murine colorectal	nude	EPI	1 × 9	20	0
	MMSN + EPI(MAG-)	—	—	—	—	—	—	—	22
	EPI	—	—	—	—	—	—	—	37
	MSMN + EPI(MAG +)	—	—	—	—	—	—	—	48
	MMSN + EPI(MAG-)	—	—	—	—	—	—	—	32
	EPI	—	—	—	—	—	1 × 12	—	45
	MSMN + EPI(MAG +)	—	—	—	—	—	—	—	59
Babaei 2020[319]	Camptothecin	AS1411 DNA aptamer	N/A	C-26 murine colorectal	Balb/c	CPT; iSur shRNA	4 × (3; 2)	20	23
	PEG@MSNR/Sur	—	—	—	—	—	—	—	28
	PEG@MSNR-CPT	—	—	—	—	—	—	—	40
	PEG@ MSNR-CPT-Sur	—	—	—	—	—	—	—	56
	Apt-PEG@ MSNR-CPT/Sur	—	—	—	—	—	—	—	85
Che 2015[320]	Taxol	Mag	N/A	S180 mouse sarcoma	Kunming	PTX	3 × 10	200	41
	PTX/MMSN@ GEL-04 (MF)	—	—	—	—	—	—	—	49
	PTX/MMSN@ GEL-04 (MF +)	—	—	—	—	—	—	—	79
Chen 2020[321]	PTX	N/A	N/A	4T1 mouse epithelial breast	Balb/c	PTX	1 × 5	100	15
	HMONs-PTX	—	—	—	—	—	—	—	29

TABLE 11: (*continued*)

Study	Group	Targeting	Ext stim	Tumor	Mouse	Drug	Dose (mg/kg)	Start TV (mm^3)	%TIR
	HMONs-PTX@ PDA	—	—	—	—	—	—	—	57
	HMONs-PTX@ PDA-PEG	—	—	—	—	—	—	—	23
	PTX liposome	—	—	—	—	—	—	—	77
Chen 2019[322]	5-FU	N/A	N/A	Cal33 murine squamous cell	Balb/c	5-FU; ß-lap	3 × (5; 25)	90	12
	ß-lap	—	—	—	—	—	—	—	8
	5-FU + ß-lap	—	—	—	—	—	—	—	18
	FNQ-MSN	—	—	—	—	—	—	—	58
Choi 2016[323]	AXT	N/A	N/A	SCC7 mouse squamous cell	Balb/c	axitinib; celastrol	7 × 1 NP	65	42
	CST	—	—	—	—	—	—	—	61
	AXT/CST	—	—	—	—	—	—	—	72
	ACML	—	—	—	—	—	—	—	80
Ding 2015[324]	CMS	peptide	N/A	MCF-7 human breast	nude	EGCG	5 × 100	50	48
	EGCG	—	—	—	—	—	—	—	72
	CMS@EGCG	—	—	—	—	—	—	—	82
	CMS@peptide@ EGCG	—	—	—	—	—	—	—	90
Du 2019[325]	Taxol	HA/CD44	N/A	HepG2 human liver	Kunming	PTX; Gox	7 × 7.5 PTX	120	33
	MSN	—	—	—	—	—	—	—	38
	MSN-Gox	—	—	—	—	—	—	—	81
	MSN-Gox/PLL/HA	—	—	—	—	—	—	—	90
Fei 2017[326]	ATO-sol	RGD	N/A	H22 murine hepatic	ICR	ATO	15 × 1	50	36
	CHMSN-ATO	—	—	—	—	—	—	—	52

TABLE 11: (*continued*)

	LP-CHMSN-ATO	—	—	—	—	—	—	—	65
	RGD-LP-CHMSN-ATO	—	—	—	—	—	—	—	82
Feng 2019[327]	taxol	N/A	N/A	EMT6 murine mammary	nude	EVO; Ber	9 × 2 (EVO + BBR)	150	91
	BMEL(6:1)	—	—	—	—	—	—	—	87
	BMEL(1:6)	—	—	—	—	—	—	—	83
	Free EVO/ BBR(6:1)	—	—	—	—	—	—	—	47
	Free EVO/ BBR(1:6)	—	—	—	—	—	—	—	30
Gao 2019[328]	Tax-Cur-PLMSN iv	N/A	N/A	4T1 mouse epithelial breast	nude	PTX/Cur	1 × (6; 36)	150	57
	Tax-Cur-PLMSN pi	—	—	—	—	—	—	—	58
	Tax	—	—	—	—	—	—	—	2
	Tax-cur	—	—	—	—	—	—	—	23
	PLMSN	—	—	—	—	—	—	—	7
Goto 2017[329]	GEM-S-MSN@ PICsome	N/A	N/A	A549 human alveolar	nude	GEM	3 × 5	8.7	61
	S-MSN@PICsome	—	—	—	—	—	—	—	1
	GEM-S-MSN	—	—	—	—	—	—	—	–5
	S-MSN	—	—	—	—	—	—	—	–19
	PICsome	—	—	—	—	—	—	—	12
	GEM	—	—	—	—	—	—	—	92
Hanafi-Bojd 2015[330]	MSN-Ph2	N/A	N/A	C-26 murine colorectal	Balb/c	EPI	3 × 9	NR	9
	MSN-Ph2-EPI	—	—	—	—	—	—	—	17
	EPI	—	—	—	—	—	—	—	46
	MSN-PEI-PEG-EPI	—	—	—	—	—	—	—	64

TABLE 11: (*continued*)

Study	Group	Targeting	Ext stim	Tumor	Mouse	Drug	Dose (mg/kg)	Start TV (mm^3)	%TIR
Hanafi-Bojd 2016[331]	EPI	N/A	N/A	C-26 murine colorectal	Balb/c	EPI; siRNA	1 × (9; 1.2)	10	17
	siRNA	—	—	—	—	—	—	—	2
	MSN-PEI-PEG-EPI-siRNA	—	—	—	—	—	—	—	62
	MSN-PEI-PEG-EPI	—	—	—	—	—	—	—	41
	MSN-PEI-PEG-siRNA	—	—	—	—	—	—	—	17
	MSN-PEI-PEG-EPI-scramble siRNA	—	—	—	—	—	—	—	22
Hu 2019[332]	miR21	N/A	N/A	BGC823 human gastric	nude	RSV; anti-miR1	1 × (10; 0.45)	90	10
	RSV	—	—	—	—	—	—	—	17
	RSVmirNP	—	—	—	—	—	—	—	38
	HA/RSVmirNP	—	—	—	—	—	—	—	66
Hu 2019[356]	Laser	AE105-peptide	NIR	HeLA human cervical	nude	cisPT	NR	150	9
	NP every day	—	—	—	—	—	—	—	24
	NP + laser every other day	—	—	—	—	—	—	—	65
	NP + laser one time	—	—	—	—	—	—	—	80
Huang 2020[355]	RT	N/A	N/A	4T1 mouse epithelial breast	NR	QC	1 × 5	200	24
	RT + Q	—	—	—	—	—	—	—	57
	CQM	—	—	—	—	—	—	—	29
	RT + CQM	—	—	—	—	—	—	—	87

TABLE 11: (*continued*)

Huo 2017[333]	GFD NC 5	N/A	N/A	4T1 mouse epithelial breast	nude	Gox; Fe_3O_4	1 × 5 GOx	20	71
	GFD NC 10	—	—	—	—	—	1 × 10 GOx	—	86
	GFD NC 5	N/A		U87 human glioblastoma	nude	Gox; Fe_3O_4	1 × 5 GOx	20	40
	GFD NC 10	—	—	—	—	—	1 × 10 GOx	—	80
Ke 2018[334]	DiR-labeled sora@ HMSNs	transferring Tf	N/A	TPC-1 human thyroid	SCID	sorafenib	1 × 9 NP	65	25
	DiR-labeled sora@ Tf-HMSNs	—	—	—	—	—	—	—	55
Kundo 2020[335]	umbelliferone	FA	N/A	Ehrlich ascites	Swiss albino	umbelliferone/ coumarin	7 × 10	160	22
	Umbe@MSN-PAA	—	—	—	—	—	—	—	46
	Umbe@ MSN-PAA-FA	—	—	—	—	—	—	—	64
Liu 2020[370]	QC	chondroitin sulfate	N/A	MCF-7 human breast	nude	PTX/QC	7 × (5; 5.1)	100	17
	MSNs-ChS@QC	—	—	—	—	—	—	—	15
	PTX	—	—	—	—	—	—	—	23
	MSN-ChS@{TX	—	—	—	—	—	—	—	34
	PQ	—	—	—	—	—	—	—	44
	MSNs@PQ	—	—	—	—	—	—	—	61
	MSNs-Chs@PQ	—	—	—	—	—	—	—	74
Li 2020[336]	TanIIA	FA	N/A	NB4 human leukemia	nude	PTX; TanIIA	6 × 5 Ptx	50	48
	Ptx	—	—	—	—	—	—	—	66
	Ptx + TanIIA	—	—	—	—	—	—	—	79
	TanIIA@ FA-LB-MSN	—	—	—	—	—	—	—	70
	Ptx@FA-LB-MSN	—	—	—	—	—	—	—	77
	(Ptx + TanIIA)@ MSN	—	—	—	—	—	—	—	82

TABLE 11: (*continued*)

Study	Group	Targeting	Ext stim	Tumor	Mouse	Drug	Dose (mg/kg)	Start TV (mm^3)	%TIR
	(Ptx + TanIIA)@ LB-MSN	—	—	—	—	—	—	—	91
	(Ptx + TanIIA)@ FA-LB-MSN	—	—	—	—	—	—	—	94
Li 2020[217]	CPT-11@ GDC-MSN	asialoglycoprotein	N/A	Huh-7 human liver	nude	Ir	7 × 10	50	98
	CPT-11@GP-MSN	—	—	—	—	—	7 × 10	—	79
	CPT-11@ PDC-MSN	—	—	—	—	—	7 × 10	—	91
	CPT 100	—	—	—	—	—	7 × 100	—	74
	CPT 10	—	—	—	—	—	7 × 10	—	27
Li 2019[337]	Fe_3O_4@ PMO-NH2-Los	N/A	N/A	DSL/6A rat pancreas	Balb/c	GEM	various	60	6
	Fe_3O_4@PMO-GEM	—	—	—	—	—	7 × 40 los 1st d7	—	31
	Fe_3O_4@PMO-GEM + Fe_3O_4@ PMO-NH2-Los	—	—	—	—	—	3 × 10 GEM starting d8	—	69
Li 2019[357]	MB	FA	NIR	HeLA human cervical	nude	Pt; MB	1 × 0.0075 MB	100	11
	MB-MSNS	—	—	—	—	—	—	—	35
	FA/PtBSA@ MB-MSNS	—	—	—	—	—	—	—	88
Li 2019[218]	Ber	FA	NIR	SMMC-7721 human liver	nude	Ber	7 × 5	90	4
	FA-JGMSN-Ber	—	—	—	—	—	—	—	38
	RT	—	—	—	—	—	—	—	45
	FA-JGMSN + RT	—	—	—	—	—	—	—	65
	FA-JGMSN-Ber + RT	—	—	—	—	—	—	—	79

TABLE 11: (*continued*)

	JGMSN-Ber + RT + NIR	—	—	—	—	—	—	—	88
	FA-JGMSN-Ber + RT + NIR	—	—	—	—	—	—	—	95
Liu 2020[338]	DM-NCTD	FA	N/A	H22 murine hepatic	NR	DM-NCTD; ABT-737	1 × 2 DM-NCTD	NR	35
	ABT-737	—	—	—	—	—	—	—	21
	DM-NCTD + ABD-737	—	—	—	—	—	—	—	46
	LA-LB(ABT-737)-(DM-NCTD@ CHMSN)	—	—	—	—	—	—	—	70
Liu 2019[149]	IRIN	N/A	N/A	MC38 murine colorectal (orthotopic)	C57BL/6	Ir	4 × 40	NR*	8
	Onivydne	—	—	—	—	—	—	—	17
	IR-silicaosome	—	—	—	—	—	—	—	58
Liu 2018[339]	PAMAM-Pt	N/A	N/A	A549 human alveolar	nude	cisPT	9 × 2	100	14
	GEM	—	—	—	—	—	—	—	28
	HMSN@ GEM-CS(SA)/ PAMAM-PT	—	—	—	—	—	—	—	46
	HMSN@GEM-CS(DMA)/ PAMAM-PT	—	—	—	—	—	—	—	72
Liu 2012[216]	pGSN-NIR	Tf	NIR	MCF-7 human breast	nude	Doc	1 × 20	200	16
	Taxotere	—	—	—	—	—	—	—	62
	pGSN-Doc-NIR	—	—	—	—	—	—	—	84
	pGSN-Doc-Tf-NIR	—	—	—	—	—	—	—	99
Lu 2010[340]	CPT	FA	N/A	MCF-7 human breast	nude	CPT	15 × 5 ip	15	14
	FMSN	—	—	—	—	—	—	—	6

TABLE 11: (*continued*)

Study	Group	Targeting	Ext stim	Tumor	Mouse	Drug	Dose (mg/kg)	Start TV (mm^3)	%TIR
	FMSN/CPT	—	—	—	—	—	—	—	99
	F-FMSN/CPT	—	—	—	—	—	—	—	100
Luo 2016[358]	MMSGNR-AIPcS4 NT	lactobionic acid	NIR	HepG2 human liver	nude	cisPT; AIPcS4	1 × (1.9; 1.15)	100	7
	MMSGNR-AIPcS4 NT 808 + 660 nm	—	—	—	—	—	—	—	52
	MMSGNR-AIPcS4	—	—	—	—	—	—	—	10
	MMSGNR-AIPcS4 808 nm	—	—	—	—	—	—	—	79
	MMSGNR-AIPcS4 660 nm	—	—	—	—	—	—	—	72
	MMSGNR-AIPcS4 880 + 660 nm	—	—	—	—	—	—	—	93
Meng 2015[341]	GEM	N/A	N/A	KB-31 HeLa human carcinoma	nude	GEM	6 × 100	20	59
	Abraxane	—	—	—	—	PTX	6 × 10	—	33
	GEM LB-MSNP	—	—	—	—	GEM	6 × 100 GEM	—	74
	PTX/GEM LB-MSNP	—	—	—	—	GEM; PTX	6 × (100; 10)	—	84
	GEM/Abraxane (1x)	—	—	—	—	GEM; PTX	6 × (100; 10)	—	57
	GEM/Abraxane (12x)	—	—	—	—	GEM; PTX	6 × (100; 120)	—	79
Mu 2017[342]	MSN-PLH-PEG	N/A	N/A	H22 murine hepatic	Kunming	sorafenib	6 × 10	120	28
	SF-oral	—	—	—	—	—	—	—	58
	SF iv	—	—	—	—	—	—	—	75
	SF/MSN	—	—	—	—	—	—	—	85

TABLE 11: (*continued*)

	SF/MSN-PLH-PEG	—	—	—	—	—	—	—	90
Murugan 2017[343]	TPT	RGD/TAT	N/A	MDA-MB-231 human breast	nude	Topotecan/ metformin	8 × 5 NP	200	33
	MP	—	—	—	—	—	—	—	20
	TPT + MT	—	—	—	—	—	—	—	50
	TPT + MSN-TAT	—	—	—	—	—	—	—	61
	TPT-MSN-TAT-CAH-MT	—	—	—	—	—	—	—	70
	PMS nanocomposites	—	—	—	—	—	—	—	92
Pan 2017[344]	MSN-P(OMEGA-ci0RGD)	RGD	N/A	HTC-116 human colorectal	nude	5-FU	6 × 20	100	0
	5-FU	—	—	—	—	—	—	—	50
	5-FU@MSN	—	—	—	—	—	—	—	63
	5-FU@MSN-RGD	—	—	—	—	—	—	—	74
Paredes 2020[345]	MSN-AP-Sn-AX	FA	N/A	MDA-MB-231 human breast	NOD Scid	MSN-AP-Sn	NR	NR	2
	MSN-AP-Sn-AX	—	—	—	—	—	—	—	6
	MSN-AP-FA-PEP-Sn-AX	—	—	—	—	—	—	—	41
Qu 2018[346]	TPT	FA	N/A	Y79 human retinoblastoma	nude	topotecan	NR	76	24
	TMN	—	—	—	—	—	—	—	38
	FTMN	—	—	—	—	—	—	—	67
Ren 2018[347]	CPT	N/A	N/A	Panc-1 human pancreatic	NR	CPT		NR	37
	MnOx-SPION@ MSN@CPT	—	—	—	—	—	6 × 2.5	—	81
Shao 2020[219]	PDA@hm	N/A	NIR	HepG2 human liver	Balb/c	Chloroquine; GOx	NR	100	–7
	PDA@hm@CQ	—	—	—	—	—	—	—	39

TABLE 11: (*continued*)

Study	Group	Targeting	Ext stim	Tumor	Mouse	Drug	Dose (mg/kg)	Start TV (mm^3)	%TIR
	PDA@hm@GOx	—	—	—	—	—	—	—	44
	PDA@hm + NIR	—	—	—	—	—	—	—	60
	PDA@hm@CQ + NIR	—	—	—	—	—	—	—	85
	PDA@hm@Dox + NIR	—	—	—	—	—	—	—	73
	PDA@hm@CQ@ Gox + NIR	—	—	—	—	—	—	—	98
Sun 2019[220]	Au@MSN-ZOL	N/A	NIR	MDA-MB231 human breast	nude	Zoledronate	4 × 0.2	NR	63
	Au@MSN-ZOL + NIR	—	—	—	—	—	—	—	95
Tang 2013[348]	Cpt50	N/A		mouse Lewis lung carcinoma	C57BL/6	CPT	1 × 25	300	63
	Cpt200	—	—	—	—	—	—	—	23
Tao 2019[349]	ATO-sol	angiopep-2 peptide	N/A	C6 rat glioma (intra cranial)	rat	ATO	8 × 1	NR	28
	MSN@ATO	—	—	—	—	—	—	—	34
	PAA-MSN@ATO	—	—	—	—	—	—	—	53
	LP-PAA-MSN@ ATO	—	—	—	—	—	—	—	57
	ANG-LP-PAA-MSN@ATO	—	—	—	—	—	—	—	76
Thapa 2017[222]	BIR	Cyclosporine A	NIR	PANC-1 human pancreas	nude	bortezomib	NR	100	53
	BIR + NIR	—	—	—	—	—	—	—	68
	LMSN/BIR	—	—	—	—	—	—	—	85
	LMSN/BIR + NIR	—	—	—	—	—	—	—	84
	CLSMN/BIR	—	—	—	—	—	—	—	89

TABLE 11: (*continued*)

	CLMSN/BIR + NIR	—	—	—	—	—	—	—	97
Wang 2020[359]	Ir	CCM	NIR	C-26 murine colorectal	Balb/c	Ir	1 × 30	150	36
	IR825/Ir ZGGO@ SiO_2	—	—	—	—	—	—	—	43
	IR825/Ir ZGGO@ SiO_2@CM	—	—	—	—	—	—	—	40
	IR825/Ir ZGGO@ SiO_2@MM	—	—	—	—	—	—	—	52
	IR825/Ir ZGGO@ SiO_2@CMM	—	—	—	—	—	—	—	65
	Ir + NIR	—	—	—	—	—	—	—	42
	IR825/Ir ZGGO@ SiO_2 + NIR	—	—	—	—	—	—	—	53
	IR825/Ir ZGGO@ SiO_2@CM + NIR	—	—	—	—	—	—	—	56
	IR825/Ir ZGGO@ SiO_2@CMM + NIR	—	—	—	—	—	—	—	66
	IR825/Ir ZGGO@ SiO_2@CMM + NIR	—	—	—	—	—	—	—	83
Wang 2019[360]	FA-GT-MSN	FA	NIR	SMMC-7721 human liver	nude	tirapazamine TPZ	1 × 0.5	80	8
	RT	—	—	—	—	—	—	—	35
	FA-GT-MSN + RT	—	—	—	—	—	—	—	56
	FA-GT-MSN + NIR + RT	—	—	—	—	—	—	—	40
	FA + GT-MSN@ TPZ + NIR + RT	—	—	—	—	—	—	—	73
	FA-GT-MSN@TPZ + NIR + RT	—	—	—	—	—	—	—	92
	GT-MSN@TPZ + NIR + RT	—	—	—	—	—	—	—	83

TABLE 11: (*continued*)

Study	Group	Targeting	Ext stim	Tumor	Mouse	Drug	Dose (mg/kg)	Start TV (mm^3)	%TIR
Wang 2017[350]	Cisplatin	lactobionic acid	N/A	H22 murine hepatic	Kunming	Pt	3 × 2	75	84
	MSN-P-Pt	—	—	—	—	—	—	—	74
	MSN-P/LA-Pt	—	—	—	—	—	—	—	88
Wu 2020[351]	HMSNs (H)	N/A	N/A	PC-3 human prostate	nude	CaO2	1 × 8	100	2
	HMSNs-PAA (HP),	—	—	—	—	—	—	—	4
	CaO2 (C),	—	—	—	—	—	—	—	12
	CaO2@HMSNs (CH)	—	—	—	—	—	—	—	41
	CaO2@HMSNs-PAA (CHP)	—	—	—	—	—	—	—	78
Wu 2019[221]	PTX/GEM LB-MSNP	N/A	NIR/ ultrasound	MDA-MB-231	nude	ICG; PTX	1 × (5; 4)	100	24
	ICG + NIR	—	—	—	—	—	—	—	43
	ICG/PFP@ HMOP-PEG	—	—	—	—	—	—	—	66
	ICG/PFP@HMOP-PEG + NIR	—	—	—	—	—	—	—	100
Xing 2018[361]	Janus M-MSN	Mag	ACMF	HepG2 human liver	nude	Cur	7 × 5	80	1
	Cur	—	—	—	—	—	—	—	29
	Janus M-MSNs-Cur	—	—	—	—	—	—	—	61
	Janus M-MSNs-Cur + ACMF	—	—	—	—	—	—	—	78
	Janus M-MSNs-Cur + ACMF + EMF	—	—	—	—	—	—	—	88
Xu 2017[352]	PTX	FA	N/A	SMMC-7721 human liver	nude	PTX	6 × 20	300	30

TABLE 11: (*continued*)

	MSN-PTX	—	—	—	—	—	—	—	57
	FA-PEG-MSN-PTX	—	—	—	—	—	—	—	70
Zhang 2020[353]	MON	N/A	N/A	A549 human alveolar	nude	cisPT; acriflavine	1 × 4 × 2 cisPt	150	4
	MONA	—	—	—	—	—	—	—	29
	PMON	—	—	—	—	—	—	—	66
	PMONA	—	—	—	—	—	—	—	92
Zhang 2019[362]	CM	EGFR	NIR	PC-9 human lung	nude	erlotinib; ICG	3 × 0.0025 Er	75	24
	Er	—	—	—	—	—	—	—	54
	CMI	—	—	—	—	—	—	—	39
	CMI + NIR	—	—	—	—	—	—	—	71
	ECM	—	—	—	—	—	—	—	64
	ECM + NIR	—	—	—	—	—	—	—	72
	ECMI	—	—	—	—	—	—	—	77
	ECMI + NIR	—	—	—	—	—	—	—	86
Zhao 2017[354]	GEM	Transferrin	NIR	PaCa-2 human pancreas	nude	GEM	1 × 2	100	19
	GNRS	—	—	—	—	—	—	—	32
	GNRS-GEM	—	—	—	—	—	—	—	60
	Tf-GNRS-GEM	—	—	—	—	—	—	—	93
Zhao 2017[371]	UA	lactobionic acid	N/A	H22 murine hepatic	Kunming	SO; UA	10 × 20.5	NR	26
	SO	—	—	—	—	—	10 × 9.5	—	39
	UA + SO	—	—	—	—	—	10 × (20.5; 9.5)	—	57
	USMN-CL	—	—	—	—	—	10 × (20.5; 9.5)	—	73
PDT only									
Brezániová 2018[363]	Foscan	N/A	NIR	MDA-MB-231	nude	temoporfin	1 × 0.8	250	29
	T-SiNP3	—	—	—	—	—	—	—	60

TABLE 11: (*continued*)

Study	Group	Targeting	Ext stim	Tumor	Mouse	Drug	Dose (mg/kg)	Start TV (mm^3)	%TIR
Du 2020[364]	CMHP	N/A	NIR	4T1 mouse epithelial breast	nude	Ce6; MnOx	1 × 2 Ce6	50	3
	CHP + Laser	—	—	—	—	—	—	—	26
	CMHP + Laser	—	—	—	—	—	—	—	98
Ma 2018[148]	Ru@MSN-20	N/A	NIR	HepG2 human liver	nude	RuPOP	1 × 0.2	140	46
	Ru@MSN-40	—	—	—	—	—	—	—	43
	Ru@MSN-80	—	—	—	—	—	—	—	38
	RuPOP	—	—	—	—	—	—	—	13
PTT only									
Yang 2019[365]	MSNR@Au-TPPS4(Gd) + 660 nm	N/A	NIR	4T1 mouse epithelial breast	Balb/c	TPPS4	1 × 15	100	13
	MSNR@Au-TPPS4(Gd) + 808 nm	—	—	—	—	—	—	—	29
	MSNR@Au-TPPS4(Gd) + 808/660 nm	—	—	—	—	—	—	—	95
Zhang 2020[366]	Cu2-xSe	N/A	NIR	MGC-803 gastric	rat	Cu2-xSe	NR	87	65
	Cu2-xSe@$mSiO_2$	—	—	—	—	—	—	—	66
	Cu2-xSe@$mSiO_2$ + NIR	—	—	—	—	—	—	—	100
PDT and TT (no chemo)									
Liu 2018[367]	ICG	N/A	NIR	MCF-7 human breast	nude	ICG	9 × 1.2	100	25
	AuNR@MSN-ICG	—	—	—	—	—	—	—	58

TABLE 11: (*continued*)

	AuNR@ MSN-RLA/ CS(DMA)-PEG	—	—	—	—	—	—	—	64
	AuNR@MSN-ICG-RLA/ CS(DMA)-PEG	—	—	—	—	—	—	—	85
Wang 2019[368]	α-CTLA-4	Cancer Cell Membrane	Mag	4T1 mouse epithelial breast	Balb/c	Ce6	5 × 12.5 NP	80	4
	CM@M-MON@ Ce6 + Laser + ACMF	—	—	—	—	—	—	—	73
	CM@M-MON@ Ce6 + Laser + α-CTLA-4	—	—	—	—	—	—	—	88
	CM@M-MON@ Ce6 + ACMF + α-CTLA-4	—	—	—	—	—	—	—	28
	CM@M-MON@ Ce6 + Laser + ACMF + α-CTLA-4	—	—	—	—	—	—	—	32
Zhang 2020[369]	PDT	FA	NIR	4T1 mouse epithelial breast	Balb/c	Ce6; CuS	1 × 10 NP	200	38
	Enhanced PDT	—	—	—	—	—	—	—	59
	PTT	—	—	—	—	—	—	—	80
	Enhanced PDT + PTT	—	—	—	—	—	—	—	98

*In this study, tumor volume at the start of treatment was not reported. 1.5–3 mm tumor "chunks" were surgically implanted into the cecum and therapy started 12 days later.

TABLE 12: TIR for pegylated liposomal DOX and Abraxane (tumor volume at the start of the therapy was not reported in all studies)

Study	Group	Tumor	Mouse	Drug	TV at start (mm^3)	TIR
Liposomes						
Brouckaert 2004[155]	DOX 1 × 4.5 mg/kg + 4 × 1 mg/kg	B16BL6 murine melanoma	C57BL/6	DOX	500	7
	Doxil 1 × 4.5 mg/kg + 4 × 1 mg/kg	—	—	—	—	34
Colbern 1999[151]	DOX 3 × 9 mg/kg	Lewis Lung	B6C3-F1	DOX	850	60
	DOXIL 3 × 4 mg/kg	—	—	—	—	86
	DOXIL 3 × 9 mg/kg	—	—	—	—	93
Colbern 1999[151]	DOX 9 mg/kg	Lewis Lung	B6C3-F1	DOX	—	38
	DOXIL 4 mg/kg	—	—	—	—	69
Colbern 1999[151]	DOX 9 mg/kg	—	—	—	—	47
	DOXIL 4 mg/kg	—	—	—	—	96
Colbern 1999[151]	DOX 3 × 9 mg/kg	C26 murine colorectal	Balb/c	DOX	245	50
	PL-DOX 3 × 4 mg/kg	—	—	—	—	78
	PL-DOX 3 × 9 mg/kg	—	—	—	—	95
Gabizon 2002[372]	DOX 2.5 mg/kg	M109	Balb/c	—	—	–7
	DOX 10 mg/kg	—	—	—	—	29
	DOXIL 2.5 mg/kg	—	—	—	—	55
	DOXIL 10 mg/kg	—	—	—	—	83
Huang 1992[373]	DOX 3 × 6 mg/kg	—	—	DOX	8	18
	SL-DOX 3 × 6 mg/kg	—	—	—	—	100
	SL-DOX 3 × 9 mg/kg	—	—	—	—	100
	EPI 3 × 6 mg/kg	—	—	—	—	42
	SL-EPI 3 × 6 mg/kg	—	—	EPI	—	100
	SL-EPI 3 × 9 mg/kg	—	—	—	—	100
Mayer 1990[374]	DOX 3.25 mg/kg	SC115 mouse breast	NR	DOX	(palpable)	8
	DOX 6.5 mg/kg	—	—	—	—	76
	Lipodox 3.2 mg/kg	—	—	—	—	42

TABLE 12: (*continued*)

	Lipodox 6.5 mg/kg	—	—	—	—	89
	Lipodox 13 mg/kg	—	—	—	—	89
Mayhew 1992[375]	L-EPI 3 × 6 mg/kg	C26 murine colorectal	Balb/c	EPI	—	41
	L-EPI 3 × 9 mg/kg	—	—	—	—	20
	S-EPI 3 × 6 mg/kg	—	—	—	—	100
	S-EPI 3 × 9 mg/kg	—	—	—	—	100
Papahadjopoulos 1991[376]	EPI 6 mg/kg	C26 murine colorectal	Balb/c	EPI	(1 day)	23
	Lipo-EPI 6 mg/kg	—	—	—	—	97
	Lipo-EPI 12 m/kg	—	—	—	—	100
Shinozawa 1981[76]	DOX 3 × 1.25 mg/kg	Ehrlich ascites	ICR	DOX	—	13
	Liposomes + DOX	—	—	—	—	53
	Liposomes – DOX	—	—	—	—	60
	Neutralliposomes + DOX	—	—	—	—	64
Singh 2020 3D[167]	DOX 5 mg/kg	primary human ovarian ascites	nude	DOX	10	26
	Doxil 5 mg/kg	—	—	—	—	80
Singh 2020 2D[167]	DOX 5 mg/kg	—	—	DOX	25	41
	Doxil 5 mg/kg	—	—		—	27
Unezaki 1995[377]	DXR 5 mg	C26 murine colorectal	Balb/c	DOX	—	46
	DXR-LP 5 mg	—	—	—	—	39
	DXR-LCL 5 mg	—	—	—	—	69
	DXR 10 mg	—	—	—	—	55
	DXR-LP 10 mg	—	—	—	—	54
	DXR-LCL 10 mg	—	—	—	—	88
	DXR 5 mg	—	—	—	—	44
	DXR-LP 5 mg	—	—	—	—	42
	DXR-LCL 5 mg	—	—	DOX	—	68
	DXR 10 mg	—	—	—	—	62
	DXR-LP 10 mg	—	—	—	—	65

TABLE 12: (*continued*)

Study	Group	Tumor	Mouse	Drug	TV at start (mm^3)	TIR
	DXR-LCL 10 mg	—	—	—	—	91
Vaage 1993a[378]	DOX 3 × 6 mg/kg	HEY human ovarian	nude	DOX	45	6
	DOX 3 × 9 mg/kg	—	—	—	—	23
	Doxil 3 × 6 mg/kg	—	—	—	—	64
	Doxil 3 × 9 mg/kg	—	—	—	—	50
Vaage 1993b[379]	Oncovin 3 × 1.0 mg	MC2 murine mammary	C3H/He	VCR	40	39
	Oncovin 3 × 1.3 mg	—	—	—	30	42
	S-VCR 3 × 1 mg	—	—	—	58	56
	S-VCR 3 × 1.3 mg	—	—	—	20	86
	S-VCR 3 × 0.5 mg	—	—	—	89	18
	S-VCR 3 × 0.7 mg	—	—	—	27	75
	S-VCR 3 × 1.0 mg	—	—	—	10	81
	DOX 3 × 6 mg	—	—	DOX	52	14
	Doxil 3 × 1 mg	—	—	—	83	36
	Doxil 3 × 3 mg	—	—	—	52	60
	Doxil 3 × 6 mg/kg	—	—	—	10	94
Vaage 1994a[380]	DOX 4 × 6 mg/kg	PC3 human prostate	nude	DOX	2	58
	DOX 4 × 9 mg/kg	—	—	—	—	67
	Doxil 4 × 6 mg/kg	—	—	—	—	82
	Doxil 4 × 9 mg/kg	—	—	—	—	82
	DOX 4 × 9 mg/kg	—	—	—	—	57
	Doxil 4 × 9 mg/kg	—	—	—	—	69
Abraxane						
Desai 2008 [82]	Abraxane 15 mg/kg	MX-1	nude	PTX	—	80
	Docetaxel 15 mg/kg	—	—	—	—	29
	Abraxane 50 mg/kg	LX-1 human hepatic	—	—	—	84

TABLE 12: (*continued*)

	Abraxane 120 mg/kg	—	—	—	—	98
	Docetaxel 15 mg/kg	—	—	—	—	61
	Nab-paclitaxel (120 mg/kg)	MDA-MB-231 human breast	—	—	—	99
	Nab-paclitaxel (180 mg/kg)		—	—	—	98
	Docetaxel 15 mg/kg		—	—	—	78
	Abraxane 50 mg/kg	MDA-MB-231/ HER2 +	—	—	—	94
	Abraxane 120 mg/kg		—	—	—	99
	Docetaxel 15 mg/kg		—	—	—	96
	Abraxane 50 mg/kg	PC3 human prostate	—	—	—	94
	Abraxane 120 mg/kg		—	—	—	99
	Docetaxel 15 mg/kg		—	—	—	97
	Abraxane 50 mg/kg	HT29 human colorectal	—	—	—	50
	Abraxane 120 mg/kg		—	—	—	65
	Docetaxel 15 mg/kg		—	—	—	36
Desai 2006[81]	Cremophor-Taxol	H522 lung	—	PTX	155	—
	Abraxane		—	—	—	100
	Abraxane	MX-1 breast	—	—	100	100
	Cremophor-Taxol	SKOV-3 ovarian	—	—	165	—
	Abraxane		—	—	—	75
	Cremophor-Taxol	PC3 human prostate	—	—	165	—
	Abraxane		—	—	—	99
	Cremophor-Taxol	HT29 colon	—	—	180	—
	Abraxane		—	—	—	50
Huang 2019[184]	Abraxane 5 × 20 mg/kg	BCap37 human breast	—	PTX	51	52

Note that earlier studies were reported only in abstract form and thus not included in this analysis.

of the studies, chemotherapy was combined with photo-dynamic therapy (PDT), photo-thermal therapy (PTT), or magnetically induced thermal therapy (MTT). Three studies with PDT and three studies with TT but without another drug are included. Some papers present multiple formulations so, where practical, data/results will be presented for each of the different formulations. Studies in which the drug was injected directly into the tumors are not included in this analysis.

A detailed analysis is provided for the formulations with DOX alone (50 studies), DOX combined with thermal therapy (22 studies), DOX combined with photodynamic therapy (7 studies), or DOX combined with radiation therapy (one study). Figure 2 presents the size, zeta potential and loading capacities of the various formulations included in the analysis and Fig. 3 the percent TIR and Fig. 4 a plot of mean and 95% confidence interval for comparisons by ANOVA. All groups are different from both free-DOX and MSN-DOX by ANOVA followed by a Dunnett *post hoc* test ($p < 0.01$ in all comparisons).

Drug release is a critical feature of a drug carrier. If the drug is released too quickly in the plasma space, the advantage of employing the carrier is largely lost. If the drug releases too slowly, or incompletely, the cancer treatment efficacy is not optimal. High "burst" release has been a particular problem for Nanomedicine drug carriers. As described

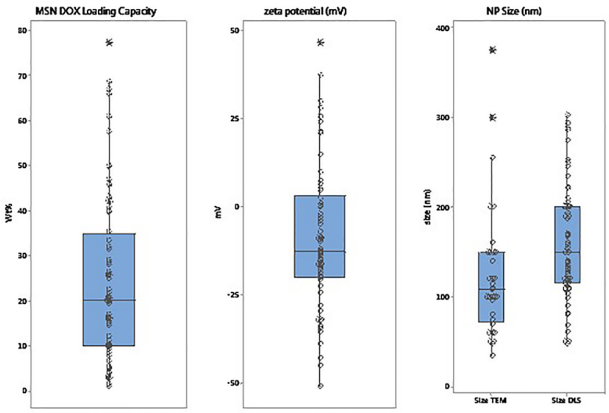

FIG. 2: Comparisons of loading capacity (LC), size by SEM/TEM and DLS and zeta potential for the formulations that include DOX without other drugs

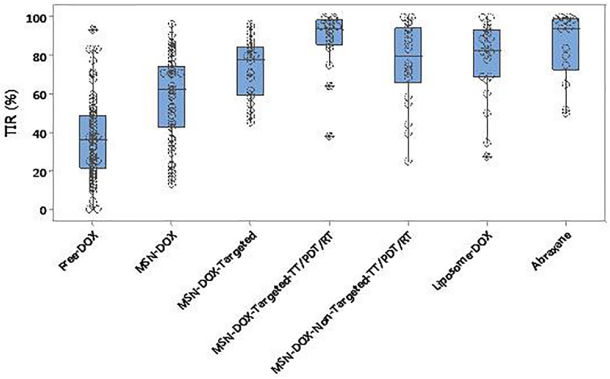

FIG. 3: Comparisons of TIR for the formulations that include DOX. F-DOX (free DOX; $n = 89$); NP-DOX (MSNs containing DOX without targeting (T), photodynamic therapy (PDT) or thermal therapy (TT); $n = 53$). NP-DOX-T (targeted MSNs carrying DOX; 27); NP-DOX-T-TT/PDT/RT (targeted MSNs carrying DOX combined with TT, PDT or RT; $n = 18$); NP-DOX-NT-TT (non-targeted MSNs carrying DOX plus TT/PDT or RT; $n = 26$); Lipo-DOX (pegylated liposomal DOX; $n = 22$); Abraxane (nab-paclitaxel; $n = 14$).

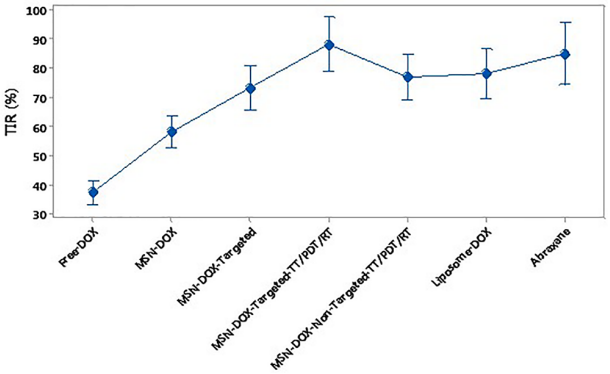

FIG. 4: Mean and 95% confidence interval for TIR. The pooled standard deviation is used to calculate the intervals. All groups are different from both free-DOX and MSN-DOX by ANOVA followed by a Dunnett *post hoc* test ($p < 0.01$ in all comparisons). Groups names are provided in Fig. 3.

previously, a negatively charged carrier (like MSNs) carrying a positively charged drug (like DOX-HCl) will generally not undergo "burst" release but will hold onto a high percentage of the cargo (drug) until it reaches an environment with a "low" pH. Drug

release data were extracted from the published plots and the measured or predicted release of various formulations at various conditions at 48 h was plotted (Fig. 5). For experiments that were not carried out to at least 48 h, the data were fit to a model to predict the 48 h cumulative release. The cumulative release of DOX from MSNs suspended in buffer (typically PBS) at ~ pH 7.4 and with exposure to ~ pH 5.5 (between 5 to 6), following molecular stimulation (e.g., GSH, enzyme, ROS) at either ~ pH 7.4 or ~ pH 5.5 and/or following exposure to an external stimulus (NIR, RF, AMF) is presented. However, the specific conditions varied considerably. Generally, the external stimulus increased the temperature of the buffer solution to ~ 42°C or greater.

Drug release from nanoparticles is generally measured either by (1) incubating the drug loaded nanoparticles and periodically spinning down a sample and measuring the amount of the drug in the supernatant or (2) by using a dialysis membrane and monitoring the amount of drug that has leaked from the nanoparticles and crossed the dialysis membrane into a reservoir of dialysate. Yu et al.[145] compared the release of DOX from Doxil using regenerated cellulose (RC) and biotech-grade cellulose ester (CE) dialysis membranes of various molecular weight cutoff (MWCO). For RC type dialysis membranes a MWCO of 8–10 kDa appeared sufficient, but for CE type membranes the MWCO of at least 50 kDa should be used to minimize the error due to the delay in released drug crossing from the donor compartment to the receiver compartment. Including a free-DOX group should be used to correct the errors in release measurements using dialysis membrane tubing. However, the experiment in[145] was done at 45°C to accelerate release and therefore the actual rate reported cannot be compared with that from MSNs. Russell et al.[142] on the other hand, reported slow DOX release (leakage) from Doxil, 20–30% at 12 d at 37°C. About 50% of the studies included in this paper measured drug release using the dialysis method, but several did not state the MWCO and none clearly identified the membrane type. Only one study included a curve for free-DOX. It is likely that for many of the studies, the true release kinetics is faster than what was reported. However, for the purpose of the analysis of this paper, the error is not likely of practical significance. Nevertheless, the release of DOX from MSNs at normal pH with no other stimulation is typically slow. Even at low pH, or following a molecular or external stimulus, the cumulative release reaches 100% by 48 h in only a few cases.

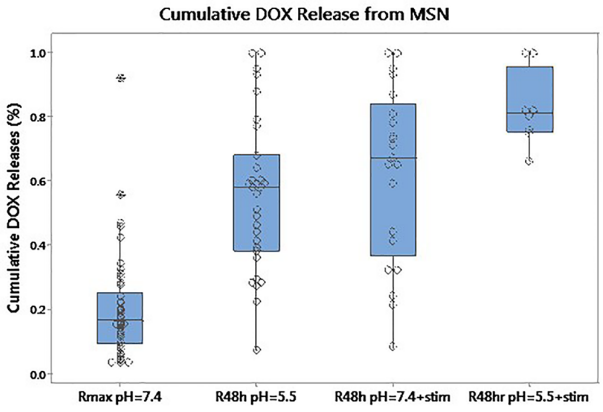

FIG. 5: DOX release from MSNs under various conditions. Stimulation (stim) includes cytosolic or intracellular molecular stimulation, or stimulation by an external energy source. Rmax: maximal release. R48: release at 48 h.

IV. DISCUSSION

This paper provides a review and analysis of the application of mesoporous nanoparticles for drug delivery for cancer and compares against pre-clinical, *in vivo* studies of PEGylated liposomal DOX (e.g., Doxil) and human albumin-bound paclitaxel (nab-paclitaxel, Abraxane, ABI-007). Only *in vivo* studies that reported drug release from the MSNs and tumor volume response to treatment were included. Several of the MSN formulations had a core-shell structure, several had coatings or chemical constructs to cap the pores to restrict/control drug release, and some formulations had hollow cores to improve drug loading capacity (Table 7). Studies varied considerably in the drug dose, the dosing schedule, tumor model and the size of the tumor at the start of the treatment. A total of 166 published studies were reviewed for this paper. The majority of the formulations used CTAB (122) or CTAC (27) as the template, and seven used the standard Stöber technique without a template. While not

strictly mesoporous based on the synthesis method, the authors using the Stöber technique referred to their particles as such, with the exception of one[20] (but that study was included in this analysis because three different sizes of particles were directly compared). The MSNs were commercially obtained for two of the studies. Other templates besides CTAB or CTAC were also used (Table 7). Some studies did not report the template used. One formulation included a porous silica shell over a liposome, but did not use a traditional template. The data analyzed statistically and graphically (in the figures) are from the 80 studies that used DOX but without other chemotherapy drugs (other than drugs to induce TT or PDT).

For these 80 studies, regression analyses between LC and NP size, charge, hollow or solid core, shell, coating, presence or absence of PEG, or type of template used were all not correlated. There was also no correlation between TIR% and these variables. There was however a statistical difference in the electron microscope measured size based on surfactant (template). The use of CTAC (71 ± 26 nm) resulted in smaller particles than CTAB (120 ± 45) with $p < 0.0001$. Although it was expected that LC would be higher in hollow compared with solid core MSNs and that TIR would correlate to LC and MSN size, the pooled data from the studies did not support these hypotheses. This is not surprising given the variability among studies of tumor model, tumor size at the start of treatment, dose, dose schedule, length of the study, nanoparticle formulation (physical and chemical characteristics) etc. Nevertheless, in terms of tumor inhibition, there is a clear benefit to targeting and combining with TT or PDT (Figs. 3 and 4).

A recent article evaluated the effect of the surfactant/template removal step on the polydispersity of the particles, the BET surface area and pore size.[146] The colloidal stability of MSNs was analyzed by dynamic light scattering (DLS) and differential centrifugal sedimentation (DCS) and particle aggregation subjectively evaluated by SEM. The methods compared were calcination, solvent extraction and dialysis. The pore size was largest using solvent extraction (EtOH:NH_4NO_3). However, the dialysis method (with EtOH:AcOOH dialysate) was better for preserving particle size and reducing particle aggregation. However, the dialysis method described requires a considerable amount of relatively expensive dialysate and is relatively time-consuming. Calcination appears to be best at removing organics from the final product, but also results in the highest amount of aggregation and decreases the pore size. The analysis from the studies included in this paper is inconclusive in terms of the effects of the surfactant/template removal process on particle size or other characteristics. The BET surface area, pore volume and pore size were reported in many of the studies but reported inconsistently.

Li et al.[147] compared the TIR of MSNs carrying DOX with different pore sizes and drug LC. The MSN size was ~ 130 nm, charge ~ –36 mV, pore sizes were 2.3, 5.4, and 8.2 nm, pore volumes were 0.492, 1.229, and 1.697 cm^3/g, and the LC values were 8.2, 21.1, and 21.1 wt% respectively. The TIR calculated were 85%, 97%, and 93%, respectively, suggesting a likely correlation between TIR and LC. Tang et al.[20] evaluated camptothecin-silica nanoconjugates of 25, 53, and 199 nm sizes (by TEM, 44, 65, and 238 nm, respectively, by DLS). LC was 16.6 wt% and charge was near neutral for all three sizes. TIR was 43%, 74%, and 34% for the small, medium and large nanoparticles respectively. Finally, Ma et al.[148] compared 20, 40, and 80 nm size MSNs (by TEM, 24, 44, and 106 nm, respectively, by DLS) loaded with PDT anticancer ruthenium complex (RuPOP) and conjugated with folate acid (FA). The MSN charge ranged from 19 to 37 mV. TIR was 46%, 43%, and 38% for the small, medium and large nanoparticles, respectively. These studies suggest that TIR may be correlated with LC and carrier size, but that other factors related to the MSN formulation and animal model and drug dosing are also important and therefore controlled experiments must be designed to adequately test such hypotheses.

Some of the studies reviewed deserve a closer look. Liu et al.[149] described an elegant method of "manufacturing" a 20 L batch irinotecan loaded "silicasome." The paper provided a detailed toxicity analysis and physiochemical characterization. Their study should serve as a model for the level of detail needed in order to establish feasibility supporting a clinical trial. However, the increased

life survival (ILS) for the model (colorectal tumor "chunk" surgically implanted into the cecum) was only ~ 39%. The TIR (58%) result was not as impressive as many of the other formulations reviewed. In Tables 8–11, the TIR that reached at least 99% are highlighted. From Fig. 3, we observe that the TIR of MSN-DOX formulations that incorporate TT compare favorably to PEGylated liposomal DOX. However, except when in combination with TT, in none of the MSN-DOX studies (with or without targeting) did the TIR reach 100%. Most of the TT studies required exposure of the tumor to NIR light for at least several minutes. This may not be very practical in a human clinical setting, except perhaps as part of a surgical procedure. Lu[150] delivered CPT with folic acid (FA) targeting that reached 100% TIR. Interestingly, the non-targeted formulation performed almost as well (99% TIR). Of course, even 100% TIR does not necessarily mean that the cancer has been eradicated, just that it was not palpable. Only long-term survival studies can prove "cure."

Drummond et al.[11] published a comprehensive review of pre-clinical and clinical studies of liposomal-based chemotherapeutics, appearing 4 years after Doxil was approved by the FDA. It provides an excellent comparison of various liposome formulations, PD-PK, drug accumulation, and survival rates. The percent ILS was reported for 16 pre-clinical studies, with different tumor models, different drug doses, and different treatment schedules. Considering Doxil specifically (5 experiments), the ILS ranged from 40% to 116%. Considering PEGylated DOX loaded liposomes more broadly (two experiments with PEG-DSPE/DSPC/Chol), the ILS was 144% in one and 168% in another. This demonstrated the wide variability expected in studies with different experimental designs, even for an approved (or soon to be approved) nanoparticle anti-cancer formulation. Of the MSN studies reviewed in this paper 18 performed survival studies (Table 13), with ILS of the MSN group ranging from a low 15% to a high of 133%, with one study reporting 100% animals surviving > 50 d and another with 100% surviving > 60 d. However, the length of survival studies reported for liposomal DOX was generally longer (60–120 d).

In the years after the approval of Doxil, numerous studies have been published evaluating tumor targeting or newer chemotherapy against PEGylated liposomal DOX formulations in tumor-bearing mice.[151–170] The studies evaluated in this paper for the TIR of PEGylated liposomal DOX in tumor-bearing mice were published mostly between 1990 and 2002, but there was also a very interesting study published in 2020.[167] In that recent study Singh et al.[167] evaluated the response to Doxil of human ovarian tumors inoculated into mice as individual cells (2D model) and after growing spheroids (3D model) and reported that the 3D tumor response was very good and was enhanced even further by combining with Avastin. The 2D tumor model response was lower. Also interesting, the response of the 2D model to free-DOX was better than the response of the 3D model to free DOX. A study by Brouckaert et al.[155] evaluated Doxil in B16BL6 murine melanoma and found that Doxil did not perform well, but response was enhanced by adding tumor necrosis factor-α (TNF). The animals received 1 × 4.5 mg/kg + 4 × 1 mg/kg equivalent doxorubicin. These examples demonstrate the importance of the model on results as well as the potential for enhancing efficacy with companion therapies.

In the three years following the approval of Abraxane, Desai et al.[81,82] published studies in several different tumor-models in mice and found quite variable results. MDA-MB-231 (breast), (H522 (lung) and MX-1 (breast) responded very well, SKOV-3 (ovarian) and PC-3 (prostate) responded well, but the tumors continued to grow in volume after the end of treatment, while the response of HT29 (colon) tumors was not much better than Cremophor-based paclitaxel. Karmali et al.[171] found virtually no inhibition of MDA-MB-435 tumor (cells originally identified as breast, but now known to be melanoma). Desai et al.,[82] Shao et al.,[172] and Yang et al.[173] investigated tumor response to Abraxane with respect to expression of SPARC (secreted protein acidic and rich in cysteine) and HER-2 (human epithelial growth receptor). Desai found that efficacy of Abraxane was higher in HER-2-negative tumors and in HER-2 positive tumors with high expression of SPARC. Yang observed very good tumor inhibition (98.8%) of Abraxane in an osteosarcoma model

TABLE 13: Percent increased life survival (ILS) of MSN groups

Author	Group	Targeting	Tumor	Mouse	Drug	Dose	TV at start	ILS %
Jin 2018[287]	MSN-Fe-AuNP	N/A	WHU-HN6- human squamous	nude	DOX	10	100	25
	DOX	—	—	—	—	—	—	38
	MSN-Fe-AuNP-DOX	—	—	—	—	—	—	63
	MSN-Fe-AuNP + NIR	—	—	—	—	—	—	80% > 28 d
	MSN-Fe-AuNP-DOX + NIR	—	—	—	—	—	—	100% > 28 d
Kang 2019[253]	DOX	HA/CD44	4T1 mouse epithelial breast	NR	DOX	5 mg/kg	86	–32
	oHA-DOX@ MSN/HAP	—	—	—	—	—	—	100% > 60 d
Liu 2016[260]	DOX	N/A	HepG2 human liver	nude	DOX	9 × 3 mg/kg	100	0
	HMSNs@DOX	—	—	—	—	—	—	24
	HMSNs-b-CD/ Ada-PEG@DOX	—	—	—	—	—	—	48% > 60 d
Liu 2019b[257]	DOX	HA/CD44	A549- human alveolar carcinoma	nude	DOX	8 × 5 mg/kg	100	57
	HA-JMSN/ DOX-DMMA	—	—	—	—	—	—	70% > 40 d
Ramaya 2017[263]	DOX	FA	EAC murine Ehrlich ascites carcinoma	Balb/c	DOX	14 × 1 mg/kg	145	70
	Lipodox	—	—	—	—	—	—	80
	Au@ SiO_2-DOX-CS-FA	—	—	—	—	—	—	125
Zhoa 2018[277]	DOX	N/A	MCF-7/MDR human breast	SCID	DOX	5 mg/kg	100	NR
	DOX@ MSN-TPGS	—	—	—	—	—	—	15
Zhou 2018[279]	DOX	Tf	MDA-MB-231 human breast	nude	DOX	7 × 1 mg/kg	110	13

TABLE 13: (*continued*)

	HMSN-S-S-Tf@ DOX	—	—	—	—	—	—	65% > 60 d
Zhu 2017[280]	DOX	VEGF	SH-Sy5Y	nude	DOX	7 × 5 mg/kg	150	32% > 11 d
	SiO_2@LDH-DOX	—	—	—	—	—	—	83% > 11 d
	SiO_2@ LDH-Bev-DOX	—	—	—	—	—	—	100% > 11 d
Wang 2019[300]	DOX	Mag	MCF-7/MDR human breast	nude	DOX; Ce6	3 mg/kg	200	98
	nanocomposite +	—	—	—	—	—	—	35% > 35 d
Wang 2018[197]	GNR/Ppy/m-SiO_2 + Laser	N/A	CT26 mouse colon	Balb/c	DOX	1 × 5 mg/kg	100	100% > 30 d
	GNR/ Ppy/m-SiO_2-DOX	—	—	—	—	—	—	73
	GNR/Ppy/m-SiO_2-DOX + Laser	—	—	—	—	—	—	100% > 30 d
Zhong 20200[294]	GNR@HPMO@ PVMSN–DOX	N/A	H22	nude	DOX	1 × 5 mg/kg	200	16
	GNR@HPMO@ PVMSN–DOX + NIR	—	—	—	—	—	—	100% > 50 d
Ansari 2018[318]	EPI	Mag	C-26 murine colorectal	nude	EPI	9 mg/kg	20	NR
	MSMN + EPI(MAG +)	—	—	—	—	—	—	35% > 35 d
Fei 2017[326]	ATO-sol	RGD	H22 murine hepatic	ICR	ATO	15 × 1 mg/kg	50	10
	RGD-LP-CHMSN-ATO	—	—	—	—	—	—	65
Liu 2019[149]	IRIN	N/A	MC38 murine colorectal (orthotopic)	C57BL/6	IRIN	4 × 40 mg/kg	NR	11
	Onivydne	—	—	—	—	—	—	7
	IR-silicaosome	—	—	—	—	—	—	39

TABLE 13: (*continued*)

Author	Group	Targeting	Tumor	Mouse	Drug	Dose	TV at start	ILS %
Liu 2018[367]	ICG	N/A	MCF-7	nude	ICG	9 × 1.2 mg/kg	100	8
	AuNR@ MSN-ICG	—	—	—	—	—	—	27
	AuNR@ MSN-RLA/ CS(DMA)-PEG	—	—	—	—	—	—	31
	AuNR@MSN-ICG-RLA/ CS(DMA)-PEG	—	—	—	—	—	—	50% > 60 d
Tao 2019[349]	ATO-sol	angiopep-2 peptide	C6 rat glioma (intra cranial)	Rat	ATO	8 × 1 mg/kg	NR	29
	ANG-LP-PAA-MSN@ATO	—	—	—	—	—	—	133
Wu 2020[351]	HMSNs (H)	N/A	PC-3	nude	ICG; paclitaxel	1 × (5; 4) mg/kg	100	0
	HMSNs-PAA (HP)	—	—	—	—	—	—	10
	CaO2 (C)	—	—	—	—	—	—	10
	CaO2@HMSNs-PAA (CHP)	—	—	—	—	—	—	60% > 14 d
Yang 2019[365]	MSNR@Au-TPPS4(Gd) + 660nm	N/A	4T1	Balb/c	TPPS4 (PTT sensitizer)	15 mg/kg	100	20% > 40 d
	MSNR@Au-TPPS4(Gd) + 808nm	—	—	—	—	—	—	39% > 40 d
	MSNR@Au-TPPS4(Gd) + 808/660nm	—	—	—	—	—	—	80% > 40 d

ILS = 100*(treated mean survival)/(control mean survival) – 100. Mean survival time is determined from a Kaplan-Meier plot as (number of days of the first death + number of days of the last death)/2.

with high SPARC expression. Conversely, Shao[172] found no increased response to Abraxane in SPARC positive NSCLC. Beyer et al.[174] demonstrated that the epithelial junction opener JO-1 improved the efficacy and safety of Doxil, Abraxane, and other chemotherapy drugs. In subsequent years, various non-albumin-bound formulations of nanoparticle-PTX were investigated in tumor-bearing mice to demonstrate improved outcomes compared with Abraxane.[175–188] Again, these studies suggest that the selection of the tumor model is critical and adding companion therapies might improve clinical outcomes in some carefully selected patients.

The synthesis of drug-loaded MSNs is very different from that of liposomes and protein-bound drugs. However, the size and loading capacities of the MSN formulations are similar to those of liposomal and protein-bound drugs. Liposomes are formed by the hydration of a thin lipid film, and the loading capacity of remote loaded liposomal doxorubicin is as high as 0.25 mg drug/mg lipid, or 25 wt%, and the size is about 100 nm in diameter.[11] The composition of the lipid was highly optimized, as reviewed by.[11] Liposomes can be synthesized within a narrow size distribution, which is controlled by extrusion through nano-porous membranes. High drug loading (up to 98% efficiency) is driven by a high liposome transmembrane ammonium salt (pH) gradient.[141] Abraxane, on the other hand, contains 10 wt% paclitaxel and a diameter between 130 and 150 nm[189,190] (see also the Abraxane package insert). It is prepared by high-pressure homogenization of paclitaxel with human serum albumin. The improved efficacy of Abraxane is likely not due to tumor EPR since it is reported that "upon dilution, nab-paclitaxel nanoparticles quickly dissociated into soluble albumin-paclitaxel complexes with size similar to native albumin."[191]

There was wide variability in the size and loading capacities of the MSN formulations reviewed (Fig. 2). The loading capacity of MSN-DOX-only formulations analyzed in this paper ranged from a low of only 1 wt%[192] to a high of 77 wt%[193] with a mean of 25 wt% and median of 20 wt%. A hollow core did not correlate to LC; range of 10 wt% to 50 wt%, mean 30% and median 35%. The high 77 wt% LC formulation was 150 nm (by electron microscopy, DLS size not provided) had a MSN core capped with black phosphorous quantum dots for PTT with exposure to near infrared laser, was targeted against folic acid (FA) and resulted in 94% TIR against H22 murine hepatic tumors. The DOX release at pH 7.4 was about 35% at 32 h, about 50% at pH 5 without exposure to the laser and over 70% at pH 5 and exposure to laser. The DLS (hydrodynamic) size of the MSN-DOX-only formulations ranged from 48 nm[194] to 302 nm,[195] with a mean of 159 nm and a median of 150 nm (not including one outlier of 750 nm and two of 600 nm). Nineteen of the MSN-DOX-only formulations were larger than 200 nm (by DLS). One of the 600 nm MSN formulation[196] was unusual in that it had a 14 nm Fe_3O_4 core, but the TEM size of the core-shell MSNs was reported to be only 114 nm. Although the hydrodynamic size of the MSN is always larger than the size by SEM/TEM, and correlates well, this difference (600–114 nm) is an outlier. These MSNs are peptide and targeted using an external magnet resulting in a TIR of 84%. They were designed to be enzyme (MMP-2) responsive and the DOX is predicted to reach 100% cumulative release in the presence of enzyme. The other 600 nm MSN formulation consisted of a 9 × 145 nm gold nanorod core to induce PTT upon exposure to near infrared laser.[197] The loading capacity was 69% and the TIR was 99% against C26 mouse colon tumor. The rod shape likely overestimates the DLS size. A third apparent outlier was a 750 nm MSN.[198] These MSNs consist of a Fe_3O_4 core that served as a template for growing a MSN shell with very large pores containing ultra-small Fe_3O_4 nanoparticles. The large pores also provide for a high LC (46 wt%). They are FA targeted and AMF stimulated for MTT and drug release. The TIR was 88% in MCF-7 tumors. The cumulative DOX release at 48 h was not much different between the sample at pH 7.4 not exposed to AMF (44%) compared with the sample exposed to AMF (48%). DOX release was not measured at low pH. The zeta potential of the MSN formulations in this paper ranged from –51.0 mV[199] to +46.7 mV[200] with mean –8.9 mV and median –12.8 mV. The MSN size and charge did not correlate to TIR%, suggesting that other characteristics have a greater effect.

The mean drug loading and size of the MSNs compare favorably to Doxil and Abraxane. The

highest level of TIR for the DOX-only, non-targeted MSN formulation (without TT or PDT) was 97% (against H22 murine hepatic tumor).[147] These MSNs had negative ZP (–35 mV) and 134 nm size (by DLS) and DOX release was about 78% at 24 h at pH 7.4. Even with targeting, only four DOX-only formulations without TT or PDT achieved greater than 95% TIR.[201–204] The MSNs reported by Gao et al.[201] demonstrated TIR of 96% (against H22 tumor). These near neutral MSNs were 131 nm (by DLS) with LC of 15 wt% and targeted to FA. These particles were interesting in that they possess a solid SiO_2 core and porous SiO_2 shell coating. DOX release reached only 27% after 48 h at pH 5. The MSNs by Turan et al.[202] reached 99% TIR (against GL261 tumors). These were 74 nm (by TEM) targeted to both RGD and CREKA (on separate MSNs) with Fe_3O_4 cores. DOX release was stimulated by RF (without increasing temperature). The LC was 20 wt%. The drug release without RF stimulation was low (4%) but with 30 min of RF stimulation the cumulative DOX release reached 66% and reached 90% with 2 h of stimulation. The *in vivo* therapy study consisted of 60 min exposure to the RF following MSN administration. This formulation may be more practical than exposure to NIR light since RF exposure might be applied systemically. But achieving uniform and desired RF in a large body region will also be a challenge. Six of the MSN-DOX-only formulations with TT achieved 99 or 100% TIR.[197,205–209] Although promising, requiring exposure to NIR light may be difficult to implement clinically and limited to localized disease.

Of the formulations combining DOX with another drug, six reached at least 95% TIR.[64,210–214] Three are of particular interest because they do not depend on external stimulation. A formulation combining DOX and MPH in a core shell structure of an MSN surrounded by a cancer cell membrane and lipid achieved 95% TIR (MCF-7 tumor).[212] However, this formulation seems to be quite complicated with formidable regulatory and manufacturing hurdles before becoming a commercially marketed product. Another formulation[215] reached 97% TIR (in H22 tumors). These dendritic MSNs combined DOX and survivin shRNA-expressing plasmid. The third combined DOX with Bcl-2 siRNA (97% TIR in MCF-7 tumor).[214] Of the MSN non-DOX formulations, eight reached TIR of at least 95%.[150,216–222] Six depend on an external stimulus and five are targeted. So, the best performing MSN formulations compare favorably to Doxil and Abraxane in tumor-bearing mice, but is that enough to warrant further development of these particular formulations, or are there other considerations and thus further improvements that must be made?

Long circulating liposomal doxorubicin and nab-paclitaxel were initially proposed to modify the PK-PD and reduce toxicities, cardiac toxicity in the case of liposomal doxorubicin and toxicities associated with the Cremophor solvent in the case of nab-paclitaxel, but pre-clinical data showed impressive improvements in survival over free doxorubicin and Cremophor-based paclitaxel, respectively. He et al. recently provided a review of nanomedicine clinical trials.[223] The authors state that there have been "marginal prolongations in the clinic." Doxil (and equivalent) in breast cancer patients found no improvements in progression-free survival, overall survival or overall response rate. Outcomes were more promising for ovarian cancer and myeloma. Abraxane showed statistically significant prolongations for breast cancer, pancreatic adenocarcinoma and non-small-cell lung cancer patients. Again, selection of patient populations is important since the therapies may be effective only in particular cancer types, with (as yet) unknown specific characteristics. However, certainly the hoped-for cure has not been realized as prolongation was on the order of days or weeks.

Petersen et al.[165] provided a meta-analysis of pre-clinical and clinical (randomized) studies comparing liposomal to conventional non-liposomal doxorubicin and found that "efficacy in patients was not different between liposomal and conventional chemotherapy as assessed by objective response." Their analysis also found that "in contrast with clinical results, animal studies showed significantly increased survival in mice." Conclusions from the paper: "…discuss the possible reasons why the pharmacological advantages of carrier mediated chemotherapy did not translate into enhanced clinical efficacy including the role of the enhanced permeability and retention (EPR) effect and

the tumor microenvironment, the optimal dosing regimen for carrier mediated agents, and the lack of standardization in the conduct and reporting of preclinical studies evaluating anticancer efficacy of these agents. Our study shows that the full clinical potential of carrier-mediated drugs remains to be realized and highlights some of the critical knowledge gaps that must be addressed in order to move the field forward." Other critical knowledge gaps include a thorough understanding of how the rate of drug release and the precise location of the drug release (intracellular or interstitial) affects tumor response, and what is optimal. There is considerable evidence that drug pegylation interferes with cellular internalization. It is also not fully understood if subsequent doses of pegylated drugs leads to increased clearance, the so-called "PEG dilemma." Clearly there are substantial differences between human disease and animal models. Compared with human disease, most animal models use immune compromised mice, with well-defined and homogenous localized disease and large tumor burden. Study time-spans are shorter and cancer recurrence is typically not studied. But, even in the pre-clinical studies, out of 11 studies analyzed, only 4 had $p < 0.05$ comparing overall survival, though when combined there was an overall $p < 0.0001$. A more recent meta-analysis of clinical studies compares liposomal to conventional cisplatin in patients with non-small-cell lung cancer.[224] As already well established, the liposomal form reduced toxicities, but there was "no significant difference in partial response or stable disease." So, is there evidence to suggest that other nanoparticle formulations will do better? Do the data demonstrate a high potential for MSN formulations to provide outcomes better than Doxil, Abraxane and other already approved nanomedicines? Several of the formulations reviewed in this paper showed excellent response, particularly those that included "active" targeting and combination therapy, multiple anti-cancer drugs, photodynamic therapy (PDT) and/or thermal therapy (TT). However, much more research is needed to bring any of these formulations into human trials, particularly manufacturing at scale and the development of technologies for applying PDT and TT to metastases. Nevertheless, if the following recommendations are followed by the research community perhaps the questions can be answered in the affirmative.

A. Recommendations

The following is a list of recommended nanomedicine characteristics that should be reported in all studies:

- Size (SEM/TEM and hydrodynamic). If size measured by SEM/TEM provide details of how many particles were measured.
- Size distribution (PDI or SD)
- Charge (in H_2O, PBS and in the presence of plasma proteins)
- Shape (SEM/TEM)
- Stability
- Drug-loading capacity (%wt/wt)
- Mechanisms of drug loading (bound, encapsulated, adsorbed, etc.)
- Drug release kinetics (in H_2O, PBS, serum or plasma proteins at physiological temperature and pH)
- When dialysis is used for release kinetics: type and MWCO of dialysis membrane
- Short-term and long-term release kinetics (to be able to extrapolate to > 90% release)
- Initial and late drug release rates
- Change in size, size distribution and charge in plasma
- Detailed description of synthesis
- Cell toxicity IC_{50} for nano-formulations compared with free drug.
- Surface area, pore size and pore volume (for porous structured systems)
- Storage conditions and changes in chemical and physical characteristics after storage, in particular after drying and resuspending
- Yield

The following is a list of recommended nanomedicine characteristics that should be reported in *in vivo* studies:

- Tumor type, source and if implanted as cells or tumor tissue
- Strain and weight (or age) of animal
- Location of implant

- Dose (in mg/kg of active drug), administration route, dose schedule
- Size (volume) of tumor at start of treatment
- *Ex vivo* tumor weight at end of study
- Tumor inhibition ratio (TIR)
- Comparison with free drug or comparable clinical drug treatment
- Rationale for selection of dose and dose schedule relative to that of clinical drug treatment
- Comparison group of commercially available drug carrier with the same or similar drug
- Survival studies should be > 120 d or until all animals have died or reached a health endpoint criteria

V. CONCLUSION

Impressive strides have been achieved in the development of MSNs for cancer therapy and the data to date are very promising. Some formulations appear to compare favorably to FDA approved Doxil and Abraxane in pre-clinical studies. However, formalizing experimental design and data reporting among research groups and making the data available in a repository (such as[127]) for more detailed analysis is needed in order to start making sense of the huge amount of data becoming available and to make the incremental improvements necessary for commercial and clinical success. Perhaps such an effort can ultimately provide sufficient evidence for an entrepreneur to make the needed investment to bring some of these promising formulations to the clinic. If the requirement for consideration of an MSN formulation to be considered for further development is how it compares to already approved formulations such as Doxil and Abraxane, it might be hard to justify the high cost that will inevitably be required to bring such products through testing and into the market. Potential advantages that MSNs have over liposomes cited in the literature include: wider array of drugs that can be incorporated, greater drug release control, potentially greater stability in circulation, prolonged drug release (which may or may not be beneficial), the inherent ability to release positively charged drugs in a low pH environment, or design thiol cleavage of the drug for release in the high glutathione tumor environment (which has not been proven to occur *in vivo*), potentially higher loading capacity (as demonstrated by some formulations) and perhaps greater flexibility for "active" targeting and delivering multiple drugs simultaneously. Studies should carefully consider a dose and dose schedule that more closely resemble the human clinical setting and compare to existing approved formulations. Studies are needed that carefully examine how drug release rate affects outcomes and if a low pH, high glutathione environment actually occurs *in vivo* and if so, how uniform and for what cancers. Studies need to be designed with models of metastatic disease and with realistic tumor volumes at the start of therapy. Survival studies need to be performed, and extended to 120 d. Attention must be given to design for manufacturing, sterilization, and minimal endotoxin levels, residue levels of surfactant and other chemicals, etc. Such therapies are unlikely to be first-line therapy, so nanomedicine use in combination with first-line therapies should be studied. Only then can an informed decision be made as to the clinical (and thus commercial) potential of the newly proposed drug delivery formulation.

Considering the versatility of MSNs for drug delivery compared with liposomes it seems likely that one or more formulations will eventually make it into clinical trials. Despite somewhat limited (but real) efficacy advantages of liposomal doxorubicin over free drug, it has been a commercial success. The systemic toxicity of silica is low and therefore toxicity should not be a major limitation. Given the extensive infrastructure for porous silica nano and microparticle synthesis for industrial applications, the likelihood of overcoming the manufacturing barrier is promising. However, the better-performing MSN formulations analyzed in this paper are rather complex and therefore the manufacturing will be more complex than for MSNs used as sieves and other industrial applications. Nevertheless, I believe that the primary factors limiting the development of MSNs for cancer therapy are market and regulatory uncertainties limiting capital investments.

REFERENCES

1. Gerlowski L, Jain RK. Microvascular permeability of normal and neoplastic tissues. Microvasc Res. 1986;31:288–305.
2. Jain RK, Gerlowski LE. Extravascular transport in normal and tumor–tissues. Crit Rev Oncol Hematol 1986;5:115–70.
3. Matsumura Y, Maeda H. A new concept for macromolecular therapeutics in cancer–chemotherapy – mechanism of tumoritropic accumulation of proteins and the antitumor agent smancs. Cancer Res. 1986;46:6387–92.
4. Maeda NY, Takeuchi M, Takada Y, Sadzuka Y, Namba, Oku N. Anti–neovascular therapy by use of tumor neovasculature–targeted long–circulating liposome. J Control Release. 2004;100:41–52.
5. Farjadian F, Ghasemi A, Gohari O, Roointan A, Karimi M, Hamblin MR. Nanopharmaceuticals and nanomedicines currently on the market: Challenges and opportunities. Nanomedicine. 2019;14:93–126.
6. Wolfram J, Ferrari M. Clinical cancer nanomedicine. Nano Today. 2019;25:85–98.
7. Bhardwaj V, Kaushik A, Khatib ZM, Nair M, McGoron AJ. Recalcitrant issues and new frontiers in nano–pharmacology. Front Pharmacol. 2019;10:1369.
8. Martinelli, C, Pucci C, Ciofani G. Nanostructured carriers as innovative tools for cancer diagnosis and therapy. APL Bioeng. 2019;3:011502.
9. McGoron AJ. Perspectives on the future of nanomedicine to impact patients: An analysis of US federal funding and interventional clinical trials. Bioconjug Chem. 2020;31:436–47.
10. Kiaie SH, Mojarad-Jabali S, Khaleseh F, Allahyari S, Taheri E, Zakeri-Milani P, Valizadeh H. Axial pharmaceutical properties of liposome in cancer therapy: Recent advances and perspectives. Int J Pharm. 2020;581:119269.
11. Drummond DC, Meyer O, Hong K, Kirpotin DB, Papahadjopoulos D. Optimizing liposomes for delivery of chemotherapeutic agents to solid tumors. Pharmacol Rev. 1999;51:691.
12. Ahmed KS, Hussein SA, Ali AH, Korma SA, Qiu L, Chen J. Liposome: Composition, characterisation, preparation, and recent innovation in clinical applications. J Drug Target. 2019;27:742–61.
13. Beltran-Gracia E, Lopez-Camacho A, Higuera-Ciapara I, Velazquez-Fernandez JB, Vallejo-Cardona AA. Nanomedicine review: Clinical developments in liposomal applications. Cancer Nanotechnol. 2019;10:UNSP 11.
14. Harshita M, Barkat A, Beg S, Pottoo FH, Ahmad FJ. Nanopaclitaxel therapy: An evidence based review on the battle for next–generation formulation challenges. Nanomedicine. 2019;14:1323–41.
15. Lamichhane S, Lee S. Albumin nanoscience: Homing nanotechnology enabling targeted drug delivery and therapy. Arch Pharm Res. 2020;43:118–33.
16. Frank LA, Onzi GR, Morawski AS, Pohlmann AR, Guterres SS, Contri RV. Chitosan as a coating material for nanoparticles intended for biomedical applications. React Funct Polym. 2020;147:104459.
17. Essa D, Kondiah PPD, Choonara YE, Pillay V. The design of poly(lactide–co–glycolide) nanocarriers for medical applications. Front Bioengineer Biotechnol. 2020;8:48.
18. Croissant JG, Fatieiev Y, Khashab NM. Degradability and clearance of silicon, organosilica, silsesquioxane, silica mixed oxide, and mesoporous silica nanoparticles. Adv Mater. 2017;29:1604634.
19. Feng Y, Panwar N, Tng DJH, Tjin SC, Wang K, Yong K. The application of mesoporous silica nanoparticle family in cancer theranostics. Coord Chem Rev. 2016;319:86–109.
20. Tang L, Yang X, Yin Q, Cai K, Wang H, Chaudhury I, Yao C, Zhou Q, Kwon M, Hartman JA, Dobrucki IT, Dobrucki LW, Borst LB, Lezmi S, Helferich WG, Ferguson AL, Fan TM, Cheng J. Investigating the optimal size of anticancer nanomedicine. Proc Natl Acad Sci U S A. 2014;111:15344–9.
21. Balakrishnan S, Bhat FA, Jagadeesan A. Applications of gold nanoparticles in cancer. In: Khosrow-Pour M, editor. Biomedical engineering: Concepts, methodologies, tools, and applications. Hershey, PA: Information Resources Management Association; 2018. p. 780–808.
22. Angelakeris M. Magnetic nanoparticles: A multifunctional vehicle for modern theranostics. Biochim Biophys Acta. 2017;1861:1642–51.
23. Ajdary M, Moosavi MA, Rahmati M, Falahati M, Mahboubi M, Mandegary A, Jangjoo S, Mohammadinejad R, Varma RS. Health concerns of various nanoparticles: A review of their in vitro and in vivo toxicity. Nanomaterials. 2018;8:634.
24. Li W, Cao Z, Liu R, Liu L, Li H, Li X, Chen Y, Lu C, Liu Y. AuNPs as an important inorganic nanoparticle applied in drug carrier systems. Artif Cells Nanomed Biotechnol. 2019;47:4222–33.
25. Yang B, Chen Y, Shi J. Mesoporous silica/organosilica nanoparticles: Synthesis, biological effect and biomedical application. Mater Sci Eng R Rep. 2019;137:66–105.
26. Arnbekar RS, Choudhary M, Kandasubramanian B. Recent advances in dendrimer–based nanoplatform for cancer treatment: A review. Eur Polymer J. 2020;126: UNSP109546.
27. Kavand A, Anton N, Vandamme T, Serra CA, Chan-Seng D. Synthesis and functionalization of hyperbranched polymers for targeted drug delivery. J Control Release. 2020;321:285–311.
28. Domingues C, Alvarez-Lorenzo C, Concheiro A, Veiga F, Figueiras A. Nanotheranostic pluronic–like polymeric micelles: Shedding light into the dark shadows of tumors. Mol Pharm. 2019;16(12):4757–74.
29. Fan W, Zhang L, Li Y, Wu H. Recent progress of cross-linking strategies for polymeric micelles with enhanced drug delivery in cancer therapy. Curr Med Chem. 2019;26(13):2356–76.

30. Parveen S, Sahoo SK. Polymeric nanoparticles for cancer therapy. J Drug Target. 2008;16:108–23.
31. de la Torre BG, Albericio F. The pharmaceutical industry in 2019. An analysis of FDA drug approvals from the perspective of molecules. Molecules. 2020;25(3):745.
32. Gauzy-Lazo L, Sassoon I, Brun MP. Advances in antibody–drug conjugate design: Current clinical landscape and future innovations. SLAS Discov. 2020;25(8):843–68.
33. Tanaka K, Shinoda S, Takai N, Takahashi H, Saito Y. The preparation of mesoporous silica–gel and the nature of the modification of its surface with organo–alkoxysilane. Bull Chem Soc Jpn. 1980;53:1242–6.
34. Coffer J, Li X, John J, Pinizzotto R, Chen Y, Newey J, Canham L. Fabrication and characterization of calcium phosphate/porous silicon/silicon structures doped with platinum antitumor compounds. MRS Proceedings. 1999;599:61. doi: 10.1557/PROC-599-61.
35. Lai CY, Trewyn BG, Jeftinija DM, Jeftinija K, Xu S, Jeftinija S, Lin VSY. A mesoporous silica nanosphere–based carrier system with chemically removable CdS nanoparticle caps for stimuli–responsive controlled release of neurotransmitters and drug molecules. J Am Chem Soc. 2003;125:4451–9.
36. Szczesniak B, Choma J, Jaroniec M. Major advances in the development of ordered mesoporous materials. Chem Commun. 2020;56:7836–48.
37. Stober W, Fink A, Bohn E. Controlled growth of monodisperse silica spheres in micron size range. J Colloid Interface Sci. 1968;26:62–9.
38. Beck JS, Vartuli JC, Roth WJ, Leonowicz ME, Kresge CT, Schmitt KD, Chu CTW, Olson DH, Sheppard EW, Mccullen SB, Higgins JB, Schlenker JL. A new family of mesoporous molecular–sieves prepared with liquid–crystal templates. J Am Chem Soc. 1992;114:10834–43.
39. Antonelli DM, Nakahira A, Ying JY. Ligand–assisted liquid crystal templating in mesoporous niobium oxide molecular sieves. Inorg Chem. 1996;35(11):3126–36.
40. Inagaki, S, Guan S, Fukushima Y, Ohsuna T, Terasaki O. Novel mesoporous materials with a uniform distribution of organic groups and inorganic oxide in their frameworks. J Am Chem Soc. 1999;121:9611–4.
41. Wan Y, Zhao D. On the controllable soft–templating approach to mesoporous silicates. Chem Rev. 2007;107:2821–60.
42. Chen F, Hableel G, Zhao ER, Jokerst JV. Multifunctional nanomedicine with silica: Role of silica in nanoparticles for theranostic, imaging, and drug monitoring. J Colloid Interface Sci. 2018;521:261–79.
43. Hoffmann F, Cornelius M, Morell J, Froeba M. Silica–based mesoporous organic–inorganic hybrid materials. Angew Chem Int Ed Engl. 2006;45:3216–51.
44. Rouquerol J, Avnir D, Fairbridge CW, Everett DH, Haynes JH, Pernicone N, Ramsay J, Sing K, Unger KK. Recommendations for the characterization of porous solids. Pure Appl Chem. 1994;66:1739–58.
45. McCusker LB, Liebau F, Engelhardt G. Nomenclature of structural and compositional characteristics of ordered microporous and mesoporous materials with inorganic hosts–(IUPAC recommendations 2001). Pure Appl Chem. 2001;73:381–394.
46. Oroyo M. International tables for crystallography, Volume A, Space-group symmetry: Wiley. For The International Union Of Crystallography; 2016.
47. Dauter Z, Jaskolski M. How to read (and understand) volume A of international tables for crystallography: An introduction for nonspecialists. J Appl Crystallogr. 2010;43:1150–71.
48. Ohsuna T, Sakamoto Y, Terasaki O, Kuroda K. TEM image simulation of mesoporous crystals for structure type identification. Solid State Sci. 2011;13:736–44.
49. Arkhireeva A, Hay JN, Lane JM, Manzano M, Masters H, Oware W, Shaw SJ. Synthesis of organic–inorganic hybrid particles by sol–gel chemistry. J Sol Gel Sci Technol. 2004;31:31–6.
50. Bharali DJ, Klejbor I, Stachowiak EK, Dutta P, Roy I, Kaur N, Bergey EJ, Prasad PN, Stachowiak MK. Organically modified silica nanoparticles: A nonviral vector for in vivo gene delivery and expression in the brain. Proc Natl Acad Sci U S A. 2005;102(32):11539–44.
51. Tang W, Xu H, Kopelman R, Philbert MA. Photodynamic characterization and in vitro application of methylene blue–containing nanoparticle platforms. Photochem Photobiol. 2005;81(2):242–9.
52. Espiard P, Revillon A, Guyot A, Mark JE. Nucleation of emulsion polymerization in the presence of small silica particles. In: Daniels ES, Sudol ED, El-Aasser MS, editors. Polymer latexes preparation, characterization, and applications. Washington, DC: American Chemical Society; 1992. p. 387–404.
53. Fornasieri G, Badaire W, Backov R, Mondain-Monval O, Zakri U, Poulin P. Mesoporous and homothetic silica capsules in reverse–emulsion microreactors. Adv Mater. 2004;16:1094–7.
54. Jaramillo N, Paucar C, Garcia C. Influence of the reaction time and the Triton x–100/Cyclohexane/Methanol/H2O ratio on the morphology and size of silica nanoparticles synthesized via sol–gel assisted by reverse micelle microemulsion. J Mater Sci. 2014;49:3400–6.
55. Roy I, Ohulchanskyy TY, Pudavar HE, Bergey EJ, Oseroff AR, Morgan J, Dougherty TJ, Prasad PN. Ceramic–based nanoparticles entrapping water–insoluble photosensitizing anticancer drugs: A novel drug–carrier system for photodynamic therapy. J Am Chem Soc. 2003;125(26):7860–5.
56. Roy I, Kumar P, Kumar R, Ohulchanskyy TY, Yong K, Prasad PN. Ormosil nanoparticles as a sustained–release drug delivery vehicle. RSC Adv. 2014;4:53498–504.
57. Nagesetti A, McGoron AJ. Multifunctional organically modified silica nanoparticles for chemotherapy, adjuvant hyperthermia and near infrared imaging. Colloids Surf B Biointerfaces. 2016;147:492–500.
58. Nagesetti A, Srinivasan S, McGoron AJ. Polyethylene glycol modified ORMOSIL theranostic nanoparticles for triggered doxorubicin release and deep drug delivery

into ovarian cancer spheroids. J Photochem Photobiol B. 2017;174:209–16.
59. Ravaine D, Seminel A, Charbouillot Y, Vincens M. A new family of organically modified silicates prepared from gels. J Non Cryst Solids. 1986;82:210–9.
60. Frasch J, Lebeau B, Soulard M, Patarin J, Zana R. In situ investigations on cetyltrimethyl ammonium surfactant/silicate systems, precursors of organized mesoporous MCM–41–type siliceous materials. Langmuir. 2000;16:9049–57.
61. Han SH, Hou WG, Dang WX, Xu J, Hu JF, Li DQ. Synthesis of rod–like mesoporous silica using mixed surfactants of cetyltrimethylammonium bromide and cetyltrimethylammonium chloride as templates. Mater Lett. 2003;57:4520–4.
62. Atkin R, Craig V, Wanless EJ, Biggs S. The influence of chain length and electrolyte on the adsorption kinetics of cationic surfactants at the silica–aqueous solution interface. J Colloid Interface Sci. 2003;266:236–44.
63. Lin Y, Zhang J, Liu S, Ye H. Doxorubicin loaded silica nanoparticles with dual modification as a tumor–targeted drug delivery system for colon cancer therapy. J Nanosci Nanotechnol. 2018;18:2330–6.
64. Wang Y, Liu X, Deng G, Sun J, Yuan H, Li Q, Wang Q, Lu J. Se@SiO_2–FA–CuS nanocomposites for targeted delivery of DOX and nano selenium in synergistic combination of chemo–photothermal therapy. Nanoscale. 2018;10:2866–75.
65. Fang J, Zhang S, Xue X, Zhu X, Song S, Wang B, Jiang L, Qin M, Liang H, Gao L. Quercetin and doxorubicin co–delivery using mesoporous silica nanoparticles enhance the efficacy of gastric carcinoma chemotherapy. Int J Nanomed. 2018;13:5113–26.
66. Tabor RF, Eastoe J, Dowding PJ, Grillo I, Heenan RK, Hollamby M. Formation of surfactant–stabilized silica organosols. Langmuir. 2008;24:12793–7.
67. Shaparenko N, Beketova D, Demidova M, Bulavchenko A. Regulation of the charge and hydrodynamic diameter of silica nanoparticles in AOT microemulsions. Colloid J. 2019;81:43–9.
68. Nagesetti A, McGoron AJ. Corrigendum to "Multifunctional organically modified silica nanoparticles for chemotherapy, adjuvant hyperthermia and near infrared imaging" Colloids Surf B Biointerfaces 147 (2016) 492–500. Colloids Surf B Biointerfaces. 2018;170:663.
69. Kumar D, Mutreja I, Keshvan PC, Bhat M, Dinda AK, Mitra S. Organically modified silica nanoparticles interaction with macrophage cells: Assessment of cell viability on the basis of physicochemical properties. J Pharm Sci. 2015;104(11):3943–51.
70. Jiang S, Hua L, Guo Z, Sun L. One–pot green synthesis of doxorubicin loaded–silica nanoparticles for in vivo cancer therapy. Mater Sci Eng C. 2018;90:257–63.
71. Mannerström M, Zou J, Toimela T, Pyykkö I, Heinonen T. The applicability of conventional cytotoxicity assays to predict safety/toxicity of mesoporous silica nanoparticles, silver and gold nanoparticles and multi–walled carbon nanotubes. Toxicol In Vitro. 2016;37:113–20.
72. Pham DH, De Roo B, Nguyen XB, Vervaele M, Kecskés A, Ny A, Copmans D, Vriens H, Locquet JP, Hoet P, de Witte PA. Use of zebrafish larvae as a multi–endpoint platform to characterize the toxicity profile of silica nanoparticles. Sci Rep. 20162;6:37145.
73. Hadipour Moghaddam SP, Mohammadpour R, Ghandehari H. In vitro and in vivo evaluation of degradation, toxicity, biodistribution, and clearance of silica nanoparticles as a function of size, porosity, density, and composition. J Control Release. 2019;311–312:1–15.
74. Mohammadpour R, Cheney DL, Grunberger JW, Yazdimamaghani M, Jedrzkiewicz J, Isaacson KJ, Dobrovolskaia MA, Ghandehari H. One–year chronic toxicity evaluation of single dose intravenously administered silica nanoparticles in mice and their ex vivo human hemocompatibility. J Control Release. 2020;324:471–81.
75. Barenholz Y. Doxil((R)) – The first FDA–approved nano–drug: From an idea to a product. In: Peer D, editor. Handbook of harnessing biomaterials in nanomedicine. Singapore: Jenny Stanford Publishing; 2012. p. 335–98.
76. Shinozawa S, Araki Y, Oda T. Tissue distribution and anti–tumor effect of liposome–entrapped doxorubicin (adriamycin) in Ehrlich solid tumor–bearing mouse. Acta Med Okayama. 1981;35:395–405.
77. Rahman A, Herman E, Ferrang V, Schein P. Protection of doxorubicin induced cardiotoxicity in beagle dogs by administration in cardiolipin liposomes. Clin Res. 1982;30:A534.
78. Smith F, Rahman A, Jenson A, Kline I, Schein PS. Toxicity evaluation of doxorubicin entrapped in cardiolipin liposomes in mice. Proc Am Assoc Cancer Res. 1983;24:260.
79. Goldin A, Rahman A, Harris M, Fumagalli A, Schein PS. Anti–tumor and pharmacologic disposition studies of free doxorubicin and doxorubicin entrapped in cardiolipin liposomes. Proc Am Assoc Cancer Res. 1983;24:260.
80. Delgado G, Potkul RK, Treat JA, Lewandowski GS, Barter JF, Forst D, Rahman A. A phase I/II study of intraperitoneally administered doxorubicin entrapped in cardiolipin liposomes in patients with ovarian cancer. Am J Obstet Gynecol. 1989;160(4):812–817; discussion 817–9.
81. Desai N, Trieu V, Yao Z, Louie L, Ci S, Yang A, Tao C, De T, Beals B, Dykes D, Noker P, Yao R, Labao E, Hawkins M, Soon-Shiong P. Increased antitumor activity, intratumor paclitaxel concentrations, and endothelial cell transport of cremophor–free, albumin–bound paclitaxel, ABI–007, compared with cremophor–based paclitaxel. Clin Cancer Res. 2006;12(4):1317–24.
82. Desai NP, Trieu V, Hwang LY, Wu R, Soon-Shiong P, Gradishar WJ. Improved effectiveness of nanoparticle albumin–bound (nab) paclitaxel versus polysorbate–based docetaxel in multiple xenografts as a function of HER2 and SPARC status. Anticancer Drugs. 2008;19(9):899–909.
83. Antunes A, Fierro I, Guerrante R, Mendes F, de M Alencar

MS. Trends in nanopharmaceutical patents. Int J Mol Sci. 2013;14:7016–31.
84. Gabizon A, Peretz T, Sulkes A, Amselem S, Benyosef R, Benbaruch N, Catane R, Biran S, Barenholz Y. Systemic administration of doxorubicin–containing liposomes in cancer–patients – a phase–1 study. Eur J Cancer Clin Oncol. 1989;25:1795–803.
85. Segal AW, Gregoriadis G, Lavender JP, Tarin D, Peters TJ. Tissue and hepatic subcellular distribution of liposomes containing bleomycin after intravenous administration to patients with neoplasms. Clin Sci Mol Med. 1976;51(4):421–5.
86. Damascelli B, Cantù G, Mattavelli F, Tamplenizza P, Bidoli P, Leo E, Dosio F, Cerrotta AM, Di Tolla G, Frigerio LF, Garbagnati F, Lanocita R, Marchianò A, Patelli G, Spreafico C, Tichà V, Vespro V, Zunino F. Intraarterial chemotherapy with polyoxyethylated castor oil free paclitaxel, incorporated in albumin nanoparticles (ABI–007): Phase I study of patients with squamous cell carcinoma of the head and neck and anal canal: Preliminary evidence of clinical activity. Cancer. 2001; 92(10):2592–602.
87. Bawa R, Barenholz Y, Owen A. The challenge of regulating nanomedicine: Key issues. Nanomedicines. 2016;51:290–314.
88. Phillips E, Penate-Medina O, Zanzonico PB, Carvajal RD, Mohan P, Ye Y, Humm J, Gönen M, Kalaigian H, Schöder H, Strauss HW, Larson SM, Wiesner U, Bradbury MS. Clinical translation of an ultrasmall inorganic optical–PET imaging nanoparticle probe. Sci Transl Med. 2014;6(260):260ra149.
89. Ma K, Mendoza C, Hanson M, Werner-Zwanziger U, Zwanziger J, Wiesner U. Control of ultrasmall sub–10 nm ligand–functionalized fluorescent core–shell silica nanoparticle growth in water. Chem Mater. 2015;27:4119–33.
90. Morigi V, Tocchio A, Bellavite Pellegrini C, Sakamoto JH, Arnone M, Tasciotti E. Nanotechnology in medicine: From inception to market domination. J Drug Deliv. 2012;2012:389485.
91. Paliwal R, Babu RJ, Palakurthi S. Nanomedicine scale–up technologies: Feasibilities and challenges. AAPS PharmSciTech. 2014;15(6):1527–34.
92. Hua S, de Matos MBC, Metselaar JM, Storm G. Current trends and challenges in the clinical translation of nanoparticulate nanomedicines: Pathways for translational development and commercialization. Front Pharmacol. 2018;9:790.
93. Nichols JW, Bae YH. EPR: Evidence and fallacy. J Control Release. 2014;190:451–64.
94. Danhier F. To exploit the tumor microenvironment: Since the EPR effect fails in the clinic, what is the future of nanomedicine? J Control Release. 2016;244(Pt A):108–121.
95. Ekdawi SN, Jaffray DA, Allen C. Nanomedicine and tumor heterogeneity: Concept and complex reality. Nano Today. 2016;11:402–14.
96. Nel A, Ruoslahti E, Meng H. New insights into "permeability" as in the enhanced permeability and retention effect of cancer nanotherapeutics. Acs Nano. 2017;11:9567–9.
97. van der Worp HB, Howells DW, Sena ES, Porritt MJ, Rewell S, O'Collins V, Macleod MR. Can animal models of disease reliably inform human studies? PLoS Med. 2010;7(3):e1000245.
98. McGonigle P, Ruggeri B. Animal models of human disease: Challenges in enabling translation. Biochem Pharmacol. 2014;87(1):162–71.
99. Björnmalm M, Thurecht KJ, Michael M, Scott AM, Caruso F. Bridging bio–nano science and cancer nanomedicine. ACS Nano. 2017;11(10):9594–613.
100. Gbabe OF, Okwundu CI, Dedicoat M, Freeman EE. Treatment of severe or progressive Kaposi's sarcoma in HIV–infected adults. Cochrane Database Syst Rev. 2014:CD003256.
101. Duggan ST, Keating GM. Pegylated liposomal doxorubicin A review of its use in metastatic breast cancer, ovarian cancer, multiple myeloma and AIDS–related Kaposi's sarcoma. Drugs. 2011;71:2531–58.
102. Hung CC, Yang Y, Tsai IC, Hsu CY, Liu CH, Yang JR. The efficacy of pegylated liposomal doxorubicin–based neoadjuvant chemotherapy in breast cancer: A retrospective case–control study in Taiwan. Biochem Res Int. 2020;2020:5729389.
103. Yao J, Pan S, Fan X, Jiang X, Yang Y, Jin J, Liu Y. Pegylated liposomal doxorubicin as neoadjuvant therapy for stage II–III locally advanced breast cancer. J Chemother. 2020;32(4):202–7.
104. Venkatraman S. Has nanomedicine lived up to its promise? Nanotechnology. 2014;25:372501.
105. Torrice M. Does nanomedicine have a delivery problem? ACS Central Sci. 2016;2:434–7.
106. Park K. The drug delivery field at the inflection point: Time to fight its way out of the egg. J Control Release. 2017;267:2–14.
107. van der Meel R, Lammers T, Hennink WE. Cancer nanomedicines: Oversold or underappreciated? Expert Opin Drug Deliv. 2017;14(1):1–5.
108. Greish K, Mathur A, Bakhiet M, Taurin S. Nanomedicine: Is it lost in translation? Ther Deliv. 2018;9(4):269–85.
109. Sarmento B. Have nanomedicines progressed as much as we'd hoped for in drug discovery and development? Expert Opin Drug Discov. 2019;14(8):723–5.
110. Chan WCW. Nanomedicine 2.0. Acc Chem Res. 2017;50: 627–632.
111. Park K. The beginning of the end of the nanomedicine hype. J Control Release. 2019;305:221–2.
112. Thomas OS, Weber W. Overcoming physiological barriers to nanoparticle delivery–are we there yet? Front Bioeng Biotechnol. 2019;7:415.
113. Crommelin DJA, van Hoogevest P, Storm G. The role of liposomes in clinical nanomedicine development. What now? Now what? J Control Release. 2020;318:256–63.

114. Würbel H. Behaviour and the standardization fallacy. Nat Genet. 2000;26:263.
115. Roberts I, Kwan I, Evans P, Haig S. Does animal experimentation inform human healthcare? Observations from a systematic review of international animal experiments on fluid resuscitation. BMJ. 2002;324(7335):474–6.
116. Martić-Kehl M, Schibli R, Schubiger P. Can animal data predict human outcome? Problems and pitfalls of translational animal research. Eur J Nucl Med Mol Imaging. 2012;39:1492–6.
117. Pound P, Ritskes-Hoitinga M. Is it possible to overcome issues of external validity in preclinical animal research? Why most animal models are bound to fail. J Transl Med. 2018;16(1):304.
118. Seyhan AA. Lost in translation: The valley of death across preclinical and clinical divide – identification of problems and overcoming obstacles. Transl Med Commun. 2019;4:1–19.
119. DiMasi JA, Grabowski HG, Hansen RW. Innovation in the pharmaceutical industry: New estimates of R&D costs. J Health Econ. 2016;47:20–33.
120. Wouters OJ, McKee M, Luyten J. Estimated research and development investment needed to bring a new medicine to market, 2009–2018. JAMA. 2020;323(9):844–53.
121. Wong CH, Siah KW, Lo AW. Estimation of clinical trial success rates and related parameters. Biostatistics. 2019;20(2):273–86.
122. Abou-El-Enein M, Duda GN, Gruskin EA, Grainger DW. Strategies for derisking translational processes for biomedical technologies. Trends Biotechnol. 2017;35(2):100–8.
123. Anchordoquy TJ, Barenholz Y, Boraschi D, Chorny M, Decuzzi P, Dobrovolskaia MA, Farhangrazi ZS, Farrell D, Gabizon A, Ghandehari H, Godin B, La-Beck NM, Ljubimova J, Moghimi SM, Pagliaro L, Park JH, Peer D, Ruoslahti E, Serkova NJ, Simberg D. Mechanisms and barriers in cancer nanomedicine: Addressing challenges, looking for solutions. ACS Nano. 2017;11(1): 12–8.
124. Sanna V, Pala N, Sechi M. Targeted therapy using nanotechnology: Focus on cancer. Int J Nanomed. 2014;9:467–83.
125. Floc'h N, Ashton S, Ferguson D, Taylor P, Carnevalli LS, Hughes AM, Harris E, Hattersley M, Wen S, Curtis NJ, Pilling JE, Young LA, Maratea K, Pease EJ, Barry ST. Modeling dose and schedule effects of AZD2811 nanoparticles targeting aurora b kinase for treatment of diffuse large B–cell lymphoma. Mol Cancer Ther. 2019;18(5):909–19.
126. Johnson ML, Cosaert JGCE, Falchook GS, Jones SF, Strickland D, Greenlees C, Charlton J, MacDonald A, Overend P, Adelman C, Burris HA, Pease EJ, Patel GS, Wang JS-Z. A phase I, open label, multicenter dose escalation study of AZD2811 nanoparticle in patients with advanced solid tumors. J Clin Oncol. 2019;37.
127. Wilhelm S, Tavares AJ, Dai Q, Ohta S, Audet J, Dvorak HF, Chan WCW. Analysis of nanoparticle delivery to tumours. Nat Rev Mater. 2016;1.
128. Dai Q, Wilhelm S, Ding D, Syed AM, Sindhwani S, Zhang Y, Chen YY, MacMillan P, Chan WCW. Quantifying the ligand–coated nanoparticle delivery to cancer cells in solid tumors. ACS Nano. 2018;12:8423–35.
129. Cheng Y, He, Riviere JE, Monteiro-Riviere NA, Lin Z. Meta–analysis of nanoparticle delivery to tumors using a physiologically based pharmacokinetic modeling and simulation approach. ACS Nano. 2020;14:3075–95.
130. Gerweck LE, Seetharaman K. Cellular pH gradient in tumor versus normal tissue: Potential exploitation for the treatment of cancer. Cancer Res. 1996;56:1194–8.
131. Pillai SR, Damaghi M, Marunaka Y, Spugnini EP, Fais S, Gillies RJ. Causes, consequences, and therapy of tumors acidosis. Cancer Metastasis Rev. 2019;38:205–22.
132. Logozzi M, Spugnini E, Mizzoni D, Di Raimo R, Fais S. Extracellular acidity and increased exosome release as key phenotypes of malignant tumors. Cancer Metastasis Rev. 2019;38:93–101.
133. Boedtkjer E, Pedersen SF. The acidic tumor microenvironment as a driver of cancer. Annu Rev Physiol. 2020;82:103–26.
134. Stubbs M, McSheehy PM, Griffiths JR, Bashford CL. Causes and consequences of tumour acidity and implications for treatment. Mol Med Today. 2000;6:15–9.
135. Lutz NW, Le Fur Y, Chiche J, Pouysségur J, Cozzone PJ. Quantitative in vivo characterization of intracellular and extracellular pH profiles in heterogeneous tumors: A novel method enabling multiparametric pH analysis. Cancer Res. 2013;73:4616–28.
136. Koltai T. Cancer: Fundamentals behind pH targeting and the double–edged approach. Onco Targets Ther. 2016;9:6343–60.
137. Qiao Y, Wan J, Zhou L, Ma W, Yang Y, Luo W, Yu Z, Wang H. Stimuli-responsive nanotherapeutics for precision drug delivery and cancer therapy. Wiley Interdiscip Rev Nanomed Nanobiotechnol. 2019;11:e1527.
138. Tebaldi ML, Oda CMR, Monteiro LOF, de Barros ALB, Santos CJ, Ferreira Soares DC. Biomedical nanoparticle carriers with combined thermal and magnetic response: Current preclinical investigations. J Magn Magn Mater. 2018;461:116–27.
139. Liu JF, Jang B, Issadore D, Tsourkas A. Use of magnetic fields and nanoparticles to trigger drug release and improve tumor targeting. Wiley Interdiscip Rev Nanomed Nanobiotechnol. 2019;11:e1571.
140. White BD, Duan C, Townley HE. Nanoparticle activation methods in cancer treatment. Biomolecules. 2019;9:202.
141. Fritze A, Hens F, Kimpfler A, Schubert R, Peschka-Suess R. Remote loading of doxorubicin into liposomes driven by a transmembrane phosphate gradient. Biochim Biophys Acta. 2006;1758:1633–40.
142. Russell LM, Hultz M, Searson PC. Leakage kinetics of the liposomal chemotherapeutic agent Doxil: The role of

dissolution, protonation, and passive transport, and implications for mechanism of action. J Control Release. 2018;269:171–6.
143. Leong HS, Butler KS, Brinker CJ, Azzawi M, Conlan S, Dufés C, Owen A, Rannard S, Scott C, Chen C, Dobrovolskaia MA, Kozlov SV, Prina-Mello A, Schmid R, Wick P, Caputo F, Boisseau P, Crist RM, McNeil SE, Fadeel B, Tran L, Hansen SF, Hartmann NB, Clausen LPW, Skjolding LM, Baun A, Ågerstrand M, Gu Z, Lamprou DA, Hoskins C, Huang L, Song W, Cao H, Liu X, Jandt KD, Jiang W, Kim BYS, Wheeler KE, Chetwynd AJ, Lynch I, Moghimi SM, Nel A, Xia T, Weiss PS, Sarmento B, das Neves J, Santos HA, Santos L, Mitragotri S, Little S, Peer D, Amiji MM, Alonso MJ, Petri-Fink A, Balog S, Lee A, Drasler B, Rothen-Rutishauser B, Wilhelm S, Acar H, Harrison RG, Mao C, Mukherjee P, Ramesh R, McNally LR, Busatto S, Wolfram J, Bergese P, Ferrari M, Fang RH, Zhang L, Zheng J, Peng C, Du B, Yu M, Charron DM, Zheng G, Pastore C. On the issue of transparency and reproducibility in nanomedicine. Nat Nanotechnol. 2019;14:629–35.
144. Faria M, Björnmalm M, Thurecht KJ, Kent SJ, Parton RG, Kavallaris M, Johnston APR, Gooding JJ, Corrie SR, Boyd BJ, Thordarson P, Whittaker AK, Stevens MM, Prestidge CA, Porter CJH, Parak WJ, Davis TP, Crampin EJ, Caruso F. Minimum information reporting in bio–nano experimental literature. Nat Nanotechnol. 2018;13:777–85.
145. Yu M, Yuan W, Li D, Schwendeman A, Schwendeman SP. Predicting drug release kinetics from nanocarriers inside dialysis bags. J Control Release. 2019;315:23–30.
146. Schneid ADC, Silveira CP, Galdino FE, Ferreira LF, Bouchmella K, Cardoso MB. Colloidal stability and redispersibility of mesoporous silica nanoparticles in biological media. Langmuir. 2020;36:11442–9.
147. Li J, Shen S, Kong F, Jiang T, Tang C, Yin C. Effects of pore size on in vitro and in vivo anticancer efficacies of mesoporous silica nanoparticles. RSC Adv. 2018;8:24633–40.
148. Ma B, He L, You Y, Mo J, Chen T. Controlled synthesis and size effects of multifunctional mesoporous silica nanosystem for precise cancer therapy. Drug Deliv. 2018;25:293–306.
149. Liu X, Jiang J, Chan R, Ji Y, Lu J, Liao YP, Okene M, Lin J, Lin P, Chang CH, Wang X, Tang I, Zheng E, Qiu W, Wainberg ZA, Nel AE, Meng H. Improved efficacy and reduced toxicity using a custom–designed irinotecan–delivering silicasome for orthotopic colon cancer. ACS Nano. 2019;13:38–53.
150. Lu J, Liong M, Li Z, Zink JI, Tamanoi F. Biocompatibility, biodistribution, and drug–delivery efficiency of mesoporous silica nanoparticles for cancer therapy in animals. Small. 2010;6:1794–805.
151. Colbern GT, Hiller AJ, Musterer RS, Pegg E, Henderson IC, Working PK. Significant increase in antitumor potency of doxorubicin HCl by its encapsulation in pegylated liposomes. J Liposome Res. 1999;9:523–38.
152. Colbern G, Vaage J, Donovan D, Uster P, Working P. Tumor uptake and therapeutic effects of drugs encapsulated in long–circulating pegylated stealth (R) liposomes. J Liposome Res. 2000;10:81–92.
153. Charrois G, Allen T. Rate of biodistribution of STEALTHR liposomes to tumor and skin: Influence of liposome diameter and implications for toxicity and therapeutic activity. Biochim Biophys Acta. 2003;1609:102–8.
154. Peer D, Margalit R. Tumor–targeted hyaluronan nanoliposomes increase the antitumor activity of liposomal doxorubicin in syngeneic and human xenograft mouse tumor models. Neoplasia. 2004;6:343–53.
155. Brouckaert P, Takahashi N, van Tiel ST, Hostens J, Eggermont AM, Seynhaeve AL, Fiers W, ten Hagen TL. Tumor necrosis factor–alpha augmented tumor response in B16BL6 melanoma–bearing mice treated with stealth liposomal doxorubicin Doxil correlates with altered Doxil pharmacokinetics. Int J Cancer. 2004;109:442–48.
156. Frenkel V, Etherington A, Greene M, Quijano J, Xie J, Hunter F, Dromi S, Li KC. Delivery of liposomal doxorubicin (Doxil) in a breast cancer tumor model: Investigation of potential enhancement by pulsed–high intensity focused ultrasound exposure. Acad Radiol. 2006;13:469–79.
157. Shan S, Flowers C, Peltz CD, Sweet H, Maurer N, Kwon EJ, Krol A, Yuan F, Dewhirst MW. Preferential extravasation and accumulation of liposomal vincristine in tumor comparing to normal tissue enhances antitumor activity. Cancer Chemother Pharmacol. 2006;58:245–55.
158. ElBayoumi, TA, Torchilin VP. Tumor–specific anti–nucleosome antibody improves therapeutic efficacy of doxorubicin–loaded long–circulating liposomes against primary and metastatic tumor in mice. Mol Pharm. 2009;6:246–54.
159. Seip R, Leyvi E, Raju BI, Shi WT, Bohmer M, Chlon C, Sio C, Reibling K, Swanson T. Ultrasound and microbubble mediated Doxil delivery in a murine breast cancer model: Therapeutic efficacy dependence on tumor growth rate. ULTSYM, 2011:1894–7.
160. Apte A, Koren E, Koshkaryev A, Torchilin VP. Doxorubicin in TAT peptide–modified multifunctional immunoliposomes demonstrates increased activity against both drug–sensitive and drug–resistant ovarian cancer models. Cancer Biol Ther. 2014;15:69–80.
161. Gaillard PJ, Appeldoorn CC, Dorland R, van Kregten J, Manca F, Vugts DJ, Windhorst B, van Dongen GA, de Vries HE, Maussang D, van Tellingen O. Pharmacokinetics, brain delivery, and efficacy in brain tumor–bearing mice of glutathione pegylated liposomal doxorubicin (2B3–101). PLoS One. 2014;9:e82331.
162. Wang T, Hartner WC, Gillespie JW, Praveen KP, Yang S, Mei LA, Petrenko VA, Torchilin VP. Enhanced tumor delivery and antitumor activity in vivo of liposomal doxorubicin modified with MCF–7–specific phage fusion protein. Nanomedicine. 2014;10:421–30.
163. Kohli AG, Kivimäe S, Tiffany MR, Szoka FC. Improving the distribution of Doxil® in the tumor matrix

by depletion of tumor hyaluronan. J Control Release. 2014;191:105–14.
164. Arabi L, Badiee A, Mosaffa F, Jaafari MR. Targeting CD44 expressing cancer cells with anti–CD44 monoclonal antibody improves cellular uptake and antitumor efficacy of liposomal doxorubicin. J Control Release. 2015;220:275–86.
165. Petersen AL, Henriksen JR, Binderup T, Elema DR, Rasmussen PH, Hag AM, Kjær A, Andresen TL. In vivo evaluation of PEGylated Cu–64–liposomes with theranostic and radiotherapeutic potential using micro PET/CT. Eur J Nucl Med Mol Imaging. 2016;43:941–52.
166. Moosavian SA, Abnous K, Badiee A, Jaafari MR. Improvement in the drug delivery and anti–tumor efficacy of PEGylated liposomal doxorubicin by targeting RNA aptamers in mice bearing breast tumor model. Colloids Surf B Biointerfaces. 2016;139:228–36.
167. Singh MS, Goldsmith M, Thakur K, Chatterjee S, Landesman-Milo D, Levy T, Kunz-Schughart LA, Barenholz Y, Peer D. An ovarian spheroid based tumor model that represents vascularized tumors and enables the investigation of nanomedicine therapeutics. Nanoscale. 2020;12:1894–903.
168. Charrois G, Allen TM. Drug release rate influences the pharmacokinetics, biodistribution, therapeutic activity, and toxicity of pegylated liposomal doxorubicin formulations in murine breast cancer. Biochim Biophys Acta. 2004;1663:167–77.
169. Ogawara K, Un K, Minato K, Tanaka K, Higaki K, Kimura T. Determinants for in vivo anti–tumor effects of PEG liposomal doxorubicin: Importance of vascular permeability within tumors. Int J Pharm. 2008;359:234–40.
170. Razavi-Azarkhiavi K, Jafarian AH, Abnous K, Razavi BM, Shirani K, Zeinali M, Jaafari MR, Karimi G. The comparison of biodistribution, efficacy and toxicity of two PEGylated liposomal doxorubicin formulations in mice bearing C–26 colon carcinoma: A preclinical study. Drug Res. 2016;66:330–6.
171. Karmali PP, Kotamraju VR, Kastantin M, Black M, Missirlis D, Tirrell M, Ruoslahti E. Targeting of albumin–embedded paclitaxel nanoparticles to tumors. Nanomedicine. 2009;5:73–82.
172. Shao H, Tang H, Salavaggione OE, Yu C, Hylander B, Tan W, Repasky E, Adjei AA, Dy GK. Improved response to nab–paclitaxel compared with cremophor–solubilized paclitaxel is independent of secreted protein acidic and rich in cysteine expression in non–small cell lung cancer. J Thorac Oncol. 2011;6:998–1005.
173. Yang Y, Niu X, Zhang Q, Hao L, Ding Y, Xu H. The efficacy of abraxane on osteosarcoma xenografts in nude mice and expression of secreted protein, acidic and rich in cysteine. Am J Med Sci. 2012;344:199–205.
174. Beyer I, Cao H, Persson J, Song H, Richter M, Feng Q, Yumul R, van Rensburg R, Li Z, Berenson R, Carter D, Roffler S, Drescher C, Lieber A. Coadministration of epithelial junction opener jo–1 improves the efficacy and safety of chemotherapeutic drugs. Clin Cancer Res. 2012;18:3340–51.
175. Xiao K, Luo J, Fowler WL, Li Y, Lee JS, Xing L, Cheng RH, Wang L, Lam KS. A self–assembling nanoparticle for paclitaxel delivery in ovarian cancer. Biomaterials. 2009;30:6006–16.
176. Rivkin I, Cohen K, Koffler J, Melikhov D, Peer D, Margalit R. Paclitaxel–clusters coated with hyaluronan as selective tumor–targeted nanovectors. Biomaterials. 2010;31:7106–14.
177. Pandya AD, Jäger E, Bagheri Fam S, Höcherl A, Jäger A, Sincari V, Nyström B, Štěpánek P, Skotland T, Sandvig K, Hrubý M, Mælandsmo GM. Paclitaxel–loaded biodegradable ROS–sensitive nanoparticles for cancer therapy. Int J Nanomed. 2019;14:6269–85.
178. Feng Z, Zhao G, Yu L, Gough D, Howell SB. Preclinical efficacy studies of a novel nanoparticle–based formulation of paclitaxel that out–performs Abraxane. Cancer Chemother Pharmacol. 2010;65:923–30.
179. Ernsting MJ, Murakami M, Undzys E, Aman A, Press B, Li SD. A docetaxel–carboxymethylcellulose nanoparticle outperforms the approved taxane nanoformulation, Abraxane, in mouse tumor models with significant control of metastases. J Control Release. 2012;162:575–81.
180. Yin T, Cai H, Liu J, Cui B, Wang L, Yin L, Zhou J, Huo M. Biological evaluation of PEG modified nanosuspensions based on human serum albumin for tumor targeted delivery of paclitaxel. Eur J Pharm Sci. 2016;83:79–87.
181. Koo H, Min KH, Lee SC, Park JH, Park K, Jeong SY, Choi K, Kwon IC, Kim K. Enhanced drug–loading and therapeutic efficacy of hydrotropic oligomer–conjugated glycol chitosan nanoparticles for tumor–targeted paclitaxel delivery. J Control Release. 2013;172:823–31.
182. Simón-Gracia L, Hunt H, Scodeller P, Gaitzsch J, Kotamraju VR, Sugahara KN, Tammik O, Ruoslahti E, Battaglia G, Teesalu T. iRGD peptide conjugation potentiates intraperitoneal tumor delivery of paclitaxel with polymersomes. Biomaterials. 2016;104:247–57.
183. Bhattacharyya J, Bellucci JJ, Weitzhandler I, McDaniel JR, Spasojevic I, Li X, Lin CC, Chi JT, Chilkoti A. A paclitaxel–loaded recombinant polypeptide nanoparticle outperforms Abraxane in multiple murine cancer models. Nat Commun. 2015;6:7939.
184. Huang J, Wu B, Zhou Z, Hu S, Xu H, Piao Y, Zheng H, Tang J, Liu X, Shen Y. Drug–binding albumins forming stabilized nanoparticles for efficient anticancer therapy. Nanomedicinee. 2019;21:102058.
185. Lee JE, Kim MG, Jang YL, Lee MS, Kim NW, Yin Y, Lee JH, Lim SY, Park JW, Kim J, Lee DS, Kim SH, Jeong JH. Self–assembled PEGylated albumin nanoparticles (SPAN) as a platform for cancer chemotherapy and imaging. Drug Delivery. 2018;25:1570–8.
186. Xiong J, Zhang H. Antibody–nanoparticle conjugate constructed with trastuzumab and nab–paclitaxel for the

targeted therapy of positive human epidermal growth factor receptor 2 gastric cancer. J Clin Oncol. 2017;35:e15506.
187. Banskota S, Saha S, Bhattacharya J, Kirmani N, Yousefpour P, Dzuricky M, Zakharov N, Li X, Spasojevic I, Young K, Chilkoti A. Genetically Encoded stealth nanoparticles of a zwitterionic polypeptide–paclitaxel conjugate have a wider therapeutic window than abraxane in multiple tumor models. Nano Lett. 2020;20:2396–409.
188. Teijeiro-Valiño C, Novoa-Carballal R, Borrajo E, Vidal A, Alonso-Nocelo M, de la Fuente Freire M, Lopez-Casas PP, Hidalgo M, Csaba N, Alonso MJ. A multifunctional drug nanocarrier for efficient anticancer therapy. J Control Release. 2019;294:154–64.
189. Pinder MC, Ibrahim NK. Nanoparticle albumin–bound paclitaxel for treatment of metastatic breast cancer. Drugs of Today. 2006;42:599–6.4.
190. Stinchcombe TE. Nanoparticle albumin–bound paclitaxel: A novel Cremophor–EL(R)–free formulation of paclitaxel. Nanomedicine. 2007;2:415–23.
191. Desai N, De T, Ci S, Louis L, Trieu V. Characterization and in vitro/in vivo dissolution of nab–paclitaxel nanoparticles. 99th AACR Annual Meeting, 2008:5624.
192. Jiang S, Hua L, Guo Z, Sun L. One–pot green synthesis of doxorubicin loaded–silica nanoparticles for in vivo cancer therapy. Mater Sci Eng C Mater Biol Appl. 2018;90:257–63.
193. Ren X, Shi L, Yu X, Liu W, Sheng J, Wan J, Li Y, Wan Y, Luo Z, Yang X. Multifunctional hierarchical mesoporous silica and black phosphorus nanohybrids as chemo–photothermal synergistic agents for enhanced cancer therapy. Nanoscale. 2020;12:12578–88.
194. Han L, Tang C, Yin C. pH–responsive core–shell structured nanoparticles for triple–stage targeted delivery of doxorubicin to tumors. ACS Appl Mater Interfaces. 2016;8:23498–508.
195. Chen L, Zhou X, Nie W, Zhang Q, Wang W, Zhang Y, He C. Multifunctional redox–responsive mesoporous silica nanoparticles for efficient targeting drug delivery and magnetic resonance imaging. ACS Appl Mater Interfaces. 2016;8:33829–41.
196. Li E, Yang Y, Hao G, Yi X, Zhang S, Pan Y, Xing B, Gao M. Multifunctional magnetic mesoporous silica nanoagents for in vivo enzyme–responsive drug delivery and MR imaging. Nanotheranostics. 2018;2:233–42.
197. Wang J, Han J, Zhu C, Han N, Xi J, Fan L, Guo R. Gold nanorods/polypyrrole/m–SiO_2 core/shell hybrids as drug nanocarriers for efficient chemo–photothermal therapy. Langmuir. 2018;34:14661–9.
198. Gao Q, Xie W, Wang Y, Wang D, Guo Z, Gao F, Zhao L, Cai Q. A theranostic nanocomposite system based on radial mesoporous silica hybridized with Fe3O4 nanoparticles for targeted magnetic field responsive chemotherapy of breast cancer. RSC Adv. 2018;8:4321–8.
199. Chen Z, Wan L, Yuan Y, Kuang Y, Xu X, Liao T, Liu J, Xu Z, Jiang B, Li C. pH/GSH–dual–sensitive hollow mesoporous silica nanoparticle–based drug delivery system for targeted cancer therapy. ACS Biomater Sci Eng. 2020;6:3375–87.
200. Meng H, Xue M, Xia T, Ji Z, Tarn DY, Zink JI, Nel AE. Use of size and a copolymer design feature to improve the biodistribution and the enhanced permeability and retention effect of doxorubicin–loaded mesoporous silica nanoparticles in a murine xenograft tumor model. ACS Nano. 2011;5:4131–44.
201. Gao F, Li L, Liu T, Hao N, Liu H, Tan L, Li H, Huang X, Peng B, Yan C, Yang L, Wu X, Chen D, Tang F. Doxorubicin loaded silica nanorattles actively seek tumors with improved anti–tumor effects. Nanoscale. 2012;4:3365–72.
202. Turan O, Bielecki P, Perera V, Lorkowski M, Covarrubias G, Tong K, Yun A, Rahmy A, Ouyang T, Raghunathan S, Gopalakrishnan R, Griswold MA, Ghaghada KB, Peiris PM, Karathanasis E. Delivery of drugs into brain tumors using multicomponent silica nanoparticles. Nanoscale. 2019;11:11910–21.
203. Turan O, Bielecki P, Tong K, Covarrubias G, Moon T, Rahmy A, Cooley S, Park Y, Peiris PM, Ghaghada KB, Karathanasis E. Effect of dose and selection of two different ligands on the deposition and antitumor efficacy of targeted nanoparticles in brain tumors. Mol Pharm. 2019;16:4352–60.
204. Yang S, Chen D, Li N, Xu Q, Li H, Gu F, Xie J, Lu J. Hollow mesoporous silica nanocarriers with multifunctional capping agents for in vivo cancer imaging and therapy. Small. 2016;12:360–70.
205. Li L, Lu Y, Jiang C, Zhu Y, Yang X, Hu X, Lin Z, Zhang Y, Peng M, Xia H, Mao C. Actively targeted deep tissue imaging and photothermal–chemo therapy of breast cancer by antibody–functionalized drug–loaded x–ray–responsive bismuth sulfide@mesoporous silica core–shell nanoparticles. Adv Funct Mater. 2018;28:1704623.
206. Li C, Feng K, Xie N, Zhao W, Ye L, Chen B, Tung C, Wu L. Mesoporous silica–coated gold nanorods with designable anchor peptides for chemo–photothermal cancer therapy. ACS Appl Nanomater. 2020;3:5070–8.
207. Li C, Yang XQ, An J, Cheng K, Hou XL, Zhang XS, Song XL, Huang KC, Chen W, Liu B, Zhao YD, Liu TC. A near–infrared light–controlled smart nanocarrier with reversible polypeptide–engineered valve for targeted fluorescence–photoacoustic bimodal imaging–guided chemo–photothermal therapy. Theranostics. 2019;9:7666–79.
208. Wei Q, Chen Y, Ma X, Ji J, Qiao Y, Zhou B, Ma F, Ling D, Zhang H, Tian M, Tian J, Zhou M. High–efficient clearable nanoparticles for multi–modal imaging and image–guided cancer therapy. Adv Funct Mater. 2018;28:1704634.
209. Zhang M, Liu X, Luo Q, Wang Q, Zhao L, Deng G, Ge R, Zhang L, Hu J, Lu J. Tumor environment responsive degradable CuS@mSiO_2@MnO_2/DOX for MRI guided synergistic chemo–photothermal therapy and chemodynamic therapy. Chem Eng J. 2020;389:124450.
210. Li C, Yang XQ, Zhang MZ, Song YY, Cheng K, An J,

Zhang XS, Xuan Y, Liu B, Zhao YD. In vivo imaging–guided nanoplatform for tumor targeting delivery and combined chemo–, gene– and photothermal therapy. Theranostics. 2018;8:5662–75.
211. Li Z, Zhang L, Tang C, Yin C. Co–delivery of doxorubicin and survivin shRNA–expressing plasmid via microenvironment–responsive dendritic mesoporous silica nanoparticles for synergistic cancer therapy. Pharm Res. 2017;34:2829–41.
212. Nie D, Dai Z, Li J, Yang Y, Xi Z, Wang J, Zhang W, Qian K, Guo S, Zhu C, Wang R, Li Y, Yu M, Zhang X, Shi X, Gan Y. Cancer–cell–membrane–coated nanoparticles with a yolk–shell structure augment cancer chemotherapy. Nano Lett. 2020;20:936–46.
213. Xing Y, Zhou Y, Zhang Y, Zhang C, Deng X, Dong C, Shuang S. Facile fabrication route of janus gold–mesoporous silica nanocarriers with dual–drug delivery for tumor therapy. ACS Biomater Sci Eng. 2020;6:1573–81.
214. Zhao S, Xu M, Cao C, Yu Q, Zhou Y, Liu J. A redox–responsive strategy using mesoporous silica nanoparticles for co–delivery of siRNA and doxorubicin. J Mater Chem B. 2017;5:6908–19.
215. Li S, Zhang D, Sheng S, Sun H. Targeting thyroid cancer with acid–triggered release of doxorubicin from silicon dioxide nanoparticles. Int J Nanomed. 2017;12:5993–6003.
216. Liu H, Liu T, Wu X, Li L, Tan L, Chen D, Tang F. Targeting gold nanoshells on silica nanorattles: A drug cocktail to fight breast tumors via a single irradiation with near–infrared laser light. Adv Mater. 2012;24:755–61.
217. Li Y, Miao Y, Chen M, Chen X, Li F, Zhang X, Gan Y. Stepwise targeting and responsive lipid–coated nanoparticles for enhanced tumor cell sensitivity and hepatocellular carcinoma therapy. Theranostics. 2020;10:3722–36.
218. Li XD, Wang Z, Wang XR, Shao D, Zhang X, Li L, Ge MF, Chang ZM, Dong WF. Berberine–loaded Janus gold mesoporous silica nanocarriers for chemo/radio/photothermal therapy of liver cancer and radiation–induced injury inhibition. Int J Nanomedicine. 2019;14:3967–82.
219. Shao L, Li Y, Huang F, Wang X, Lu J, Jia F, Pan Z, Cui X, Ge G, Deng X, Wu Y. Complementary autophagy inhibition and glucose metabolism with rattle–structured polydopamine@mesoporous silica nanoparticles for augmented low –temperature photothermal therapy and in vivo photoacoustic imaging. Theranostics. 2020;10:7273–86.
220. Sun W, Ge K, Jin Y, Han Y, Zhang H, Zhou G, Yang X, Liu D, Liu H, Liang XJ, Zhang J. Bone–targeted nanoplatform combining zoledronate and photothermal therapy to treat breast cancer bone metastasis. ACS Nano. 2019;13:7556–67.
221. Wu J, Williams GR, Niu S, Gao F, Tang R, Zhu LM. A multifunctional biodegradable nanocomposite for cancer theranostics. Adv Sci. 2019;6:1802001.
222. Thapa RK, Nguyen HT, Gautam M, Shrestha A, Lee ES, Ku SK, Choi HG, Yong CS, Kim JO. Hydrophobic binding peptide–conjugated hybrid lipid–mesoporous silica nanoparticles for effective chemo–photothermal therapy of pancreatic cancer. Drug Deliv. 2017;24:1690–102.
223. He H, Liu L, Morin EE, Liu M, Schwendeman A. Survey of clinical translation of cancer nanomedicines–lessons learned from successes and failures. Acc Chem Res. 2019;52:2445–61.
224. Xu J, Zhang Y, Yin H, Zhong H, Su M, Tian Z, Li J. Shell–isolated nanoparticle–enhanced raman and fluorescence spectroscopies: Synthesis and applications. Adv Opt Mater. 2018;6:1701069.
225. Bangham AD. Liposomes – the Babraham connection. Chem Phys Lipids. 1993;64:275–85.
226. Vartuli JC, KD Schmitt, CT Kresge, WJ Roth, ME Leonowicz, SB Mccullen, SD Hellring, JS Beck, JL Schlenker, DH Olson, EW Sheppard. Development of a formation mechanism for M41s materials. Amsterdam; Sara Burgerhartstraat 25, Po Box 211, 1000 AE Amsterdam, Netherlands: Elsevier Science Publ B V; 1994. p. 60.
227. Huo QS, Margolese DI, Stucky GD. Surfactant control of phases in the synthesis of mesoporous silica–based materials. Chem Mater. 1996;8:1147–60.
228. Schumacher K, Ravikovitch PI, Du Chesne A, Neimark A, Unger KK. Characterization of MCM–48 materials. Langmuir. 2000;16:4648–54.
229. Huo Q, Leon R, Petroff PM, Stucky GD. Mesostructure design with gemini surfactants: Supercage formation in a 3-dimensional hexagonal array. Science. 1995;268:1324–7.
230. Sakamoto Y, Kaneda M, Terasaki O, Zhao DY, Kim JM, Stucky G, Shin HJ, Ryoo R. Direct imaging of the pores and cages of three–dimensional mesoporous materials. Nature. 2000;408:449–53.
231. El Haskouri J, Cabrera S, Caldes M, Guillem C, Latorre J, Beltran A, Beltran D, Marcos MD, Amoros P. Surfactant–assisted synthesis of the SBA–8 mesoporous silica by using nonrigid commercial alkyltrimethyl ammonium surfactants. Chem Mater. 2002;14:2637–43.
232. Zhao DY, Huo QS, Feng JL, Kim JM, Han YJ, Stucky GD. Novel mesoporous silicates with two–dimensional mesostructure direction using rigid bolaform surfactants. Chem Mater. 1999;11:2668–72.
233. Zhao DY, Huo QS, Feng JL, Chmelka BF, Stucky GD. Nonionic triblock and star diblock copolymer and oligomeric surfactant syntheses of highly ordered, hydrothermally stable, mesoporous silica structures. J Am Chem Soc. 1998;120:6024–36.
234. Sakamoto Y, Diaz I, Terasaki O, Zhao DY, Perez-Pariente J, Kim JM, Stucky GD. Three–dimensional cubic mesoporous structures of SBA–12 and related materials by electron crystallography. J Phys Chem B. 2002;106:3118–23.
235. Zhao D, Feng J, Huo Q, Melosh N, Fredrickson GH, Chmelka BF, Stucky GD. Triblock copolymer syntheses of mesoporous silica with periodic 50 to 300 angstrom pores. Science. 1998;279:548–52.
236. Yu CZ, Yu YH, Zhao DY. Highly ordered large caged

cubic mesoporous silica structures templated by triblock PEO–PBO–PEO copolymer. Chem Commun. 2000; 575–576.
237. Shen S, Li Y, Zhang Z, Fan J, Tu B, Zhou W, Zhao D. A novel ordered cubic mesoporous silica templated with tri–head group quaternary ammonium surfactant. Chem Commun. 2002;19:2212–3.
238. Liu X, Tian B, Yu C, Gao F, Xie S, Tu B, Che R, Peng LM, Zhao D. Room–temperature synthesis in acidic media of large–pore three–dimensional bicontinuous mesoporous silica with Ia3d symmetry. Angew Chem Int Ed Engl. 2002;41:3876–8.
239. Shen S, Garcia-Bennett AE, Liu Z, Lu Q, Shi Y, Yan Y, Yu C, Liu W, Cai Y, Terasaki O, Zhao D. Three–dimensional low symmetry mesoporous silica structures templated from tetra–headgroup rigid bolaform quaternary ammonium surfactant. J Am Chem Soc. 2005;127:6780–7.
240. Hodgkins RP, Garcia-Bennett AE, Wright PA. Structure and morphology of propylthiol–functionalised mesoporous silicas templated by non–ionic triblock copolymers. Microporous Mesoporous Mater. 2005;79: 241–52.
241. Yu T, Zhang H, Yan X, Chen Z, Zou X, Oleynikov P, Zhao D. Pore structures of ordered large cage–type mesoporous silica FDU–12s. J Phys Chem B. 2006;110:21467–72.
242. Schmidt-Winkel P, Glinka CJ, Stucky GD. Microemulsion templates for mesoporous silica. Langmuir. 2000;16:356–61.
243. Inagaki S, Fukushima Y, Kuroda K. Synthesis and characterization of highly ordered mesoporous material – Fsm–16, from a layered polysilicate. Amsterdam; Sara Burgerhartstraat 25, Po Box 211, 1000 AE Amsterdam, Netherlands: Elsevier Science Publ B V; 1994. p. 132.
244. Bagshaw SA, Prouzet E, Pinnavaia TJ. Templating of mesoporous molecular–sieves by nonionic polyethylene oxide surfactants. Science. 1995;269:1242–4.
245. Chen M, Hu J, Wang L, Li Y, Zhu C, Chen C, Shi M, Ju Z, Cao X, Zhang Z. Targeted and redox–responsive drug delivery systems based on carbonic anhydrase IX–decorated mesoporous silica nanoparticles for cancer therapy. Sci Rep. 2020;10:14447.
246. Cheng W, Nie J, Xu L, Liang C, Peng Y, Liu G, Wang T, Mei L, Huang L, Zeng X. pH–sensitive delivery vehicle based on folic acid–conjugated polydopamine–modified mesoporous silica nanoparticles for targeted cancer therapy. ACS Appl Mater Interfaces. 2017;9: 18462–73.
247. Cheng W, Liang C, Xu L, Liu G, Gao N, Tao W, Luo L, Zuo Y, Wang X, Zhang X, Zeng X, Mei L. TPGS–functionalized polydopamine–modified mesoporous silica as drug nanocarriers for enhanced lung cancer chemotherapy against multidrug resistance. Small. 2017;13. doi: 10.1002/smll/201700623.
248. Dai L, Zhang Q, Li J, Shen X, Mu C, Cai K. Dendrimer like mesoporous silica nanoparticles as pH–responsive nanocontainers for targeted drug delivery and bioimaging. ACS Appl Mater Interfaces. 2015;7:7357–72.
249. Fang Z, Li X, Xu Z, Du F, Wang W, Shi R, Gao D. Hyaluronic acid–modified mesoporous silica–coated superparamagnetic Fe3O4 nanoparticles for targeted drug delivery. Int J Nanomedicine. 2019;14:5785–97.
250. Hou J, Guo C, Shi Y, Liu E, Dong W, Yu B, Liu S, Gong J. A novel high drug loading mussel–inspired polydopamine hybrid nanoparticle as a pH–sensitive vehicle for drug delivery. Int J Pharm. 2017;533:73–83.
251. Hou R, Wang Y, Xu Y, Zheng Y, Ma M, Hu B. Theranostic hollow/mesoporous organosilica nanospheres enhance the therapeutic efficacy of anticancer drugs in metastatic hormone–resistant prostate cancer. RSC Adv. 2016;6:94058–67.
252. Huang L, Zhang Q, Dai L, Shen X, Chen W, Cai K. Phenylboronic acid–modified hollow silica nanoparticles for dual–responsive delivery of doxorubicin for targeted tumor therapy. Regen Biomater. 2017;4:111–24.
253. Kang Y, Sun W, Li S, Li M, Fan J, Du J, Liang XJ, Peng X. Oligo hyaluronan-coated silica/hydroxyapatite degradable nanoparticles for targeted cancer treatment. Adv Sci. 2019;6:1900716.
254. Khatoon S, Han HS, Lee M, Lee H, Jung DW, Thambi T, Ikram M, Kang YM, Yi GR, Park JH. Zwitterionic mesoporous nanoparticles with a bioresponsive gatekeeper for cancer therapy. Acta Biomater. 2016;40:282–92.
255. Li QL, Sun Y, Sun YL, Wen J, Zhou Y, Bing QM, Isaacs LD, Jin Y, Gao H, Yang YW. Mesoporous silica nanoparticles coated by layer–by–layer self–assembly using cucurbit[7]uril for in vitro and in vivo anticancer drug release. Chem Mater. 2014;26:6418–31.
256. Liu J, Zhao L, Shi L, Yuan Y, Fu D, Ye Z, Li Q, Deng Y, Liu X, Lv Q, Cheng Y, Xu Y, Jiang X, Wang G, Wang L, Wang Z. A sequentially responsive nanosystem breaches cascaded bio–barriers and suppresses P–glycoprotein function for reversing cancer drug resistance. ACS Appl Mater Interfaces. 2020;12(49):54343–55.
257. Liu Y, Dai R, Wei Q, Li W, Zhu G, Chi H, Guo Z, Wang L, Cui C, Xu J, Ma K. Dual–functionalized janus mesoporous silica nanoparticles with active targeting and charge reversal for synergistic tumor–targeting therapy. ACS Appl Mater Interfaces. 2019;11:44582–92.
258. Liu CM, Chen GB, Chen HH, Zhang JB, Li HZ, Sheng MX, Weng WB, Guo SM. Cancer cell membrane–cloaked mesoporous silica nanoparticles with a pH–sensitive gatekeeper for cancer treatment. Colloids Surf B Biointerfaces. 2019;175:477–86.
259. Liu J, Li Q, Zhang J, Huang L, Qi C, Xu L, Liu X, Wang G, Wang L, Wang Z. Safe and effective reversal of cancer multidrug resistance using sericin–coated mesoporous silica nanoparticles for lysosome–targeting delivery in mice. Small. 2017;13:1602567.
260. Liu J, Luo Z, Zhang J, Luo T, Zhou J, Zhao X, Cai K. Hollow mesoporous silica nanoparticles facilitated drug

delivery via cascade pH stimuli in tumor microenvironment for tumor therapy. Biomaterials. 2016;83:51–65.
261. Palanikumar L, Choi ES, Oh JY, Park SA, Choi H, Kim K, Kim C, Ryu JH. Importance of encapsulation stability of nanocarriers with high drug loading capacity for increasing in vivo therapeutic efficacy. Biomacromolecules. 2018;19:3030–9.
262. Qiao H, Jia J, Shen H, Zhao S, Chen E, Chen W, Di B, Hu C. Capping silica nanoparticles with tryptophan–mediated cucurbit[8]uril complex for targeted intracellular drug delivery triggered by tumor–overexpressed IDO1 enzyme. Adv Healthc Mater. 2019;8:1900174.
263. Ramya AN, Joseph MM, Maniganda S, Karunakaran V, Sreelekha TT, Maiti KK. Emergence of gold-mesoporous silica hybrid nanotheranostics: Dox-encoded, folate targeted chemotherapy with modulation of SERS fingerprinting for apoptosis toward tumor eradication. Small. 2017;13. doi: 10.1002/smll.201700819.
264. Shao D, Li J, Zheng X, Pan Y, Wang Z, Zhang M, Chen QX, Dong WF, Chen L. Janus "nano–bullets" for magnetic targeting liver cancer chemotherapy. Biomaterials. 2016;100:118–33.
265. Shen L, Pan S, Niu D, He J, Jia X, Hao J, Gu J, Zhao W, Li P, Li Y. Facile synthesis of organosilica–capped mesoporous silica nanocarriers with selective redox–triggered drug release properties for safe tumor chemotherapy. Biomater Sci. 2019;7:1825–32.
266. Si P, Shi J, Zhang P, Wang C, Chen H, Mi X, Chu W, Zhai B, Li W. MUC–1 recognition–based activated drug nanoplatform improves doxorubicin chemotherapy in breast cancer. Cancer Lett. 2020;472:165–74.
267. Tian Y, Guo R, Jiao Y, Sun Y, Shen S, Wang Y, Lu D, Jiang X, Yang W. Redox stimuli–responsive hollow mesoporous silica nanocarriers for targeted drug delivery in cancer therapy. Nanoscale Horiz. 2016;1:480–7.
268. Wan L, Chen Z, Deng Y, Liao T, Kuang Y, Liu J, Duan J, Xu Z, Jiang B, Li C. A novel intratumoral pH/redox–dual–responsive nanoplatform for cancer MR imaging and therapy. J Colloid Interface Sci. 2020;573:263–77.
269. Wang M, Liu W, Zhang Y, Dang M, Zhang Y, Tao J, Chen K, Peng X, Teng Z. Intercellular adhesion molecule 1 antibody–mediated mesoporous drug delivery system for targeted treatment of triple–negative breast cancer. J Colloid Interface Sci. 2019;538:630–7.
270. Wei Y, Gao L, Wang L, Shi L, Wei E, Zhou B, Zhou L, Ge B. Polydopamine and peptide decorated doxorubicin–loaded mesoporous silica nanoparticles as a targeted drug delivery system for bladder cancer therapy. Drug Deliv. 2017;24:681–91.
271. Xu J, Gao F, Li L, Ma HL, Fan Y, Liu W, Guo S, Zhao X, Wang H. Gelatin–mesoporous silica nanoparticles as matrix metalloproteinases–degradable drug delivery systems in vivo. Microporous and Mesoporous Materials. 2013;182:165–72.
272. Yang Y, Wang A, Wei Q, Schlesener C, Haag R, Li Q, Li J. Hyperbranched polyglycerol–induced porous silica nanoparticles as drug carriers for cancer therapy in vitro and in vivo. ChemistryOpen. 2017;6:158–64.
273. Yang D, Wang T, Su Z, Xue L, Mo R, Zhang C. Reversing cancer multidrug resistance in xenograft models via orchestrating multiple actions of functional mesoporous silica nanoparticles. ACS Appl Mater Interfaces. 2016;8:22431–41.
274. You Y, He L, Ma B, Chen T. High–drug–loading mesoporous silica nanorods with reduced toxicity for precise cancer therapy against nasopharyngeal carcinoma. Adv Funct Mater. 2017;27:1703313.
275. Zhang Y, Dang M, Tian Y, Zhu Y, Liu W, Tian W, Su Y, Ni Q, Xu C, Lu N, Tao J, Li Y, Zhao S, Zhao Y, Yang Z, Sun L, Teng Z, Lu G. Tumor acidic microenvironment targeted drug delivery based on pHLIP–modified mesoporous organosilica nanoparticles. ACS Appl Mater Interfaces. 2017;9:30543–52.
276. Zhang Q, Wang X, Li P, Nguyen KT, Wang X, Luo Z, Zhang H, Tan NS, Zhao Y. Biocompatible, uniform, and redispersible mesoporous silica nanoparticles for cancer–targeted drug delivery in vivo. Adv Funct Mater. 2014;24:2450–61.
277. Zhao P, Li L, Zhou S, Qiu L, Qian Z, Liu X, Cao X, Zhang H. TPGS functionalized mesoporous silica nanoparticles for anticancer drug delivery to overcome multidrug resistance. Mater Sci Eng C Mater Biol Appl. 2018;84:108–17.
278. Zhao X, Zhou S, Wang D, He W, Li J, Zhang S. Dual–intelligent functionalized silica nanoparticles for liver cancer imaging and therapy. Int J Clin Exp Med. 2016;9:13584–94.
279. Zhou J, Li M, Lim WQ, Luo Z, Phua SZF, Huo R, Li L, Li K, Dai L, Liu J, Cai K, Zhao Y. A transferrin–conjugated hollow nanoplatform for redox–controlled and targeted chemotherapy of tumor with reduced inflammatory reactions. Theranostics. 2018;8:518–32.
280. Zhu R, Wang Z, Liang P, He X, Zhuang X, Huang R, Wang M, Wang Q, Qian Y, Wang S. Efficient VEGF targeting delivery of DOX using Bevacizumab conjugated SiO_2@LDH for anti–neuroblastoma therapy. Acta Biomater. 2017;63:163–80.
281. Cao Y, Wu C, Liu Y, Hu L, Shang W, Gao Z, Xia N. Folate functionalized pH–sensitive photothermal therapy traceable hollow mesoporous silica nanoparticles as a targeted drug carrier to improve the antitumor effect of doxorubicin in the hepatoma cell line SMMC–7721. Drug Deliv. 2020;27:258–68.
282. Chai S, Kan S, Sun R, Zhou R, Sun Y, Chen W, Yu B. Fabricating polydopamine–coated MoSe2–wrapped hollow mesoporous silica nanoplatform for controlled drug release and chemo–photothermal therapy. Int J Nanomedicine. 2018;13:7607–21.
283. Chen C, Tang W, Jiang D, Yang G, Wang X, Zhou L, Zhang W, Wang P. Hyaluronic acid conjugated polydopamine functionalized mesoporous silica nanoparticles for

synergistic targeted chemo–photothermal therapy. Nanoscale. 2019;11:11012–24.
284. Cheng X, Li D, Lin A, Xu J, Wu L, Gu H, Huang Z, Liu J, Zhang Y, Yin X. Fabrication of multifunctional triple–responsive platform based on CuS–capped periodic mesoporous organosilica nanoparticles for chemo–photothermal therapy. Int J Nanomed. 2018;13:3661–77.
285. Fang J, Liu Y, Chen Y, Ouyang D, Yang G, Yu T. Graphene quantum dots–gated hollow mesoporous carbon nanoplatform for targeting drug delivery and synergistic chemo–photothermal therapy. Int J Nanomedicine. 2018;13:5991–6007.
286. Feng S, Mao Y, Wang X, Zhou M, Lu H, Zhao Q, Wang S. Triple stimuli–responsive ZnO quantum dots–conjugated hollow mesoporous carbon nanoplatform for NIR–induced dual model antitumor therapy. J Colloid Interface Sci. 2020;559:51–64.
287. Jin R, Liu Z, Bai Y, Zhou Y, Gooding JJ, Chen X. Core–satellite mesoporous silica–gold nanotheranostics for biological stimuli triggered multimodal cancer therapy. Adv Funct Mater. 2018;28:1801961.
288. Lei W, Sun C, Jiang T, Gao Y, Yang Y, Zhao Q, Wang S. Polydopamine–coated mesoporous silica nanoparticles for multi–responsive drug delivery and combined chemo–photothermal therapy. Mater Sci Eng C Mater Biol Appl. 2019;105:110103.
289. Lei Q, Qiu WX, Hu JJ, Cao PX, Zhu CH, Cheng H, Zhang XZ. Multifunctional mesoporous silica nanoparticles with thermal–responsive gatekeeper for NIR light–triggered chemo/photothermal–therapy. Small. 2016;12:4286–98.
290. Li D, Zhang T, Min C, Huang H, Tan D, Gu W. Biodegradable theranostic nanoplatforms of albumin–biomineralized nanocomposites modified hollow mesoporous organosilica for photoacoustic imaging guided tumor synergistic therapy. Chem Eng J. 2020;388:124253.
291. Lu Y, Li L, Lin Z, Li M, Hu X, Zhang Y, Peng M, Xia H, Han G. Enhancing osteosarcoma killing and CT imaging using ultrahigh drug loading and NIR–responsive bismuth sulfide@mesoporous silica nanoparticles. Adv Healthc Mater. 2018;7:1800602.
292. Wang J, Zhang W, Li S, Miao D, Qian G, Su G. Engineering of porous silica coated gold nanorods by surface–protected etching and their applications in drug loading and combined cancer therapy. Langmuir. 2019;35:14238–47.
293. Yang J, Dai D, Lou X, Ma L, Wang B, Yang YW. Supramolecular nanomaterials based on hollow mesoporous drug carriers and macrocycle–capped CuS nanogates for synergistic chemo–photothermal therapy. Theranostics. 2020;10:615–29.
294. Zhong R, Wang R, Hou X, Song L, Zhang Y. Polydopamine–doped virus–like structured nanoparticles for photoacoustic imaging guided synergistic chemo–/photothermal therapy. RSC Adv. 2020;10:18016–24.
295. Fang J, Wang Q, Yang G, Xiao X, Li L, Yu T. Albumin–MnO_2 gated hollow mesoporous silica nanosystem for modulating tumor hypoxia and synergetic therapy of cervical carcinoma. Colloids Surf B Biointerfaces. 2019;179:250–9.
296. Li Z, Han J, Yu L, Qian X, Xing H, Lin H, Wu M, Yang T, Chen Y. Synergistic Sonodynamic/chemotherapeutic suppression of hepatocellular carcinoma by targeted biodegradable mesoporous nanosonosensitizers. Adv Funct Mater. 2018;28:1800145.
297. Liu G, Ma J, Li Y, Li Q, Tan C, Song H, Cai S, Chen D, Hou Z, Chen Q, Zhu X. Core–interlayer–shell Fe3O4@mSiO(2)@lipid–PEG–methotrexate nanoparticle for multimodal imaging and multistage targeted chemo–photodynamic therapy. Int J Pharm. 2017;521:19–32.
298. Vijayakameswara RN, Han HS, Lee H, Nguyen VQ, Jeon S, Jung DW, Lee J, Yi GR, Park JH. ROS–responsive mesoporous silica nanoparticles for MR imaging–guided photodynamically maneuvered chemotherapy. Nanoscale. 2018;10:9616–27.
299. Su J, Sun H, Meng Q, Zhang P, Yin Q, Li Y. Enhanced blood suspensibility and laser–activated tumor–specific drug release of theranostic mesoporous silica nanoparticles by functionalizing with erythrocyte membranes. Theranostics. 2017;7:523–37.
300. Wang D, Li X, Li X, Kang A, Sun L, Sun M, Yang F, Xu C. Magnetic and pH dual–responsive nanoparticles for synergistic drug–resistant breast cancer chemo/photodynamic therapy. Int J Nanomed. 2019;14:7665–79.
301. Xu P, Yao J, Li Z, Wang M, Zhou L, Zhong G, Zheng Y, Li N, Zhai Z, Yang S, Wu Y, Zhang D, Dai Z. Therapeutic effect of doxorubicin–chlorin E6–loaded mesoporous silica nanoparticles combined with ultrasound on triple–negative breast cancer. Int J Nanomedicine. 2020;15:2659–68.
302. Wang Z, Shao D, Chang Z, Lu M, Wang Y, Yue J, Yang D, Li M, Xu Q, Dong WF. Janus gold nanoplatform for synergetic chemoradiotherapy and computed tomography imaging of hepatocellular carcinoma. ACS Nano. 2017;11:12732–41.
303. Chen Z, Zhu P, Zhang Y, Liu Y, He Y, Zhang L, Gao Y. Enhanced sensitivity of cancer stem cells to chemotherapy using functionalized mesoporous silica nanoparticles. Mol Pharm. 2016;13:2749–59.
304. Ding X, Yu W, Wan Y, Yang M, Hua C, Peng N, Liu Y. A pH/ROS–responsive, tumor–targeted drug delivery system based on carboxymethyl chitin gated hollow mesoporous silica nanoparticles for anti–tumor chemotherapy. Carbohydr Polym. 2020;245:116493.
305. He Y, Shao L, Usman I, Hu Y, Pan A, Liang S, Xu H. A pH–responsive dissociable mesoporous silica–based nanoplatform enabling efficient dual–drug co–delivery and rapid clearance for cancer therapy. Biomater Sci. 2020;8:3418–29.
306. He Y, Su Z, Xue L, Xu H, Zhang C. Co–delivery of erlotinib and doxorubicin by pH–sensitive charge conversion nanocarrier for synergistic therapy. J Control Release. 2016;229:80–92.

307. Hu JJ, Lei Q, Peng MY, Zheng DW, Chen YX, Zhang XZ. A positive feedback strategy for enhanced chemotherapy based on ROS–triggered self–accelerating drug release nanosystem. Biomaterials. 2017;128:136–46.
308. Kankala RK, Liu C, Yang D, Wang S, Chen A. Ultrasmall platinum nanoparticles enable deep tumor penetration and synergistic therapeutic abilities through free radical species–assisted catalysis to combat cancer multidrug resistance. Chem Eng J. 2020;383:123138.
309. Kong M, Tang J, Qiao Q, Wu T, Qi Y, Tan S, Gao X, Zhang Z. Biodegradable hollow mesoporous silica nanoparticles for regulating tumor microenvironment and enhancing antitumor efficiency. Theranostics. 2017;7:3276–92.
310. Liu H, Luan X, Feng H, Dong X, Yang S, Chen Z, Cai Q, Lu Q, Zhang Y, Sun P, Zhao M, Chen H, Lovell JF, Fang C. Integrated combination treatment using a "smart" chemotherapy and microRNA delivery system improves outcomes in an orthotopic colorectal cancer model. Adv Funct Mater. 2018;28:1801118.
311. Ramasamy T, Ruttala HB, Sundaramoorthy P, Poudel BK, Youn YS, Ku SK, Choi H, Yong CS, Kim JO. Multimodal selenium nanoshell–capped Au@mSiO(2) nanoplatform for NIR–responsive chemo–photothermal therapy against metastatic breast cancer. Npg Asia Mater. 2018;10:197–216.
312. Su T, Long Y, Deng C, Feng L, Zhang X, Chen Z, Li C. Construction of a two–in–one liposomal system (TWO-Lips) for tumor–targeted combination therapy. Int J Pharm. 2014;476:241–52.
313. Xie J, Xu W, Wu Y, Niu B, Zhang X. Macroporous organosilicon nanocomposites co–deliver Bcl2–converting peptide and chemotherapeutic agent for synergistic treatment against multidrug resistant cancer. Cancer Lett. 2020;469:340–54.
314. Xue H, Yu Z, Liu Y, Yuan W, Yang T, You J, He X, Lee RJ, Li L, Xu C. Delivery of miR–375 and doxorubicin hydrochloride by lipid–coated hollow mesoporous silica nanoparticles to overcome multiple drug resistance in hepatocellular carcinoma. Int J Nanomedicine. 2017;12:5271–87.
315. Yin PT, Pongkulapa T, Cho HY, Han J, Pasquale NJ, Rabie H, Kim JH, Choi JW, Lee KB. Overcoming chemoresistance in cancer via combined MicroRNA therapeutics with anticancer drugs using multifunctional magnetic core–shell nanoparticles. ACS Appl Mater Interfaces. 2018;10:26954–63.
316. Zhang F, Jia Y, Zheng X, Shao D, Zhao Y, Wang Z, Dawulieti J, Liu W, Sun M, Sun W, Pan Y, Cui L, Wang Y, He K, Zhang M, Li J, Dong WF, Chen L. Janus nanocarrier–based co–delivery of doxorubicin and berberine weakens chemotherapy–exacerbated hepatocellular carcinoma recurrence. Acta Biomater. 2019;100:352–64.
317. Zhang B, Luo Z, Liu J, Ding X, Li J, Cai K. Cytochrome c end–capped mesoporous silica nanoparticles as redox–responsive drug delivery vehicles for liver tumor–targeted triplex therapy in vitro and in vivo. J Control Release. 2014;192:192–201.
318. Ansari L, Jaafari MR, Bastami TR, Malaekeh-Nikouei B. Improved anticancer efficacy of epirubicin by magnetic mesoporous silica nanoparticles: In vitro and in vivo studies. Artif Cells Nanomed Biotechnol. 2018;46:594–606.
319. Babaei M, Abnous K, Taghdisi SM, Taghavi S, Sh Saljooghi A, Ramezani M, Alibolandi M. Targeted rod–shaped mesoporous silica nanoparticles for the co–delivery of camptothecin and survivin shRNA into colon adenocarcinoma in vitro and in vivo. Eur J Pharm Biopharm. 2020;156:84–96.
320. Che E, Gao Y, Wan L, Zhang Y, Han N, Bai J, Li J, Sha Z, Wang S. Paclitaxel/gelatin coated magnetic mesoporous silica nanoparticles: Preparation and antitumor efficacy in vivo. Microporous Mesoporous Mater. 2015;204:226–34.
321. Chen Q, Chen Y, Zhang W, Huang Q, Hu M, Peng D, Peng C, Wang L, Chen W. Acidity and glutathione dual–responsive polydopamine–coated organic–inorganic hybrid hollow mesoporous silica nanoparticles for controlled drug delivery. ChemMedChem. 2020;15:1940–6.
322. Chen J, Zhang S, Zhang S, Gao S, Wang J, Lei D, Du P, Xu Z, Zhu C, Sun H. Mesoporous silica nanoparticle–based combination of NQO1 inhibitor and 5–fluorouracil for potent antitumor effect against head and neck squamous cell carcinoma (HNSCC). Nanoscale Res Lett. 2019;14:387.
323. Choi JY, Ramasamy T, Kim SY, Kim J, Ku SK, Youn YS, Kim JR, Jeong JH, Choi HG, Yong CS, Kim JO. PEGylated lipid bilayer–supported mesoporous silica nanoparticle composite for synergistic co–delivery of axitinib and celastrol in multi–targeted cancer therapy. Acta Biomater. 2016;39:94–105.
324. Ding J, Yao J, Xue J, Li R, Bao B, Jiang L, Zhu JJ, He Z. Tumor–homing cell–penetrating peptide linked to colloidal mesoporous silica encapsulated (–)–epigallocatechin–3–gallate as drug delivery system for breast cancer therapy in vivo. ACS Appl Mater Interfaces. 2015;7:18145–55.
325. Du X, Zhang T, Ma G, Gu X, Wang G, Li J. Glucose–responsive mesoporous silica nanoparticles to generation of hydrogen peroxide for synergistic cancer starvation and chemistry therapy. Int J Nanomedicine. 2019;14:2233–51.
326. Fei W, Zhang Y, Han S, Tao J, Zheng H, Wei Y, Zhu J, Li F, Wang X. RGD conjugated liposome–hollow silica hybrid nanovehicles for targeted and controlled delivery of arsenic trioxide against hepatic carcinoma. Int J Pharm. 2017;519:250–62.
327. Feng Y, Li NX, Yin HL, Chen TY, Yang Q, Wu M. Thermo– and pH–responsive, lipid–coated, mesoporous silica nanoparticle–based dual drug delivery system to improve the antitumor effect of hydrophobic drugs. Mol Pharm. 2019;16:422–36.
328. Gao J, Fan K, Jin Y, Zhao L, Wang Q, Tang Y, Xu H, Liu Z, Wang S, Lin J, Lin D. PEGylated lipid bilayer coated

mesoporous silica nanoparticles co–delivery of paclitaxel and curcumin leads to increased tumor site drug accumulation and reduced tumor burden. Eur J Pharm Sci. 2019;140:105070.
329. Goto A, Yen H, Anraku Y, Fukushima S, Lai P, Kato M, Kishimura A, Kataoka K. Facile preparation of delivery platform of water–soluble low–molecular–weight drugs based on polyion complex vesicle (PICsome) encapsulating mesoporous silica nanoparticle. ACS Biomater Sci Eng. 2017;3:807–15.
330. Hanafi-Bojd MY, Jaafari MR, Ramezanian N, Xue M, Amin M, Shahtahmassebi N, Malaekeh-Nikouei B. Surface functionalized mesoporous silica nanoparticles as an effective carrier for epirubicin delivery to cancer cells. Eur J Pharm Biopharm. 2015;89:248–58.
331. Hanafi-Bojd MY, Jaafari MR, Ramezanian N, Abnous K, Malaekeh-Nikouei B. Co–delivery of epirubicin and siRNA using functionalized mesoporous silica nanoparticles enhances in vitro and in vivo drug efficacy. Curr Drug Deliv. 2016;13:1176–82.
332. Hu Y, Wang Z, Qiu Y, Liu Y, Ding M, Zhang Y. Anti–miRNA21 and resveratrol–loaded polysaccharide–based mesoporous silica nanoparticle for synergistic activity in gastric carcinoma. J Drug Target. 2019;27:1135–43.
333. Huo M, Wang L, Chen Y, Shi J. Tumor–selective catalytic nanomedicine by nanocatalyst delivery. Nat Commun. 2017;8:357.
334. Ke Y, Xiang C. Transferrin receptor–targeted HMSN for sorafenib delivery in refractory differentiated thyroid cancer therapy. Int J Nanomedicine. 2018;13:8339–54.
335. Kundu M, Chatterjee S, Ghosh N, Manna P, Das J, Sil PC. Tumor targeted delivery of umbelliferone via a smart mesoporous silica nanoparticles controlled–release drug delivery system for increased anticancer efficiency. Mater Sci Eng C Mater Biol Appl. 2020;116:111239.
336. Li Z, Zhang Y, Zhu C, Guo T, Xia Q, Hou X, Liu W, Feng N. Folic acid modified lipid–bilayer coated mesoporous silica nanoparticles co–loading paclitaxel and tanshinone IIA for the treatment of acute promyelocytic leukemia. Int J Pharm. 2020;586:119576.
337. Li Y, Tang Y, Chen S, Liu Y, Wang S, Tian Y, Wang C, Teng Z, Lu G. Sequential therapy for pancreatic cancer by losartan– and gemcitabine–loaded magnetic mesoporous spheres. RSC Adv. 2019;9:19690–8.
338. Liu M, Tu J, Feng Y, Zhang J, Wu J. Synergistic co–delivery of diacid metabolite of norcantharidin and ABT–737 based on folate–modified lipid bilayer–coated mesoporous silica nanoparticle against hepatic carcinoma. J Nanobiotechnology. 2020;18:114.
339. Liu J, Guo X, Luo Z, Zhang J, Li M, Cai K. Hierarchically stimuli–responsive nanovectors for improved tumor penetration and programed tumor therapy. Nanoscale. 2018;10:13737–50.
340. Lu J, Liong M, Li Z, Zink JI, Tamanoi F. Biocompatibility, biodistribution, and drug–delivery efficiency of mesoporous silica nanoparticles for cancer therapy in animals. Small. 2010;6:1794–805.
341. Meng H, Wang M, Liu H, Liu X, Situ A, Wu B, Ji Z, Chang CH, Nel AE. Use of a lipid–coated mesoporous silica nanoparticle platform for synergistic gemcitabine and paclitaxel delivery to human pancreatic cancer in mice. ACS Nano. 2015;9:3540–57.
342. Mu S, Liu Y, Wang T, Zhang J, Jiang D, Yu X, Zhang N. Unsaturated nitrogen–rich polymer poly(L–histidine) gated reversibly switchable mesoporous silica nanoparticles using "graft to" strategy for drug controlled release. Acta Biomater. 2017;63:150–62.
343. Murugan C, Venkatesan S, Kannan S. Cancer therapeutic proficiency of dual–targeted mesoporous silica nanocomposite endorses combination drug delivery. ACS Omega. 2017;2:7959–75.
344. Pan G, Jia TT, Huang QX, Qiu YY, Xu J, Yin PH, Liu T. Mesoporous silica nanoparticles (MSNs)–based organic/inorganic hybrid nanocarriers loading 5–fluorouracil for the treatment of colon cancer with improved anticancer efficacy. Colloids Surf B Biointerfaces. 2017; 159:375–85.
345. Ovejero Paredes K, Díaz-García D, García-Almodóvar V, Lozano Chamizo L, Marciello M, Díaz-Sánchez M, Prashar S, Gómez-Ruiz S, Filice M. Multifunctional silica–based nanoparticles with controlled release of organotin metallodrug for targeted theranosis of breast cancer. Cancers. 2020;12:187.
346. Qu W, Meng B, Yu Y, Wang S. Folic acid–conjugated mesoporous silica nanoparticles for enhanced therapeutic efficacy of topotecan in retina cancers. Int J Nanomed. 2018;13:4379–89.
347. Ren S, Yang J, Ma L, Li X, Wu W, Liu C, He J, Miao L. Ternary–responsive drug delivery with activatable dual mode contrast–enhanced in vivo imaging. ACS Appl Mater Interfaces. 2018;10:31947–58.
348. Tang L, Gabrielson NP, Uckun FM, Fan TM, Cheng J. Size–dependent tumor penetration and in vivo efficacy of monodisperse drug–silica nanoconjugates. Mol Pharm. 2013;10:883–92.
349. Tao J, Fei W, Tang H, Li C, Mu C, Zheng H, Li F, Zhu Z. Angiopep–2–conjugated "core–shell" hybrid nanovehicles for targeted and pH–triggered delivery of arsenic trioxide into glioma. Mol Pharm. 2019;16:786–97.
350. Wang Z, Wu P, He Z, He H, Rong W, Li J, Zhou D, Huang Y. Mesoporous silica nanoparticles with lactose–mediated targeting effect to deliver platinum(IV) prodrug for liver cancer therapy. J Mater Chem B. 2017;5:7591–7.
351. Wu D, Zhu ZQ, Tang HX, Shi ZE, Kang J, Liu Q, Qi J. Efficacy–shaping nanomedicine by loading calcium peroxide into tumor microenvironment–responsive nanoparticles for the antitumor therapy of prostate cancer. Theranostics. 2020;10:9808–29.
352. Xu X, Wu C, Bai A, Liu X, Lv H, Liu Y. Folate–functionalized mesoporous silica nanoparticles as a liver

tumor–targeted drug delivery system to improve the antitumor effect of paclitaxel. J Nanomaterials. 2017: 2069685.
353. Zhang X, He C, Liu X, Chen Y, Zhao P, Chen C, Yan R, Li M, Fan T, Altine B, Yang T, Lu Y, Lee RJ, Gai Y, Xiang G. One–pot synthesis of a microporous organosilica–coated cisplatin nanoplatform for HIF–1–targeted combination cancer therapy. Theranostics. 2020;10:2918–29.
354. Zhao R, Han X, Li Y, Wang H, Ji T, Zhao Y, Nie G. Photothermal effect enhanced cascade targeting strategy for improved pancreatic cancer therapy by gold nanoshell@ mesoporous silica nanorod. ACS Nano. 2017;11:8103–13.
355. Huang C, Chen T, Zhu D, Huang Q. Enhanced tumor targeting and radiotherapy by quercetin loaded biomimetic nanoparticles. Front Chem. 2020;8:225.
356. Hu X, Mandika C, He L, You Y, Chang Y, Wang J, Chen T, Zhu X. Construction of urokinase–type plasminogen activator receptor–targeted heterostructures for efficient photothermal chemotherapy against cervical cancer to achieve simultaneous anticancer and antiangiogenesis. ACS Appl Mater Interfaces. 2019;11:39688–705.
357. Li Y, Jian X, Zhou S, Lu Y, Zhao C, Gao Z, Song YY. Protein shell–encapsulated pt clusters as continuous O–2–supplied biocoats for photodynamic therapy in hypoxic cancer cells. ACS Appl Mater Interfaces. 2019;11: 17215–25.
358. Luo G, Chen W, Lei Q, Qiu W, Liu Y, Cheng Y, Zhang X. A triple–collaborative strategy for high–performance tumor therapy by multifunctional mesoporous silica–coated gold nanorods. Adv Funct Mater. 2016;26:4339–50.
359. Wang Z, Liu J, Zhao N, Li C, Lv S, Hu Y, Lv H, Wang D, Wang S. Cancer cell macrophage membrane camouflaged persistent luminescent nanoparticles for imaging–guided photothermal therapy of colorectal cancer. ACS Appl Nanomater. 2020;3:7105–18.
360. Wang Z, Chang ZM, Shao D, Zhang F, Chen F, Li L, Ge MF, Hu R, Zheng X, Wang Y, Dong WF. Janus gold triangle–mesoporous silica nanoplatforms for hypoxia–activated radio–chemo–photothermal therapy of liver cancer. ACS Appl Mater Interfaces. 2019;11:34755–65.
361. Xing H, Wang Z, Shao D, Chang Z, Ge M, Li L, Wu M, Yan Z, Dong W. Janus nanocarriers for magnetically targeted and hyperthermia–enhanced curcumin therapy of liver cancer. RSC Adv. 2018;8:30448–54.
362. Zhang Y, Zhang L, Lin X, Ke L, Li B, Xu L, Lv T, Li Z, Chen H, Gao Y. Dual–responsive nanosystem for precise molecular subtyping and resistant reversal of EGFR targeted therapy. Chem Eng J. 2019;372:483–95.
363. Brezániová I, Záruba K, Králová J, Sinica A, Adámková H, Ulbrich P, Poučková P, Hrubý M, Štěpánek P, Král V. Silica–based nanoparticles are efficient delivery systems for temoporfin. Photodiagnosis Photodyn Ther. 2018;21:275–84.
364. Du W, Liu T, Xue F, Chen Y, Chen Q, Luo Y, Cai X, Ma M, Chen H. Confined nanoparticles growth within hollow mesoporous nanoreactors for highly efficient MRI–guided photodynamic therapy. Chem Eng J. 2020;379:122251.
365. Yang S, You Q, Yang L, Li P, Lu Q, Wang S, Tan F, Ji Y, Li N. Rodlike MSN@Au nanohybrid–modified supermolecular photosensitizer for nIRF/MSOT/CT/MR quadmodal imaging–guided photothermal/photodynamic cancer therapy. ACS Appl Mater Interfaces. 2019;11:6777–88.
366. Zhang X, Wang L, Wu X, Cong C. Synthesis of SiO_2@ Cu2–xSe nanospheres for efficient near–infrared radiation mediated treatment and care of gastric cancer patients. J Photochem Photobiol B. 2020;206:111849.
367. Liu J, Liang H, Li M, Luo Z, Zhang J, Guo X, Cai K. Tumor acidity activating multifunctional nanoplatform for NIR–mediated multiple enhanced photodynamic and photothermal tumor therapy. Biomaterials. 2018;157:107–24.
368. Wang Z, Zhang F, Shao D, Chang Z, Wang L, Hu H, Zheng X, Li X, Chen F, Tu Z, Li M, Sun W, Chen L, Dong WF. Janus nanobullets combine photodynamic therapy and magnetic hyperthermia to potentiate synergetic anti–metastatic immunotherapy. Adv Sci. 2019;6:1901690.
369. Zhang L, Yang Z, Ren J, Ba L, He W, Wong C. Multifunctional oxygen–enriching nano–theranostics for cancer–specific magnetic resonance imaging and enhanced photodynamic/photothermal therapy. Nano Research. 2020;13:1389–98.
370. Liu M, Fu M, Yang X, Jia G, Shi X, Ji J, Liu X, Zhai G. Paclitaxel and quercetin co–loaded functional mesoporous silica nanoparticles overcoming multidrug resistance in breast cancer. Colloids Surf B Biointerfaces. 2020;196:111284.
371. Zhao R, Li T, Zheng G, Jiang K, Fan L, Shao J. Simultaneous inhibition of growth and metastasis of hepatocellular carcinoma by co–delivery of ursolic acid and sorafenib using lactobionic acid modified and pH–sensitive chitosan–conjugated mesoporous silica nanocomplex. Biomaterials. 2017;143:1–16.
372. Gabizon A, Tzemach D, Mak L, Bronstein M, Horowitz AT. Dose dependency of pharmacokinetics and therapeutic efficacy of pegylated liposomal doxorubicin (DOXIL) in murine models. J Drug Target. 2002;10:539–48.
373. Huang SK, Mayhew E, Gilani S, Lasic DD, Martin FJ, Papahadjopoulos D. Pharmacokinetics and therapeutics of sterically stabilized liposomes in mice bearing C–26 colon–carcinoma. Cancer Res. 1992;52:6774–81.
374. Mayer LD, Bally MB, Cullis PR, Wilson SL, Emerman JT. Comparison of free and liposome encapsulated doxorubicin tumor drug uptake and antitumor efficacy in the Sc115 murine mammary–tumor. Cancer Lett. 1990;53:183–90.
375. Mayhew EG, Lasic D, Babbar S, Martin FJ. Pharmacokinetics and antitumor–activity of epirubicin encapsulated in long–circulating liposomes incorporating a polyethylene glycol–derivatized phospholipid. Int J Cancer. 1992;51:302–9.
376. Papahadjopoulos D, Allen TM, Gabizon A, Mayhew E, Matthay K, Huang SK, Lee KD, Woodle MC, Lasic DD,

Redemann C. Sterically stabilized liposomes – improvements in pharmacokinetics and antitumor therapeutic efficacy. Proc Natl Acad Sci U S A. 1991;88:11460–4.
377. Unezaki S, Maruyama K, Ishida O, Suginaka A, Hosoda J, Iwatsuru M. Enhanced tumor targeting and improved antitumor activity of doxorubicin by long–circulating liposomes containing amphipathic poly(ethylene glycol). Int J Pharm. 1995;126:41–8.
378. Vaage J, Donovan D, Mayhew E, Abra R, Huang A. Therapy of human ovarian–carcinoma xenografts using doxorubicin encapsulated in sterically stabilized liposomes. Cancer. 1993;72:3671–5.
379. Vaage J, Donovan D, Mayhew E, Uster P, Woodle M. Therapy of mouse mammary carcinomas with vincristine and doxorubicin encapsulated in sterically stabilized liposomes. Int J Cancer. 1993;54:959–64.
380. Vaage J, Barberá-Guillem E, Abra R, Huang A, Working P. Tissue distribution and therapeutic effect of intravenous free or encapsulated liposomal doxorubicin on human prostate carcinoma xenografts. Cancer. 1994;73:1478–84.